2016

ECOLOGY OF THE ALLUVIAL AQUIFER OF THE NYACK FLOODPLAIN ON THE MIDDLE FORK OF THE FLATHEAD RIVER, MONTANA

Amanda Gay DelVecchia
The University of Montana

ECOLOGY OF THE ALLUVIAL AQUIFER OF THE NYACK FLOODPLAIN ON THE MIDDLE FORK OF THE FLATHEAD RIVER, MONTANA

By: Amanda Gay DelVecchia
B.S. Environmental Science, The University of North Carolina at Chapel Hill, Chapel Hill, North Carolina, 2012

Dissertation

presented in partial fulfillment of the requirements
for the degree of

Doctor of Philosophy
in Systems Ecology

The University of Montana
Missoula, MT

May 2016

Approved by:

Scott Whittenburg, Dean of The Graduate School
Graduate School

Dr. Jack Stanford, Chair
Flathead Lake Biological Station, Division of Biological Sciences

Dr. Bonnie Ellis
Flathead Lake Biological Station, Division of Biological Sciences

Dr. Gordon Luikart
Flathead Lake Biological Station, Division of Biological Sciences

Dr. Jonathan Graham
Department of Mathematical Sciences

Dr. Ryan Jones
Department of Microbiology and Immunology, Montana State University

DelVecchia, Amanda, Doctor of Philosophy, May 14, 2016 Systems Ecology

Ecology of the alluvial aquifer of the Nyack Floodplain, Middle Fork of the Flathead River, Montana

Chairperson: Dr. Jack Stanford

The pristine Nyack Floodplain on the Middle Fork of the Flathead River in Northwestern Montana contains an expansive alluvial aquifer that is extremely limited in organic carbon, yet supports abundant and diverse hyporheic stoneflies. My dissertation focused broadly on how these large consumers persist in such an oligotrophic system. In particular, I studied the ecological role of methane dynamics.

I found that most of the dissolved methane in the aquifer was biogenic. Methane carbon ranged in age from modern to 6,900 years BP. Stonefly biomass in the Nyack floodplain included 37.3 to 66.5 % methane derived carbon contributions, even including sites where methane concentrations were low to immeasurable. Stonefly biomass carbon ages ranged up to 6,900 years BP, showing the incorporation of up to 20% ancient carbon, or 41% millennial-aged carbon. When I expanded analysis of methane-derived carbon in biomass to three other floodplains across Montana and Washington, I found that 8-41% of biomass in other floodplains was comprised of methane-derived carbon. Stonefly species had distinct trophic positions as demonstrated by $\delta^{13}C$ and $\delta^{15}N$ analysis of biomass. The differences in trophic positions between species likely resulted from varying abilities of each species to access methane-derived carbon resources at oxic-hypoxic interfaces, as suggested by respirometry experiments and analysis of 16S rRNA sequences in stonefly gut contents. Species-specific $\delta^{13}C$ signatures were consistent with variation in species assemblages because stoneflies with more depleted $\delta^{13}C$ signatures indicating assimilation of methane derived carbon in biomass tended to be present in wells with higher methane concentrations. Dissolved methane concentrations explained 19% of the variation in stonefly species assemblages. While none of the biogeochemical variables studied were consistently significant in predicting trophic positions, dissolved methane concentrations alone explained 19% of the variation in stonefly species assemblages. Finally, not only were species adapted to the use of methane-derived carbon resources, but they were adapted to the lack of temporal variation in temperature within the aquifer: these hyporheic stonefly species had desynchronized growth and emergence patterns uncharacteristic of most stonefly species.

This was the first report of a freshwater ecosystem to contain consumers dependent on ancient methane derived carbon. By demonstrating the role of methane in supporting these consumers, my work developed the contemporary understanding of basal resources supporting riverine productivity. It also underscored the of biogeochemical heterogeneity for maintaining productivity.

Contents

Figures and Tables

Chapter 2

Figures

Tables

Chapter 3

Figures

Tables

Chapter 4

Figures

Tables

Acknowledgments

This dissertation is dedicated to my parents, Peter and Gay DelVecchia, who have given their entire lives to making sure that I have every opportunity for health, happiness, and fulfillment. It is a small recognition of the doors they have opened for me, the values they have taught me, and the joy, love, and pride they have given me.

My advisor, Dr. Jack Stanford has been much more to me than a patient and furtive academic mentor. He has invested his time, effort, and trust in me, which have facilitated and motivated me along the way. He has been a doting and loyal friend that I will always count on. I cannot imagine a better advisor, and I will always do my best to uphold the high standards he has taught me.

My committee has been an extremely supportive group of mentors. From spending hours discussing concepts, to sharing their excitement for Nyack research, to ensuring I would be prepared for my examinations and checkpoints, they have invested their time in my future and I am grateful. In particular, Bonnie Ellis has guided me in both ecology and career development, was an organized and helpful committee chair for my comprehensive exams, and has been a friend to me. Gordon Luikart has paused at his busiest moments to teach me about even the most basic concepts in population genetics and to share his optimism and enthusiasm. Ryan Jones welcomed me into his lab and spent several days teaching me analysis methods in microbial ecology. Jonathan Graham has patiently taught me how to improve as a scientist in a way I consider most crucial: analyzing data as robustly as possible and presenting it accurately.

Finally, William Woessner was a creative and thoughtful committee member that taught me new approaches to my research before he retired.

FLBS has given me a great team to work with: Tom Bansak got me started on Nyack and assisted me throughout my time here. Sue Gillespie, Marie Kohler, Judy Maseman, and Teri Bales answered my endless questions. Adam Baumann, Samantha Tappenbeck, Tyler Tappenbeck, and Jim Craft constantly helped me with lab and field methods and kept me alert in the scope room (TT, AB). Jeremy Nigon helped me with all IT questions. Phil Matson provided me encouragement, help on Nyack, and assistance during travel. Shawn Devlin and Brian Hand guided me along in this early career process. Eric Anderson, Reggie Heiser, and Mark Potter ensured I had everything I needed to complete Nyack work. Tony Richards was always there to help me load up for field trips.

Outside of FLBS, I am thankful to many others who gave their time and enthusiasm to this research. Ashley Helton and Geoffrey Poole have been creative, enthusiastic, and supportive collaborators with an in-depth knowledge of Nyack hydrology. Xiaomei Xu facilitated radiocarbon dating of dissolved methane, a crucial part of the project. Tim McDermott has given me guidance on microbial ecology aspects of the project. Steve Whalen and Anne Hershey helped to begin this work and teach me methods of dissolved methane sampling. Brian Reid has shared his brilliant ideas with me from his time spent on Nyack. Meredith Wright helped to begin work on the Nyack methane story. John Bruno, as my undergraduate advisor at UNC, helped me to complete my undergraduate project that led me to grad school.

The Dalimata family has been ever-ready to help, to check in with me for a laugh or two, and to ensure I didn't do anything quite too East-Coast city girl with the work truck. And of

course, what research would be possible without incredible volunteers and technicians? Of particular mention is Hannah Coe, the legendary field and lab superstar who could handle anything, who worked endless days in anything from -10 to 90 degrees with a smile on her face, and who expected the unexpected without fail. I also would like to thank Neal Jacobi, Amelia Schirmer, Chad Reynolds, Emily Winters, Clinton Begley, Cailey Philmon, Matthew Bambach, Chris Anderson, and all others who have helped me with field and lab work.

Last but far from least, Nicholas Dalimata has supported me by broadening my horizons and reminding me to enjoy myself throughout this process. Jema Rushe and Brett Addis have been my fellow grads and close friends, helping me to get through the degree. Rachel and John Malison have always been there a step ahead of me, helping me along for the past six years.

Funding for my dissertation work was provided mainly by the Jessie M. Bierman Professorship and a philanthropically funded graduate fellowship. It was supplemented by a graduate fellowship and a graduate enhancement funding grant from The University of Montana EPSCOR program.

Chapter 1: Introduction

River ecosystems are complex because they are dynamic across three dimensions. Interactions across each of these dimensions are spatially and temporally structured and vary along the river corridor (Stanford and Ward 1993, Stanford et al. 2005). The most apparent dimension of exchange in these systems is longitudinal, as was emphasized when rivers were first viewed as driven by upstream nutrient export in the river continuum concept (Vannote et al. 1980). The role of lateral interactions as maintained by flooding and exchange with the riparian zone was recognized with the flood pulse concept (Junk et al. 1989) and the partitioning of productivity in these systems into both autochthonous and allochthonous carbon supplies (e.g. Thorp and Delong 1994, 2002). Finally, the role of vertical exchange between the surface and hyporheic zone (alluvial aquifer) in floodplains was recognized by the concept of the hyporheic corridor (Stanford and Ward 1993). Floodplains are distributed along rivers "like beads on a string" and they provide a dynamic ecotone where surface and ground water components of the river constantly interact through the exchange of water, materials, and biota (Stanford and Ward 1993, Stanford et al. 2005).

These floodplains are valuable as hot spots of biodiversity and productivity, yet they are also some of most threatened ecosystems in the world due to damming, channelization, development, and other anthropogenic influences (Tockner and Stanford 2002). In gravel-bedded rivers, the alluvial aquifers of these floodplains are in fact expansive hyporheic zones with extensive exchange with the floodplain surface (Stanford et al. 2005). In particular, the Nyack Floodplain in Northwestern Montana has served as a long term (40 year) study site for research on the shallow alluvial aquifer of a gravel-bedded floodplain. The Nyack is unique for

being so expansive, yet relatively pristine. The aquifer itself is unique for its diversity and abundance of invertebrates living in an extreme oligotrophic and carbon-limited system, and for its extensive interaction with the surface water environment (Boulton et al. 1998, Craft et al. 2002, Stanford et al. 2005). Here the fields of river ecology and groundwater ecology have been advanced with detailed studies on groundwater biota (macroinvertebrates, meiofauna, and microbiota), biogeochemistry, and flowpath dynamics.

The legacy of Nyack research facilitated me to build on a poorly understood but important aspect of river and groundwater ecology: carbon cycling within the aquifer. The biggest conundrum in Nyack research prior to my dissertation was: how do such high numbers of large-bodied hyporheic stoneflies survive in a system that is dark, cramped, and extremely limited by paucity of labile organic carbon? As described in more detail in my first chapter, the previous work on the Nyack demonstrated an imbalance in the aquifer carbon budget (Appling 2012), that could be explained by methanogenesis providing labile organic carbon fixation (Helton et al. 2015). I furthered this work by studying the ecological role of methane in the aquifer, especially in regards to how it supports top consumers, hyporheic stoneflies. I was also able to expand our understanding of these macroinvertebrates by studying how their life histories vary within the heterogenous environment of the aquifer.

My second chapter focused on the source of the methane, its carbon contribution to stonefly biomass, and the widespread occurrence of methane derived carbon in stonefly biomass in floodplains across Montana and Washington. Most of the methane in the aquifer was methanogenic, but the data indicated a potential thermogenic methane contribution, possibly from the Kishenehn shale formation underlying the aquifer (Constenius and Dyni 1983). On the

Nyack, overall biomass averaged 41.5 to 66.5 percent methane derived carbon, even including sites where methane concentrations were low to immeasurable. The three other floodplains examined averaged 8 - 41 % methane derived carbon in biomass. This was the first report of a freshwater ecosystem to contain consumers dependent on ancient methane derived carbon and showed that the Nyack aquifer was one of the most expansive ecosystems to contain a majority of site-wide biomass comprised of methane derived carbon. This paper developed the contemporary understanding of basal resources supporting riverine productivity. The paper is currently in review at *Nature Communications*.

The overarching objective of my third chapter was to understand how methane dynamics, specifically as related to various other biogeochemical and hydrologic conditions, influenced the ecology of top consumers in the aquifer. I found that dissolved methane concentration was the best predictor of dissolved organic carbon concentration in the aquifer, while methane concentration was best predicted by dissolved oxygen concentration. Stoneflies had distinct isotopic niches (trophic positions) as defined by $\delta^{13}C$ and $\delta^{15}N$ signatures. The differences in trophic positions between species likely resulted from varying abilities to access methane-derived carbon resources at oxic-hypoxic interfaces, as shown by respirometry experiments and analysis of 16S rRNA sequences in gut contents. While none of the biogeochemical variables studied were consistently significant in predicting trophic positions, dissolved methane concentrations alone explained 19% of the variation in stonefly species assemblages, while the combination of all biogeochemical variables considered explained 22%. We concluded that methanogenic methane was clearly important for production in this system, as shown by its correlation with DOC, varying levels of carbon contribution to individual stonefly species, and significance in structuring stonefly species assemblages. Furthermore, this work showed that

hyporheic stoneflies have unique adaptations to the heterogenous and carbon-limited environment. This chapter was prepared for submission to *Ecological Monographs*.

The fourth chapter elaborated a major gap in hyporheic stonefly ecology: how is growth and emergence synchronicity affected by aquifer temperature and dissolved oxygen conditions? Temperature is the most important variable in determining stream stonefly growth and emergence patterns because stoneflies require both accumulation of degree days and a threshold temperature in order to mature and emerge (Ward and Stanford 1982). Aquifer temperature patterns are different from those of stream environments in which stonefly ecology has previously been studied because in the aquifer, temperatures at longer flowpaths remain at approximately the mean annual air temperature of 6-7°C year-round. Five species of hyporheic stonefly are common in the Nyack aquifer: *Paraperla frontalis*, *Kathroperla perdita*, *Isocapnia crinita*, *Isocapnia grandis,* and *Isocapnia integra*. All species had desynchronized emergence, while *P. frontalis,* the most abundant species in our samples, additionally had desynchronized growth across the aquifer. *P. frontalis* growth was correlated with well, river, and air temperature patterns. Mean daily air temperature was the only significant predictor of *P. frontalis* emergence. We concluded that the constancy of temperature patterns in habitats within this expansive aquifer contributed to this desynchronization of both growth and emergence in hyporheic species, highlighting another stonefly behavioral adaptation to the aquifer environment.

The overall findings of my dissertation showed the importance of complex ecological interactions for maintaining consumer productivity in expansive floodplain aquifers, especially that of the Nyack. Biogeochemical heterogeneity within the aquifer was necessary for methane cycling and for the coexistence of various stonefly species. Methane cycling provided a carbon

source that both structured stonefly species assemblages and comprised up to a majority of biomass. The stonefly species in the aquifer were able to coexist because they had niche differences related to their use of methane resources: they displayed varying levels of reliance upon methane derived carbon, adaptations that facilitated their access to methane-derived carbon resources, and the ability to persist despite desynchronization in growth and emergence. In summary, my dissertation work suggested a need to reconsider the basal sources of productivity in the shallow aquifers of gravel bedded floodplains, some of the most biodiverse and valuable environments in the world.

Literature Cited

Appling, A. 2012. Connectivity drives function: carbon and nitrogen dynamics in a floodplain-aquifer ecosystem. Dissertation. Duke University, Durham, North Carolina, USA.

Boulton, A. J., S. Findlay, P. Marmonier, E. H. Stanley, and H. M. Valett. 1998. The functional significance of the hyporheic zone in streams and rivers. Annual Review of Ecology and Systematics 29:59–81.

Constenius, K. N., and J. R. Dyni. 1983. Lacustrine oil shales and stratigraphy of part of the Kishenehn Basin, Northwestern Montana. Colorado School of Mines.

Craft, J. A., J. A. Stanford, and M. Pusch. 2002. Microbial respiration within a floodplain aquifer of a large gravel-bed river. Freshwater Biology 47:251–261.

Helton, A. M., M. S. Wright, E. S. Bernhardt, G. C. Poole, R. M. Cory, and J. A. Stanford. 2015. Dissolved organic carbon lability increases with water residence time in the alluvial aquifer of a river floodplain ecosystem. Journal of Geophysical Research: Biogeosciences 120:693–706.

Junk, W. J., P. B. Bayley, and R. E. Sparks. 1989. The flood pulse concept in river-floodplain systems. Canadian special publication of fisheries and aquatic sciences 106:110–127.

Stanford, J. A., M. S. Lorang, and F. R. Hauer. 2005. The shifting habitat mosaic of river ecosystems. Verh. Internat. Verein. Limnol. 29:123–136.

Stanford, J. A., and J. V. Ward. 1993. An ecosystem perspective of alluvial rivers: connectivity and the hyporheic corridor. Journal of the North American Benthological Society:48–60.

Thorp, J. H., and M. D. Delong. 1994. The riverine productivity model: an heuristic view of carbon sources and organic processing in large river ecosystems. Oikos:305–308.

Thorp, J. H., and M. D. Delong. 2002. Dominance of autochthonous autotrophic carbon in food webs of heterotrophic rivers. Oikos 96:543–550.

Tockner, K., and J. A. Stanford. 2002. Riverine flood plains: present state and future trends. Environmental Conservation 29:308–330.

Vannote, R. L., G. W. Minshall, K. W. Cummins, J. R. Sedell, and C. E. Cushing. 1980. The River Continuum Concept. Canadian Journal of Fisheries and Aquatic Sciences 37:130–137.

Ward, J. V., and J. A. Stanford. 1982. Thermal responses in the evolutionary ecology of aquatic insects. Annual Review of Entomology 27:97–117.

In review at *Nature Communications*

Chapter 2: Ancient methane derived carbon subsidizes contemporary food web

Authors: Amanda G. DelVecchia[1], Jack A. Stanford[1], Xiaomei Xu[2]

Affiliations:

[1]Flathead Lake Biological Station, The University of Montana

[2]The University of California - Irvine

Summary

While most global productivity is driven by modern photosynthesis, river ecosystems are supplied by locally fixed and imported carbon that spans a range of ages. Alluvial aquifers of gravel-bedded river floodplains present a conundrum: despite no possibility for photosynthesis in groundwater and extreme paucity of labile organic carbon, they support diverse and abundant large-bodied consumers (stoneflies, Insecta: Plecoptera). Here we solve this long standing problem by showing that up to a majority of the biomass carbon composition of these top consumers in four floodplain aquifers of Montana and Washington is methane-derived. The methane carbon ranged in age from modern to up to >50,000 years old, mostly derived from biogenic sources although some thermogenic contribution cannot be excluded. This the first report of a freshwater ecosystem to contain consumers dependent on ancient methane derived

carbon, and one of the most expansive ecosystems to contain a majority of site-wide biomass comprised of methane derived carbon, transforming our contemporary understanding of basal resources supporting riverine productivity.

Introduction

Two landmark papers in *Science* and *Nature* in 1974 and 1988, respectively, revolutionized our view of river systems [1,2]. These works demonstrated that the shallow alluvial aquifers of river floodplains were abundantly populated by diverse large-bodied hyporheic stoneflies (Insecta:Plecoptera) that spent their nymphal stages entirely underground before emerging from the river channel as flying adults. The finding highlighted the broad extent of surface and groundwater interchange, and additionally underscored the importance of connectivity for maintaining biodiversity and productivity. In the decades that followed, our knowledge of the shallow aquifer has developed, but the question has persisted: how do these abundant large-bodied consumers survive in the highly oligotrophic, dark, and carbon-limited environment of the aquifer?

River floodplains worldwide are underlain by shallow alluvial aquifers where interstitial flow is driven by penetration of river water into the bed sediments. In gravel-bed systems these aquifers are extremely porous and generally well-oxygenated. The aquifers may contain diverse and abundant meiofauna as well as large-bodied stoneflies (Extended Data Fig. 1) [1–3]. The presence of these speciose communities is a conundrum because productivity is generally limited by labile organic carbon availability and microbial productivity is extremely low [3–5]. The Nyack Floodplain on the Middle Fork of the Flathead River in northwestern Montana (Fig.1), provides a well-documented example of an expansive alluvial aquifer that is ultra-oligotrophic, yet paradoxically supports a diverse and productive food web with large (up to 3 cm length) stonefly larvae as top consumers (Extended Data Fig. 1, Extended Data Fig. 2).

The Nyack aquifer is contained in gravel and cobble bed sediments that were deposited during the last glacial retreat approximately 7,000 to 10,000 years ago [6,7] and subsequently reworked by cut and fill alluviation associated with river flooding [6]. The 20 – 50+ m thick aquifer is occluded by Precambrian bedrock overlain by glacial outwash clays and a Tertiary shale (Kishenehn) formation that is carboniferous and thus a potential source of thermogenic carbon [8]. The aquifer is characterized by extreme hydraulic conductance up to 11.6 cm/sec [9] and is exclusively recharged by the river. It is therefore considered an voluminous "hyporheic" zone [6] where surface- and groundwater processes interchange. Water residence times vary from hours to three years in relation to lengths of flow paths from the river through the aquifer [9]. Overall, the aquifer is well oxygenated because oxygen diffuses from the vadose zone of the floodplain [10] and microbial productivity is ultra-limited by paucity of labile organic carbon (DOC <2 mg/L) [11]. Along short flow paths near the river (i.e., through gravel bars), respiration of allochthonous carbon results in a predictable drop in DO (dissolved oxygen) and DOC (dissolved organic carbon) [12]. However, along longer flow paths through the entire aquifer, an anomalous increase in organic carbon lability occurs, suggesting carbon fixation as might occur through chemoautrophy and/or methanotrophy [12]. The occurrence of chemoautotrophy and/or methanotrophy in the aquifer has also been proposed as a solution to imbalance in the Nyack aquifer carbon budget [13].

Thus, we investigated the source and role of methane as a subsidy to floodplain aquifer food webs, mainly at Nyack but also at three other locations: the Kalispell floodplain on the main stem of the Flathead River in Northwest Montana, the Jocko River floodplain in Southwest Montana, and the Methow River floodplain in Washington. At each of these sites a grid of slotted, but not screened, groundwater monitoring wells was available for sampling. Of this suite

of aquifers only the Nyack is underlain by a hydrocarbon-containing shale formation. We posited: 1) what is the source of the methane, 2) what are the contributions of various methane sources to stonefly biomass, and 3) is a methane subsidy in alluvial aquifers a widespread phenomenon? In order to identify methane sources, we measured the carbon and deuterium stable isotope ratios of dissolved methane, and the radiocarbon ages of dissolved methane along with methane, ethane, and propane concentrations. In order to understand the contributions of various methane carbon sources to biomass (question 2), we measured carbon stable isotope ratios and radiocarbon ages of stonefly biomass and organic matter, and then incorporated these values into Bayesian mixing models parameterized using a suite of scenarios to give a range of reasonable and conservative estimates of source contributions to biomass. Question 3 was addressed by comparing results among of study sites.

Methane sources

At Nyack, we collected samples from two depths, 1 and 4 m below the baseflow water table, at seven wells (Fig. 1) previously shown to contain the full suite of aquifer biota (Extended Data Fig. 1). One of the wells had a residence time of 45 days while all others ranged from 117 to 305 days (Extended Data Table 1) [9]. We sampled an additional depth near the bottom of one well (HA10; Fig 2), specifically to target potential shale off-gassing of methane, because this well had the highest concentration at the deepest depth sampled on each sampling date. Only three wells, HA10, HA12, and HA17, yielded methane concentrations higher than >1 μmol/L (Extended Data Fig. 3A). These three were the only wells with methane concentrations high enough to measure stable isotope values. Only HA10 and HA12 occasionally had high enough concentrations to measure radiocarbon. In these two wells, maximum concentration reached

10% saturation (Extended Data Fig. 3B). In wells HA10, HA12, and HA17, we compared methane stable isotope ratios to known characterizations of methane sources based on the ratios of deuterium and carbon stable isotope signatures (Fig. 2A) [14–18]. While methanogenic signatures typically are easy to identify as having light (low) carbon and hydrogen isotopic ratios, any deviation from these combinations leads to uncertainty as to whether the heaviness might be caused by variable sources, such as a thermogenic methane contribution, or by microbial oxidation of biogenic methane, which leaves the residual methane pool heavier in ^{13}C. Our measured methane stable isotopic ratios ($\delta^{13}C$ and $\delta^{2}H$) generally clustered at values suggesting a mix of acetoclastic (reduction of organic carbon) and hydrogenotrophic (reduction of carbon dioxide) methanogenesis (Fig. 2A). HA10 samples deviated from the clustering, suggesting either high levels of microbial oxidation or a thermogenic methane contribution, likely from outgassing of the underlying Kishenehn shale formation (Fig. 2A). We therefore also measured concentrations of higher chain hydrocarbons – ethane and propane – in these three wells (Fig. 2B). The high ratios of methane concentrations to concentrations of these higher chain hydrocarbons suggested that the aquifer did not contain a thermogenic methane subsidy [16,19,20]. However, none of the samples from which we were able to measure ethane and propane concentrations coincided with heavy carbon isotopic ratios. Therefore, the cause of the heavy isotopic ratios of methane was still unresolved and the possibility of a thermogenic methane subsidy remained valid.

Of the three wells with methane present, only HA10 and HA12 had high enough concentrations to determine radiocarbon ages. The methane in well HA10 was consistently older than that of HA12, and all methane samples that we aged corresponded with methanogenic ^{13}C signatures and a lack of measurable higher level hydrocarbons. Methane in HA12 ranged from

335 ± 15 years BP to 1970 ± 20 years BP, and methane in HA10 ranged from 2350 ± 15 years BP to 6910 ± 140 years BP (Extended Data Table 2). Because radiocarbon ages of dissolved methane samples are the average ages of all sources of methane present, the highly aged methane from HA10 could have included a substantial proportion of ancient methane that is radiocarbon dead; radiocarbon-dead methane could have come from off-gassed methane from the Tertiary age shale underlying the floodplain. For example, the most aged HA10 sample of 6900 years BP (11/24/2014, Extended Data Table 2) could have included up to 58% radiocarbon-dead methane with 42% modern methane: if we assumed that thermogenic methane had a $\delta^{13}C$ value of -50 ‰ [14,15] and that microbial methane had a $\delta^{13}C$ value of -100 ‰ (see methods), then the same sample which had a measured $\delta^{13}C$ value of -70.6‰ could have included a maximum of 59% thermogenic methane. The closeness of these estimates suggested that this sample in particular could have had a substantial thermogenic contribution, though we did not have measured ethane and propane concentrations from the same day to verify or refute this possibility. We concluded that measurable dissolved methane in the aquifer was mainly produced via microbial methanogenesis of modern and ancient organic matter, but a subsidy from thermogenic methane was likely, at least in the HA10 well.

Methane derived carbon in stonefly biomass

Four species of amphibitic stoneflies were very abundant in our samples: *Paraperla frontalis, Isocapnia grandis, Isocapnia crinita,* and *Kathroperla perdita* [3]. *P. frontalis* was the most common and widespread. Both *P. frontalis* and *K. perdita* have mouth parts typically associated with carnivory, but the *Isocapnia* spp have mouthparts characteristic of grazers (Extended Data Fig. 1). Stonefly samples from each species had a wide range of variation in $\delta^{13}C$ (Table 1). This indicated that the stoneflies were consuming methane derivedcarbon, rather than

deriving low $\delta^{13}C$ values from a symbiosis with methanogenic microbes [21]. Our $\delta^{13}C$ values were also significantly different between species and between dates of collection (ANOVA analysis $Pr|>F| p < 0.05$). However, both of these variables interacted with the well of collection for each sample because stonefly species each had unique habitat preferences. We therefore pooled both species and dates of collection by well for all subsequent analyses.

We used standard linear two-source mixing models to determine the methane contribution to stonefly biomass in the aquifers [22].We accounted for methane carbon isotope fractionation by MOB by implementing the most conservative possible estimate of the MOB $\delta^{13}C$ signature as our lower boundary, and the average of our methane $\delta^{13}C$ signatures as an upper boundary, terming these our "conservative" and "average" estimates of methane dependence, respectively (see Methods). We found that stonefly biomass from all wells, including those with no measurable methane, had high methane derived carbon contributions (Extended Data Fig. 5). Using a stratified average of both the conservative and average estimates of methane dependence at each well on the floodplain, we determined that 40.4 to 70.8% of stonefly biomass was comprised of methane derived carbonat Nyack. Our results therefore showed that the biomass of top consumers at Nyack was substantially dependent on methane derived carbon.

Biomass subsidized by ancient carbon

Wells HA10 and HA12 were the only wells from which we were able to date the dissolved methane because methane concentrations were low to undetectable in the other wells. Thus only in these two wells were we able to compare methane and stonefly biomass ages. To measure a biomass age most representative of river-supplied carbon, we additionally dated stonefly biomass from the well with the shortest flow path and the lowest overall stonefly

methane dependence: well HA02 (Extended Data Table 1, Extended Data Fig. 5). Biomass radiocarbon ages of individual stoneflies from these three wells were strongly correlated with calculated levels of methane derived carbon contribution (log (Age + 1000) regressed against the average estimate of methane dependence per individual; $R^2 = 0.56$, $p = 2.328 \cdot 10^{-10}$, n=52) (Fig. 3). This indicated that: a) a broad range of methane ages was present in the aquifer, b) the non-methane derived carbon was modern, and c) stoneflies assimilated methane carbon at least 6,900 years BP old.

We used the measured radiocarbon and $\delta^{13}C$ values of stonefly biomass, methane, and organic matter to parameterize a Bayesian mixing model [23] to estimate the contribution of aged or ancient methane to stonefly biomass in all wells. We estimated the distribution of radiocarbon values for organic matter (or all non-methane carbon sources) by weighting stonefly biomass ages by the percent non-methane contributions calculated from a two-source mixing model of ^{13}C signatures. We then created four scenarios considering two possibilities that represented opposite ends of ranges for each methane $\delta^{13}C$ values and the oldest possible methanogenic methane contribution (Extended Data Table 4). Regardless of scenario, the $\delta^{13}C$ values and radiocarbon ages of the stoneflies were significantly different among the three wells (Fig 4), suggesting that stoneflies were in fact dependent on local food resources that varied spatially. Where river-supplied carbon was in lower availability (i.e. in wells HA10 and HA12 with longer flow paths, Extended Data Table 1) stoneflies were dependent on methane. Only individuals collected from HA10 relied on aged to fossil methane, supporting the possibility that an ancient shale methane subsidy might indeed exist at this location. In any case, it was clear that the top consumers in the food webs of the Nyack aquifer were dependent on a methane subsidy from ancient carbon.

Methane dependency is widespread

We collected dissolved methane concentrations and stonefly samples from wells across the three other river floodplains to understand if a methane subsidy to the groundwater food web was a widespread phenomenon. We used the same standard two-source mixing model on $\delta^{13}C$ values used on Nyack to estimate ranges of proportions of stonefly biomass that were methane-derived carbon at all floodplains. We parameterized the model using the source estimates for organic matter and methane calculated at Nyack. We found higher estimates of methane dependence at Nyack than at any other floodplain, but overall methane contributions were high across the other floodplains as well, ranging from 8.5 to 36.5 % (Fig. 5, Table 1). This was surprising given that, of fifteen wells analyzed across all other floodplains, only three (two at Methow, one on the Jocko) had measurable dissolved methane (Extended Data Fig. 6). This was similar to the case we found at Nyack, where methane dependence existed at all wells regardless of methane concentrations.

Discussion

The data showed that the Nyack food web was heavily subsidized by methane carbon with various ages (from modern to millennial aged or fossil), most of which was methanogenically produced. Although we could not verify a thermogenic methane contribution through presence of ethane and propane concentrations, the documented existence of carboniferous shale at Nyack [8], presence of highly aged carbon, and presence of heavy methane $\delta^{13}C$ added credence to the possibility of a thermogenic contribution to the aquifer food web. Because methanogenesis occurs mainly in anoxic environments and MOB flourish in opposing

gradients of methane and oxygen [24], it is likely that stoneflies were directly or indirectly consuming resources produced at these interfaces (i.e. either grazing or consuming via an intermediate trophic link). In fact, the heaviness of biofilm and organic matter $\delta^{13}C$ signatures relative to stonefly biomass signatures suggested that stoneflies preferentially consume methane derived carbon. This could explain their survival in such a carbon-limited system. Furthermore, because stoneflies emerge from the river as flying or crawling adults, they are exporters of labile organic carbon from the aquifer to the floodplain surface as well as top consumers in a food web that assimilates a greenhouse gas and potential water contaminant.

This is the first report of methane dependence in top consumer species across multiple river ecosystems, and the first report of an ancient methane subsidy to a freshwater food web. While methane cycling and aged carbon have each been studied in rivers [25–28], the few published studies that document a river food web methane subsidy are site-specific) . For example, Caraco et al. documented an ancient carbon subsidy to zooplankton in the Hudson River Estuary[28], Kohzu et al. showed that some macroinvertebrate production was fueled by biogenic methane produced from detritus in backwater pools[29], and Trimmer et al. showed that caddis fly species derived up to 30% of their biomass from methanogenic methane in the River Lambourn[30]. Each of these studies was site-specific and none of these studies found that ancient carbon was integrated in a methane-based food source. Additionally, much work in lake ecosystems has documented methane subsidies in midge (Insecta: Chironomidae) species, but still information is lacking on the frequency and circumstances of methane carbon contributions to aquatic food webs[31]. Additionally, these aquifers with methane derived carbon subsidies are dark environments with no potential for photosynthesis, so the depletion measured in the stoneflies

could not have occurred from a basal resource of depleted CO_2 being converted by photosynthesis as has been suggested previously[32].

All of the floodplains which we studied had substantial site-wide methane subsidies to top consumers, and Nyack additionally had a millennial-aged to fossil methane subsidy. There are multiple possibilities for the origin of the millennial-aged to ancient methane: if methanogenic, it could have been produced from buried organic matter such as that which would have been deposited during the last glaciation[e.g. 33]; it also could have come from thermogenic methane outgassing.

The stoneflies with such high proportions of methane derived carbon in biomass as described herein exemplify the need for unperturbed spatial and biogeochemical complexity in floodplains, not just for sustaining biodiversity and productivity, but also for the natural filtration processes provided by surface and groundwater exchanges in the alluvial aquifers. River floodplains are among the most threatened ecosystems in the world [34] and the surprising details of groundwater ecology described herein provide a broader basis for river protection and conservation.

Methods

Sample Collection and Processing

The Nyack floodplain was equipped with seven 3-inch PVC wells with 2 mm slot openings down the length of the pipe. The wells were drilled 8-10 m using a hollow auger drilling rig See Extended Data Table 1–for aquifer characteristics measured at each well. Wells HA02, HA07, HA08, HA10, HA12, and HA15 (Fig 1) were equipped with sensors and data loggers that recorded dissolved oxygen, temperature, depth and specific conductance on an hourly basis. We used a peristaltic pump equipped with PTFE (Teflon) tubing to draw water

from two to three depths at each well - 1 and 4 m below the baseflow water table at all wells, with an additional depth of 0.5 m above bedrock (well base) at well HA10. The Kalispell floodplain had seven existing wells drilled similarly (slotted but not screened, and drilled to maximum possible depth). The Jocko had three wells, and the Methow four. We sampled these wells also at 1 and 4 m below the base flow water table.

We sampled methane concentrations approximately every three weeks at all wells on Nyack and in Kalispell for two years, from August 2013 to August 2015. We sampled four times during 2014-2015, once in July 2014 and four times from March to September 2015 on the Jocko and on the Methow. We used a modified active-sampling method: we pumped sample water into a BOD bottle, allowing it to overflow for one to two minutes before withdrawing 1-7 mL using a 22-gauge needle attached to a two-way stopper and 10 mL syringe. In the lab, we had capped 9.83 mL glass scintillation vials with PTFE-lined grey butyl stoppers and crimp seals, then flushed them three times with ultra-high-purity N_2. We simultaneously injected field samples to the sample vials while allowing excess N_2 to drain into a second syringe. We poisoned the samples to 0.5% $ZnCl_2$ and stored them upside down at 4° C until analysis within one week of collection. We analyzed samples on a greenhouse gas chromatograph (SRI Instruments model 8610C) equipped with a flame ionization detector and SRI PeakSimple Software. We calculated headspace methane concentrations using a three-point calibration with Scotty gas standards (Air Liquide America). We then used Henry's Law to calculate dissolved methane before headspace equilibration using the solubility constant documented by Yamamoto et al. (1976) [28]. Error averaged 0.08 µmol/L initial aqueous concentration and our detection limit was 0.11 µmol/L.

We collected samples for measurement of ethane and propane concentrations beginning

in Spring 2015 using similar methods as for methane collection. The discrepancy in timing arose because only by Spring 2015 did our stable isotope results reflect a potential thermogenic contribution. We used similar methods as for collection of samples for measurement of dissolved methane concentrations, but instead injected 30-mL samples to 38.25 mL glass serum vials capped with thick black butyl stoppers. We did this to minimize our detection limit of ethane and propane by maximizing the equilibrium headspace concentrations of ethane and propane, which we expected to be present at low concentrations if at all. We used Henry's Law and solubility constants documented by Hine and Mookerjee (1975)[35] to calculate the dissolved concentrations of ethane and propane in waters.

We collected samples for analysis of dissolved methane stable isotope composition from wells HA10, HA12, and HA17 using acid-washed Teflon tubing and the same active sampling methodology used for collecting concentration measurements. However, we instead injected samples into evacuated Exetainers® vials (Labco Limited), then similarly poisoned them to 0.5% $ZnCl_2$. We sent samples to the University of California at Davis Stable Isotope Facility for ^{2}H and ^{13}C analyses, where they were analyzed on a Thermo Scientific Delta V Plus isotope ratio mass spectrometer (IRMS, Thermo Scientific, Bremen, DE) according to the methods of Yarnes et al. (2013) [36]. Long-term standard error was 0.2 ‰ for $\delta^{13}C$ and 2 ‰ for $\delta^{2}H$.

When methane concentrations were at a minimum of 10 µmol/L, we were able to collect samples for radiocarbon analysis of dissolved methane. We pumped water into an acid-washed and baked 1 L glass microculture bottle, keeping the hose at the bottom of the bottle and timing until it filled. We then inverted the bottle underwater and allowed water to flush through for the duration of time it took for the bottle to fill; this also allowed for the capture of any outgassed components. We capped the bottle in this state with blue butyl and crimp seals, poisoned the

sample with 10 mL 50% $ZnCl_2$, and transported it back to FLBS on ice, where we injected a 4 mL UHP N_2 headspace and shipped samples to UC-Irvine's Keck Carbon Cycle AMS facility.

Upon arriving at the UC-I Keck lab, ~15% headspace was created in the sample bottle by injecting ultra zero air with a syringe and removing the displaced volume of water in the same time. Samples were shaken for 1 minute and allowed to settle for 30 minutes before extraction. An evacuated 2 L stainless steel canister attached to a needle was used to extract headspace gases from the water bottle. The canister was then filled to 1 atm pressure with ultra zero air, which served as a carrier gas in the latter extraction. On a flow-through vacuum line, the headspace CH_4 and CO_2 were separated, combusted and purified [37], and graphitized by the sealed tube Zn reduction method [38] then measured for radiocarbon (^{14}C) on a compact accelerator mass spectrometer (AMS, National Electrostatics Corp.) [39]. For dry stoneflies, the samples were weighed into prebaked quartz tubes with prebaked CuO, evacuated, sealed then combusted at 900°C for 2 hours. After combustion, sealed tubes were cracked and CO_2 was extracted on a vacuum line, graphitized and measured for ^{14}C using the same method mentioned above. Data presented here are expressed as radiocarbon age (year, BP) and $\Delta^{14}C$ (‰) as well. Both were normalized to radiocarbon activity of an oxalic acid standard OX1 and isotopic fractionation corrected to -25‰ [40]. For $\Delta^{14}C$, standard OX1 was also decay corrected to 1950. $\Delta^{14}C$ (‰) =/> 0 can be used to indicate 'modern' carbon (1950 to present), and $\Delta^{14}C$ (‰) < 0 for "aged" carbon (pre-1950), and $\Delta^{14}C$ (‰) = -1000‰ for "fossil" or ^{14}C dead carbon. The $\Delta^{14}C$ analytical error was ~ 2‰ for modern sample, based on long-term measurements of secondary standards. $\delta^{13}C$ analysis was made on CO_2 subsampled from the vacuum line and measured by using a Gas Bench II coupled with a Thermo Scientific Delta Plus XL IRMS. The $\delta^{13}C$ analytical error was ± 0.15‰ based on long-term measurements of secondary standards.

On the same days when we collected methane samples, we collected as many stonefly nymphs as possible via trapping methods. To trap, we suspended nylon ropes in the wells on which the emergent and resident stoneflies could climb. We checked the ropes every two weeks and collected larvae if present. Every six weeks, we additionally pumped the wells using a gas-operated diaphragm pump. Samples were kept at a minimum of three meters from the pump while the pump was running to avoid potential contamination. All output water was transferred through 2.5" Tigerflex tubing and emptied into a 330 micron Nitex mesh net. We elutriated the retained samples, collecting stoneflies caught in the net and transferring them to distilled water (DI). We kept the stoneflies at 4°C for a minimum of 24 hours to clear gut contents, then identified them to species level [41,42], rinsed them in DI water, and transferred them into individual sterile cryovials. We froze samples and stored them at -80° C until preparation for stable isotope analysis. We took the same collection approach for collecting organic matter and biofilm samples for stable isotope analysis, but samples were collected in June to July 2013. We used 64 and 500 µm Nitex mesh to parse out fine and coarse organic matter, respectively. These samples were also frozen until preparation for stable isotope analysis.

We collected biofilm samples by suspending ashed and autoclaved gravel bags at all sampling depths for ten weeks during July and August 2013. We collected samplers into sterile Whirl-paks and froze them. To remove biofilm and strongly associated particulate matter for stable isotope analysis, we defrosted and filled Whirl-paks with 200 mL ultra-pure distilled water, then sonicated for 40 minutes. We poured the solution into sterile glass beakers, rinsed the remaining gravel into the beakers, and dried the beakers at 60˚C until water evaporated (usually 3-4 days). We then scraped the samples into silver capsules and acidified them using them [43].

To prepare stoneflies and organic matter for stable isotope analysis, we defrosted them at room temperature, rinsed the stoneflies a second time in DI, and then transferred them directly to aluminum foil to dry at 60°C for at least 48 hours. We then milled them into a fine homogenous powder using steel milling capsules and a grinding mill for 20 seconds each. We subsampled 0.8 to 1.2 mg of each stonefly into tin capsules and replicated approximately once per 15 samples (replicate coefficient of variation = 0.2%). Samples were analyzed on a PDZ Europa ANCA-GSL elemental analyzer interfaced to a PDZ Europa 20-20 isotope ratio mass spectrometer (Sercon Ltd., Cheshire, UK) at the UC Davis Stable Isotope Laboratory. Stable isotope ratios were expressed relative to international standards: V-PDB (Vienna PeeDee Belemnite) for ^{13}C and air for ^{15}N.

Methane source determination

In order to calculate potential methane source contributions, we considered three sources: modern methanogenic methane, ancient methanogenic methane, and thermogenic methane (shale). Both classifications of methanogenic methane are biologically produced anaerobically through either acetoclastic methanogenesis or hydrogenotrophic methanogenesis. In the former scenario, methanogenic archaea require an organic carbon source. The second scenario is an autotrophic process in which methanogenic archaea produce methane from carbon dioxide and hydrogen. In both forms of methanogenesis, the methane produced is drastically depleted in ^{13}C (-50 to -80 ‰) due to methanogens preferentially assimilatinglighter carbon isotope in their metabolism (^{12}C) [15]. Methane in freshwater systems can also be released from thermogenic sources such as shale or coal, though this has not previously been documented as an ecological subsidy. In this case, hydrocarbons are produced as a result of abiotic pressure and temperature

conditions. Thermogenic methane carbon and hydrogen are both isotopically heavier than the methanogenic methane, and usually accompanied by higher level hydrocarbons such as ethane and propane [14,16]. It is also radiocarbon-dead, or greater than 50,000 years in age. Ancient organic matter can also be methanogenically decomposed to produce highly aged methane. All methane can then be consumed by methane oxidizing bacteria (MOB), which fractionate the dissolved methane by preferentially assimilating the lighter carbon isotope, leaving the residual methane enriched in the heavier isotope. In the exponential phase of MOB growth, fractionation in MOB biomass is 30.3 ‰ [20]. During normal growth phases, fractionation is 16 ‰ [17,20]. A graphical summary of source determination using carbon and hydrogen isotopes is overlaid on Figure S3A. We used isotopic signatures in combination with radiocarbon dating, and measurement of ethane and propane concentrations to determine the methane sources. These results are displayed in Figure S3.

Our results suggested that the majority of dissolved methane was derived from a mixture of acetoclastic and hydrogenotrophic methanogenesis. The samples that deviated from this general classification were both taken from well HA10 deep. Methane oxidation involves wide variation in deuterium fractionation depending on temperature and all thermogenic methane tends to have heavier deuterium isotopes [16–18]. Therefore, these samples could have resulted from high levels of oxidation or a contribution from a thermogenic methane source. This range of possibilities was reinforced by radiocarbon dating, which showed that dissolved methane collected from HA10 was consistently older than dissolved methane from HA12.

We therefore began to collect samples for the measurement of ethane and propane concentrations in May 2015. These samples corresponded with stable isotope signatures and insect and radiocarbon ages. None of the samples from which we measured ethane and propane

concentrations were found to be isotopically heavy but insects were consistently aged up to 6900 years BP. However, none of the samples we measured had ethane or propane concentrations high enough to suggest a thermogenic methane contribution. In general, if the ratio of methane concentration to the summed concentrations of ethane and propane is <100, then the source is thermogenic. If it is >1000, then the source is methanogenic [44]. Anything in between is considered a mix. No samples had ratios significantly lower than 1000 (Figure S3B). We therefore concluded that the samples which we measured had no thermogenic methane contribution, though we HA10 deep might still have a thermogenic methane contribution that is so minimal and unpredictable that we very occasionally have the opportunity to measure it.

Causes of stonefly biomass $\delta^{13}C$ depletion

We also measured the age of dissolved CO_2, which ranged from 1310 ± 15 to 1970 ± 20 years BP, suggesting that older methane carbon contributions were from organic matter rather than DIC which would be similar to the dissolved CO_2 (Extended Data Table 2). The $\delta^{13}C$ values ranged from -19.2 to -14.8‰ (n=6), which further indicates this carbon pool is not likely the main contributor for the stonefly biomass. Although the carbon isotope fractionation indicated by the low $\delta^{13}C$ values in these estimates (Table 1) can occur via other pathways such as ammonium oxidation and sulfur oxidation, the resulting $\delta^{13}C$ values would be far heavier than those we observed. Ammonium oxidation produces bulk biomass depleted in $\delta^{13}C$ by 20‰ relative to CO_2, which we measured as -16.6 ± 0.7 ‰ [45], and sulfur oxidation produces bulk biomass depleted in $\delta^{13}C$ by 24.6 to 25.1 ‰ relative to CO_2 [46].

Methane contribution to stonefly biomass: $\delta^{13}C$ models

Regardless of methane source, it was necessary to account for the variation in isotopic signatures of methane across the floodplain as we proceeded to calculate methane derived carbon contributions to stonefly biomass. We assumed that stoneflies consumed MOB as is suggested by the large variation in stonefly biomass $\delta^{13}C$ values even within species (Table 1).

We used a two-source mixing model [22] on stonefly biomass signatures to calculate relative contributions of MOB and organic matter using $\delta^{13}C$ values (Eq. 1):

$$\%\ methane\text{-}derived\text{-}carbon\ in\ biomass = \frac{Stonefly\partial^{13}C - OM\partial^{13}C}{Methane\partial^{13}C - OM\partial^{13}C} \bullet 100$$

To represent any possible contribution of organic matter to stonefly diet, we used 'organic matter' as a surrogate for any component of the stonefly biomass that was not methane-derived carbon. Means and standard errors of $\delta^{13}C$ values for each organic matter classification are displayed in Extended Data Table 3. Coarse particulate organic matter (CPOM) showed depletion relative to other organic matter pools because stonefly detritus was inevitably and visibly incorporated into the CPOM pools we collected via pumping. We used a stratified average of all OM pools, -27.83 ± 2.49 ‰ which is very close to the literature estimate of photosynthetically fixed terrestrial carbon: -28 ‰[22].

To estimate the $\delta^{13}C$ value of MOB, we bracketed estimates using our measured values of methane itself and maximum levels of fractionation by exponential growth of MOB (α = 30.3 ‰)[20]. We preferred to use a Keeling plot [47] to estimate methane signatures at the time of production, but our data showed extensive variation in isotopic signatures even in samples collected at times with high methane concentrations, making such an estimation technique unfeasible (Extended Data Fig. 4). We therefore averaged all samples (n=32) collected at times

when methane concentration was >1 µmol, yielding -68.79 ± 8.52 ‰. This was termed our "Average" estimate of source methane $\delta^{13}C$ and therefore a suitable estimate for the heaviest possible isotopic ratio representative of MOB biomass. We then applied the fractionation factor to this estimate, yielding a most conservative estimate (lightest possible isotopic ratio) of -100.86 ‰ using the equation (Eq. 2) [17]:

$$\alpha_{\mathrm{Pr}oduct}^{Source} = \frac{1000 + \partial^{13}Source}{1000 + \partial^{13}\mathrm{Pr}oduct}$$

We termed values of methane dependence using this estimate as our "Conservative" estimate. We presented both sets of data in the results.

We found a significant effect of species and date of collection on methane dependence using simple linear regression models and ANOVA analysis (main text). However, both of these variables were strongly confounded with well of collection, as stonefly life history and well conditions inevitably determined the environment which they inhabited at the time of sample collection and thereby influenced the quantities of each measured. In regards to date, we collected from time points over four seasons and during 1-2 years at all sites to avoid bias from sampling time. In order to compare overall levels of methane dependence across and within floodplains, therefore, we only considered wells as strata and pooled species at all times of collection. Please see raw data files for dates of sample collection at each well.

Methane contribution to stonefly biomass: $\delta^{13}C$ and $\Delta^{14}C$ models

We submitted 52 stoneflies from wells HA02, HA10, and HA12 for combined stable isotope analysis and radiocarbon dating at the WM Keck facility at UC Irvine (see methods above). We then were able to use both $\delta^{13}C$ and $\Delta^{14}C$ values for implementing a Bayesian framework stable isotope mixing model to infer contributions of various potential methane pools to stonefly biomass. This model considered aged methane, ancient methane, modern methane, and modern organic matter as potential sources, using scenarios of both average and conservative MOB $\delta^{13}C$ values.

We inferred the source values for organic matter by taking a weighted average of $\Delta^{14}C$ values across the 53 stoneflies. Our weights (OM dependence) were calculated as 1- (methane dependence obtained via Eq. 1). Because we could calculate methane dependence using either the Average (Avg) or Conservative (Cons) approaches, we had two estimates for OM $\Delta^{14}C$: Avg: -13.7 ± 32.2 ‰ and Cons: -65.6 ± 75.9 ‰. We used these in the Avg and Cons scenario types (Extended Data Table 4).

For each of the Avg and Cons scenarios, we also had two estimates for maximum methane age measured using $\Delta^{14}C$. The radiocarbon ages that we measured in methane, ranging from 335 to 6900 years BP, were by definition an average of the various carbon ages present in that methane sample. Each sample was therefore a mixture of methane source ages. We therefore created one methane source to represent modern methane, taken as the Avg radiocarbon age of OM, and a second methane source as either aged or ancient methane. Aged methane was given the $\Delta^{14}C$ value of the oldest measured methane (-580 ± 7.2 ‰) and ancient methane was considered to be radiocarbon dead, or >50,000 years in age (-1000 ‰). This contributed another dimension to the scenarios needed: Aged and Anc (ancient) methane. Again, the pathway for incorporation of either methane type to stonefly biomass would be via MOB and

we therefore needed to consider the possibilities of minimum and maximum fractionation (Avg and Cons). The four scenarios and their associated source values and standard deviations are displayed in Extended Data Table 4.

We implemented the mixing model in the R platform [48] using the SIAR package [23]. The SIAR package allows for the input of source mean stable isotope signatures and their standard deviations. It also requires the input of trophic enrichment factors and their standard deviation, which we took as widely used literature averages [22]. Individual stoneflies were grouped by well. The SIAR package uses a Monte Carlo Markov Chain simulation to calculate a distribution of possible contributions of each source to each group. We ran the model for 10,000 iterations with a burn-in of 1000 runs for each scenario. We then compiled the run results and calculate mean and standard deviations of each source contribution to biomass in each well analyzed (HA10, HA12, and HA02). Results for the four scenarios are all displayed in Figure 4 (main paper).

References

1. Stanford, J. A. & Gaufin, A. R. Hyporheic communities of two Montana Rivers. *Science* 185, 700–702 (1974).
2. Stanford, J. & Ward, J. The Hyporheic Habitat of River Ecosystems. *Nature* 335, 64–66 (1988).
3. Gibert, J., Danielopol, D. L. & Stanford, J. A. *Groundwater Ecology*. (Academic Press, Inc., 1994).
4. Craft, J. A., Stanford, J. A. & Pusch, M. Microbial respiration within a floodplain aquifer of a large gravel-bed river. *Freshw. Biol.* 47, 251–261 (2002).
5. Ellis, B. K., Stanford, J. A. & Ward, J. V. Microbial assemblages and production in alluvial aquifers of the Flathead River, Montana, USA. *J. North Am. Benthol. Soc.* 382–402 (1998).
6. Stanford, J. A., Lorang, M. S. & Hauer, F. R. The shifting habitat mosaic of river ecosystems. *Verh Intern. Ver. Limnol* 29, 123–136 (2005).
7. Carrara, P. E. *Late Quaternary glacial and vegetative history of the Glacier National Park region, Montana*. (USGPO; For sale by the Books and Open-File Reports Section, US Geological Survey, 1989).
8. Constenius, K. N. & Dyni, J. R. *Lacustrine oil shales and stratigraphy of part of the Kishenehn Basin, Northwestern Montana*. (Colorado School of Mines, 1983).
9. Helton, A. M., Poole, G. C., Payn, R. A., Izurieta, C. & Stanford, J. A. Relative influences of the river channel, floodplain surface, and alluvial aquifer on simulated hydrologic residence time in a montane river floodplain. *Geomorphology* (2012).
10. Smith, M. G., Parker, S. R., Gammons, C. H., Poulson, S. R. & Hauer, F. R. Tracing dissolved O 2 and dissolved inorganic carbon stable isotope dynamics in the Nyack aquifer:

Middle Fork Flathead River, Montana, USA. *Geochim. Cosmochim. Acta* 75, 5971–5986 (2011).

11. Craft, J. A., Stanford, J. A. & Pusch, M. Microbial respiration within a floodplain aquifer of a large gravel-bed river. *Freshw. Biol.* 47, 251–261 (2002).
12. Helton, A. M. *et al.* Dissolved organic carbon lability increases with water residence time in the alluvial aquifer of a river floodplain ecosystem. *J. Geophys. Res. Biogeosciences* 120, 693–706 (2015).
13. Appling, A. *Connectivity drives function: carbon and nitrogen dynamics in a floodplain-aquifer ecosystem. Dissertation*. (Duke University, 2012).
14. Schoell, M. Multiple origins of methane in the Earth. *Chem. Geol.* 71, 1–10 (1988).
15. Whiticar, M. J. Carbon and hydrogen isotope systematics of bacterial formation and oxidation of methane. *Chem. Geol.* 161, 291–314 (1999).
16. Osborn, S. G., Vengosh, A., Warner, N. R. & Jackson, R. B. Methane contamination of drinking water accompanying gas-well drilling and hydraulic fracturing. *Proc. Natl. Acad. Sci.* 108, 8172–8176 (2011).
17. Hayes, J. M. Factors controlling 13 C contents of sedimentary organic compounds: principles and evidence. *Mar. Geol.* 113, 111–125 (1993).
18. Coleman, D. D., Risatti, J. B. & Schoell, M. Fractionation of carbon and hydrogen isotopes by methane-oxidizing bacteria. *Geochim. Cosmochim. Acta* 45, 1033–1037 (1981).
19. Bernard, B. B., Brooks, J. M. & Sackett, W. M. Light hydrocarbons in recent Texas continental shelf and slope sediments. *J. Geophys. Res. Oceans 1978–2012* 83, 4053–4061 (1978).

20. Summons, R. E., Jahnke, L. L. & Roksandic, Z. Carbon isotopic fractionation in lipids from methanotrophic bacteria: relevance for interpretation of the geochemical record of biomarkers. *Geochim. Cosmochim. Acta* 58, 2853–2863 (1994).
21. Kiyashko, S. I., Narita, T. & Wada, E. Contribution of methanotrophs to freshwater macroinvertebrates: evidence from stable isotope ratios. *Aquat. Microb. Ecol.* 24, 203–207 (2001).
22. Fry, B. *Stable Isotope Ecology*. (Springer New York, 2006).
23. Parnell, A. C., Inger, R., Bearhop, S. & Jackson, A. L. Source partitioning using stable isotopes: coping with too much variation. *PloS One* 5, e9672 (2010).
24. Bussmann, I., Rahalkar, M. & Schink, B. Cultivation of methanotrophic bacteria in opposing gradients of methane and oxygen. *Fems Microbiol. Ecol.* 56, 331–344 (2006).
25. Trimmer, M., Maanoja, S., Hildrew, A. G., Pretty, J. L. & Grey, J. Potential carbon fixation via methane oxidation in well-oxygenated riverbed gravels. *Limnol. Oceanogr.* 55, 560–568 (2010).
26. Shelley, F., Grey, J. & Trimmer, M. Widespread methanotrophic primary production in lowland chalk rivers. *Proc. R. Soc. Lond. B Biol. Sci.* 281, 20132854 (2014).
27. Buriankova, I. *et al.* Methanogens and methanotrophs distribution in the hyporheic sediments of a small lowland stream. *Fundam. Appl. Limnol.* 181, 87–102 (2012).
28. Caraco, N., Bauer, J. E., Cole, J. J., Petsch, S. & Raymond, P. Millennial-aged organic carbon subsidies to a modern river food web. *Ecology* 91, 2385–2393 (2010).
29. Kohzu, A. *et al.* Stream food web fueled by methane-derived carbon. *Aquat. Microb. Ecol.* 36, 189–194 (2004).

30. Trimmer, M., Hildrew, A. G., Jackson, M. C., Pretty, J. L. & Grey, J. Evidence for the role of methane-derived carbon in a free-flowing, lowland river food web. *Limnol. Oceanogr.* 54, 1541–1547 (2009).
31. Jones, R. I. & Grey, J. Biogenic methane in freshwater food webs. *Freshw. Biol.* 56, 213–229 (2011).
32. van Duinen, G. A. *et al.* Methane as a carbon source for the food web in raised bog pools. *Freshw. Sci.* 32, 1260–1272 (2013).
33. Hood, E. *et al.* Glaciers as a source of ancient and labile organic matter to the marine environment. *Nature* 462, 1044–1047 (2009).
34. Tockner, K. & Stanford, J. A. Riverine flood plains: present state and future trends. *Environ. Conserv.* 29, 308–330 (2002).
35. Hine, J. & Mookerjee, P. K. Structural effects on rates and equilibriums. XIX. Intrinsic hydrophilic character of organic compounds. Correlations in terms of structural contributions. *J. Org. Chem.* 40, 292–298 (1975).
36. Yarnes, C. δ13C and δ2H measurement of methane from ecological and geological sources by gas chromatography/combustion/pyrolysis isotope-ratio mass spectrometry. *Rapid Commun. Mass Spectrom.* 27, 1036–1044 (2013).
37. Pack, M. A., Xu, X., Lupascu, M., Kessler, J. D. & Czimczik, C. I. A rapid method for preparing low volume CH 4 and CO 2 gas samples for 14 C AMS analysis. *Org. Geochem.* 78, 89–98 (2015).
38. Xu, X. *et al.* Modifying a sealed tube zinc reduction method for preparation of AMS graphite targets: reducing background and attaining high precision. *Nucl. Instrum. Methods Phys. Res. Sect. B Beam Interact. Mater. At.* 259, 320–329 (2007).

39. Southon, J. & Santos, G. M. Life with MC-SNICS. Part II: Further ion source development at the Keck carbon cycle AMS facility. *Nucl. Instrum. Methods Phys. Res. Sect. B Beam Interact. Mater. At.* 259, 88–93 (2007).
40. Stuiver, M. & Polach, H. A. Discussion; reporting of C-14 data. *Radiocarbon* 19, 355–363 (1977).
41. Stewart, K. W. & Stark, B. P. *Nymphs of North American stonefly genera (plecoptera)*. (Entomological Society of America, 1988).
42. Baumann, R. W., Gaufin, A. R. & Surdick, R. F. The stoneflies (Plecoptera) of the Rocky Mountains [USA]. *Mem. Am. Entomol. Soc.* (1977).
43. Hedges, J. I. & Stern, J. H. Carbon and nitrogen determinations of carbonate-containing solids [In sediments, sediment trap materials and plankton]. *Limnol. Oceanogr.* 29, (1984).
44. Schoell, M. The hydrogen and carbon isotopic composition of methane from natural gases of various origins. *Geochim. Cosmochim. Acta* 44, 649–661 (1980).
45. Sakata, S., Hayes, J. M., Rohmer, M., Hooper, A. B. & Seemann, M. Stable carbon-isotopic compositions of lipids isolated from the ammonia-oxidizing chemoautotroph Nitrosomonas europaea. *Org. Geochem.* 39, 1725–1734 (2008).
46. Ruby, E. G., Jannasch, H. W. & Deuser, W. G. Fractionation of stable carbon isotopes during chemoautotrophic growth of sulfur-oxidizing bacteria. *Appl. Environ. Microbiol.* 53, 1940–1943 (1987).
47. Keeling, C. D. The concentration and isotopic abundances of atmospheric carbon dioxide in rural areas. *Geochim. Cosmochim. Acta* 13, 322–334 (1958).
48. *R: A language and environment for statistical computing*. (R Foundation for Statistical Computing, 2008).

Acknowledgments: Many thanks for to Adam Baumann, Bonnie Ellis, Diane Whited, Hannah Coe, Jon Graham, Ashley Helton, Shawn Devlin, Geoffrey Poole, Steve Whalen, Chad Reynolds, Brian Reid, Meredith Wright, Anne Hershey, FLBS faculty and staff, volunteers, and the Dalimata family. The data reported in this paper are tabulated in the Supplementary Material. Funding was provided by the Jessie M. Bierman professorship and philanthropic donations.

Author Contributions: Amanda DelVecchia and Jack Stanford designed the study and conducted data collection, data analysis, and writing. Xiaomei Xu contributed to sample analysis and writing.

Author Information: Reprints and permissions information is available at www.nature.com/reprints. The authors declare no competing financial interests.

Correspondence and requests for materials should be addressed to amanda.delvecchia@umontana.edu.

Table 1. Average and conservative estimates of methane dependence across floodplains

Floodplain	n Wells Sampled	n Insects Sampled	Conservative Estimate of Methane Dependence (%)	Average Estimate of Methane Dependence (%)	Mean $\delta^{13}C$ (‰)
Nyack	7	528	37.3 ± 0.1	66.5 ± 0.1	-55.1 ± 0.1
Kalispell	6	31	12.9 ± 0.4	23.0 ± 1.2	-37.3 ± 0.2
Methow	4	145	8.5 ± 0.5	15.1 ± 0.2	-34.1 ± 0.1
Jocko	3	14	20.5 ± 0.7	36.5 ± 2.4	-42.8 ± 0.4
Species	**n Insects sampled**		**Conservative Estimate of Methane Dependence (%)**	**Average Estimate of Methane Dependence (%)**	**Mean $\delta^{13}C$ (‰)**
I. crinita	23		38.8 ± 3.7	69.2 ± 6.7	-56.2 ± 2.7
I. grandis	128		33.8 ± 2.2	60.2 ± 3.8	-52.5 ± 1.6
I. integra	3		14.7 ± 0.9	26.2 ± 1.6	-38.6 ± 0.7
P. frontalis	423		33.1 ± 1.0	59.1 ± 1.7	-52.0 ± 0.7
K. perdita	95		18.3 ± 1.6	32.5 ± 2.8	-41.2 ± 1.1
Isocapnia spp.	34		31.3 ± 3.6	55.9 ± 6.4	-50.7 ± 2.6

Average and conservative estimates of methane dependence across floodplains were computed as stratified means ± standard error. Sample sizes varied because a) available sampling wells varied among sites, and b) stonefly abundance varied among wells within sites. *Isocapnia spp.* includes larvae of *I. grandis* and *I. crinita*, which could not be taxonomically segregated in the larval stage, but were very abundant as easily recognizable teneral adults in both wells. *K.*

perdita was the largest species, with carnivorous mouthparts, and was also methane dependent. This suggested that methane derived carbon could be a significant indirect subsidy to higher-level consumers, or that even these presumably carnivorous species directly consume MOB.

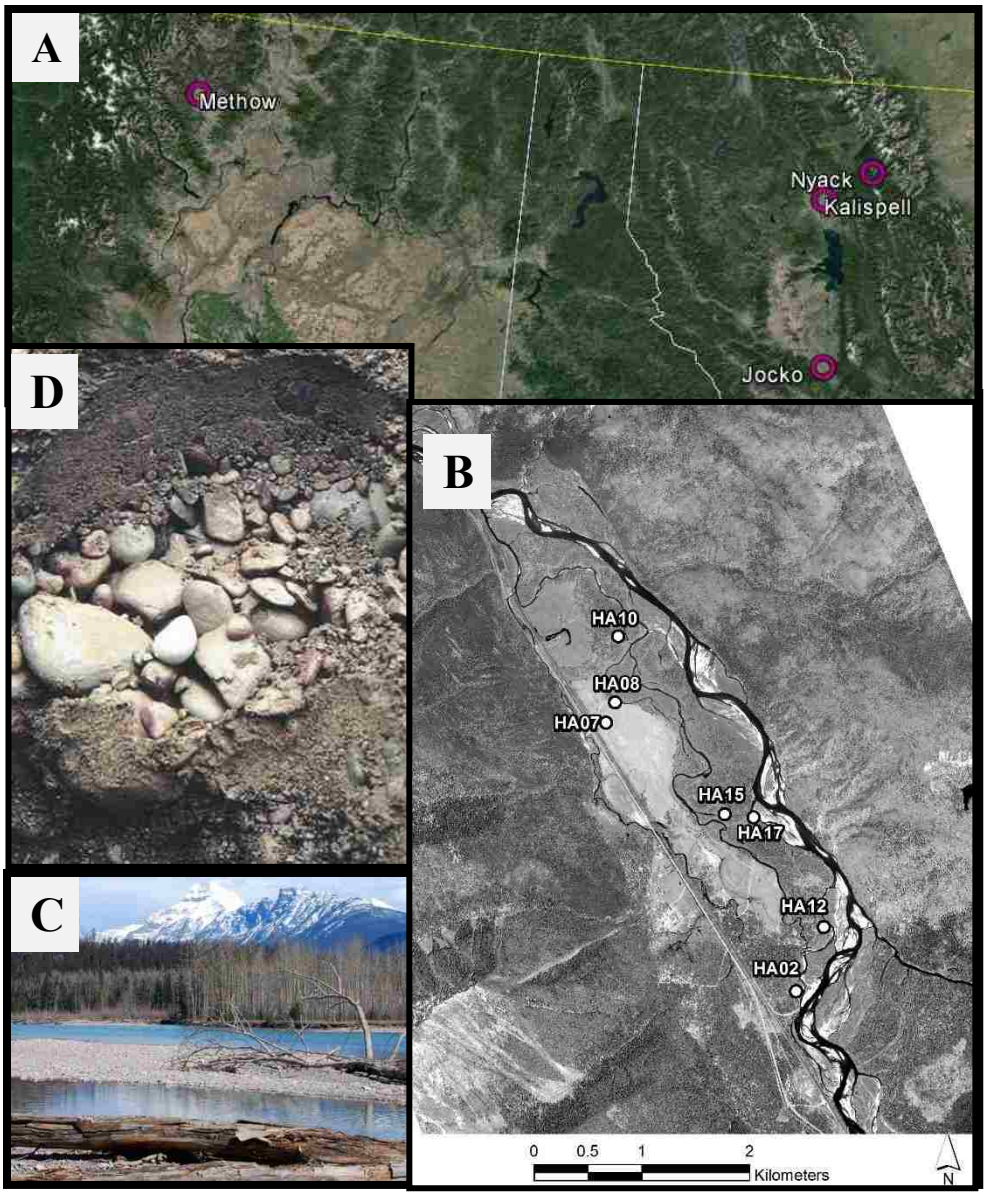

Fig. 1. Floodplain locations: A the four floodplains studied are overlaid on Google Earth Imagery. The main research site was the Nyack Floodplain. B. Aerial imagery of the Nyack Floodplain shows the locations of the 7 wells studied (see ED Table 1). . C. A view of the Nyack floodplain, near well HA02, shows the pristine nature, landscape complexity, and spatial heterogeneity typical of Nyack. D. A cross-section of the Nyack

bed-sediments highlights the heterogeneity of the matrix: sorted cobbles allow extreme hydraulic conductivity, while the fine sediment presents the opportunity to retain organic matter and develop localized hypoxia or anoxia.

a

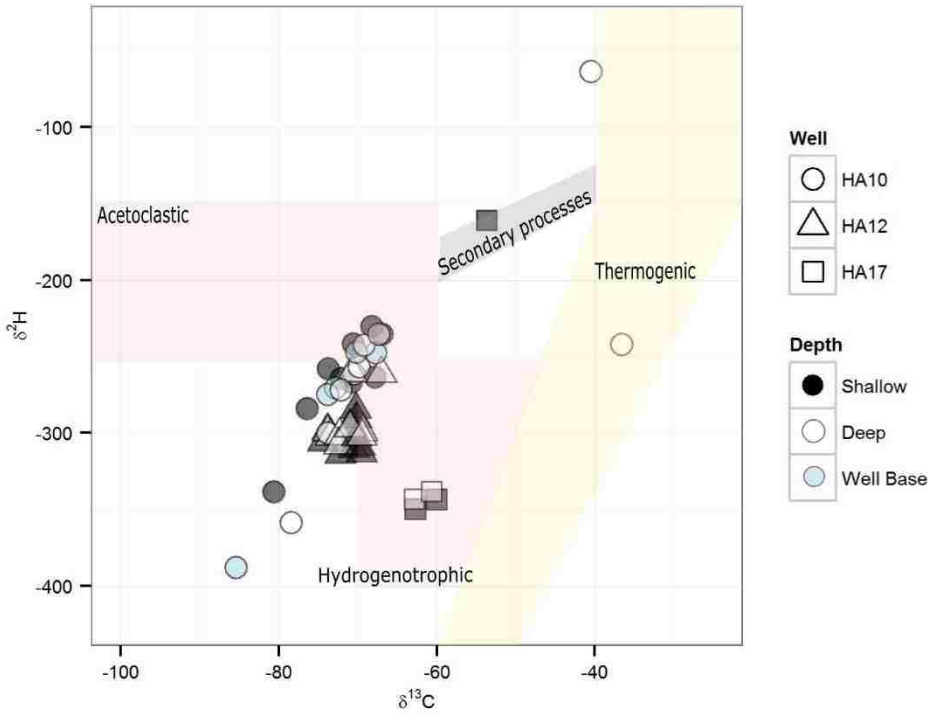
Acetoclastic
Secondary processes
Thermogenic
Hydrogenotrophic
-100
-200
-300
-400
δ^2H
-100
-80
-60
-40
$\delta^{13}C$
Well
HA10
HA12
HA17
Depth
Shallow
Deep
Well Base

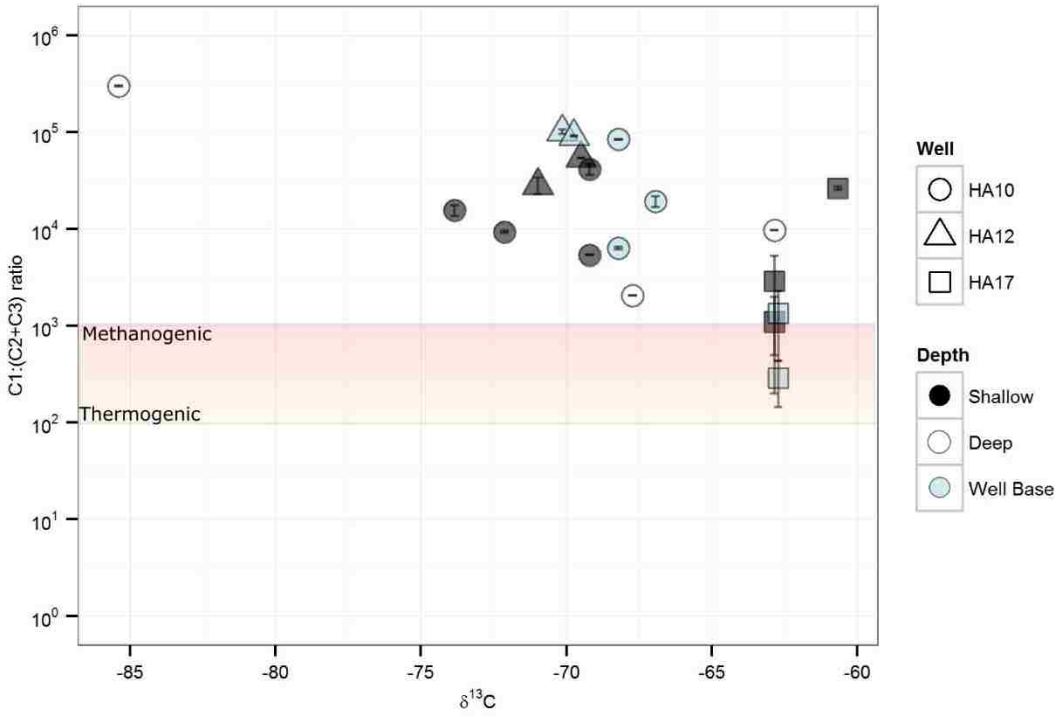
10^6
10^5
10^4
10^3
10^2
10^1
10^0
C1:(C2+C3) ratio
Methanogenic
Thermogenic
-85
-80
-75
-70
-65
-60
$\delta^{13}C$
Well
HA10
HA12
HA17
Depth
Shallow
Deep
Well Base

b

Fig. 2. Using stable isotopes to determine methane source A. A Schoell plot (22) of deuterium isotopic signatures vs. carbon isotopic signatures in individual samples. Symbols represent well; colors represent depth. Most samples cluster at a methanogenic origin, while others at HA10 deep and HA17 shallow suggest a thermogenic contribution and/or microbial oxidation. However, samples from the same day at other depths still cluster with methanogenesis. B. A Bernard plot (24) displays the ratio of methane concentration to summed concentrations of higher chain hydrocarbons (ethane and propane) vs the δ13C of methane. The high ratios (above 1000) within error, suggest a low probability of a thermogenic contribution.

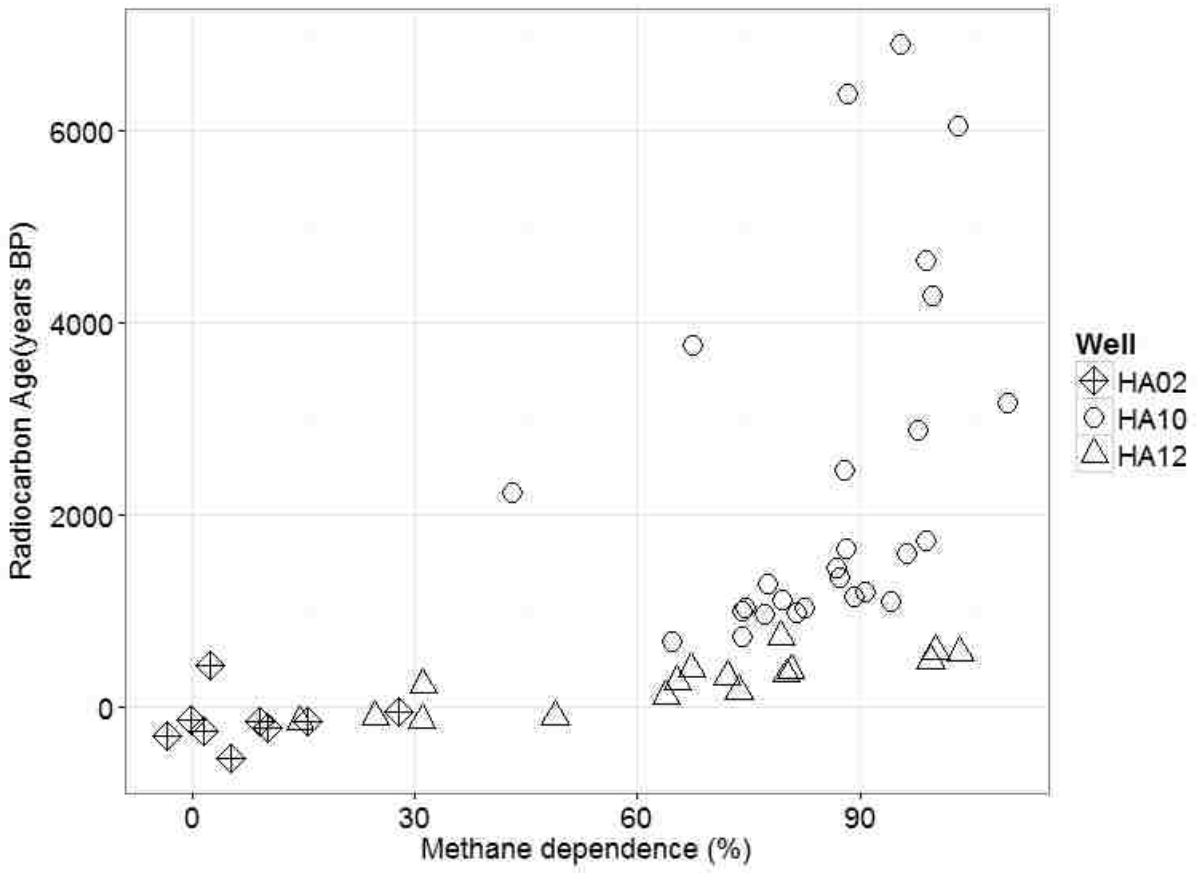

Fig. 3. Radiocarbon age vs. methane dependence: radiocarbon ages of stonefly tissue (each point is one individual) were strongly correlated with calculated levels of methane dependence, suggesting that a) a broad range of methane ages is present in the aquifer, as shown by the high variation in age even at high levels of methane dependence; b) non-methane derived carbon was modern because low levels of methane dependence correspond with younger ages; and c) the maximum methane age could be much older than 6900 years, because all stonefly tissue measured was a mixture of various organic carbon sources.

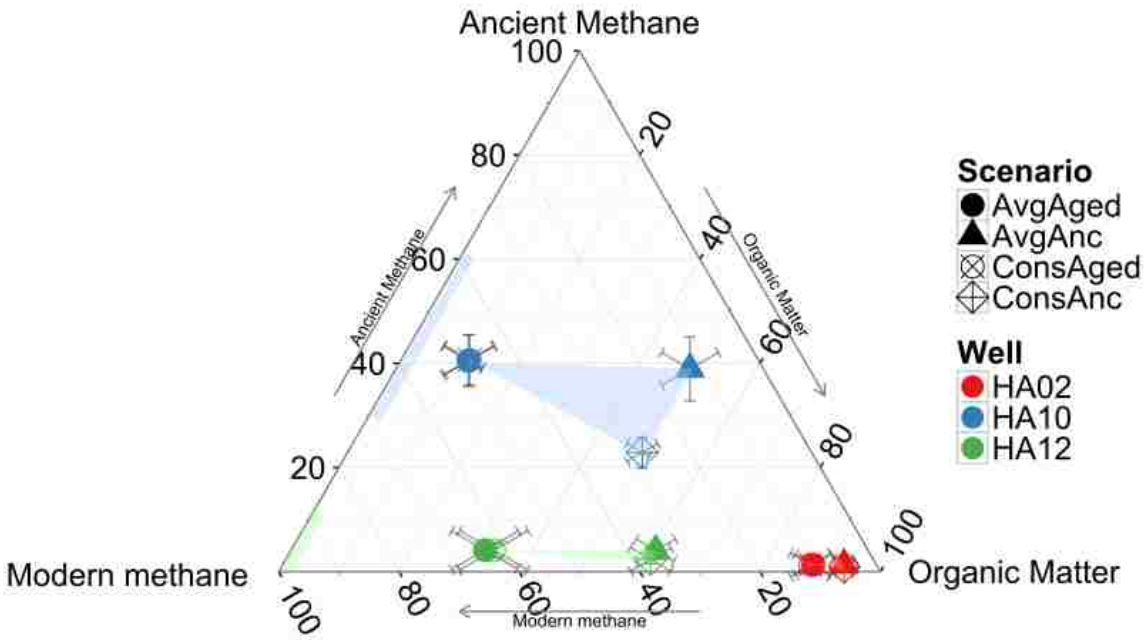

Fig. 4. Bayesian modelling outcomes: means and standard deviations of percentage source contributions to stonefly biomass from each of the three sources (modern methane, ancient methane, and organic matter) were plotted for each well (colors) for each of the four mixing-model scenarios explained in text and ED Table 4 (symbols). The shaded areasrepresent the full range of possibilities for source contributions considering the four scenarios. The shaded lines on the methane axis (left) represent the potential mixtures of modern and ancient methane in each well from which we could measure methane ages (HA10 and HA12). Wells HA10 and HA12 were the only two wells on the floodplain with high methane concentrations, and well HA02 was closest to the river with the shortest flow path and lowest levels of methane dependence in stonefly biomass across all samples.

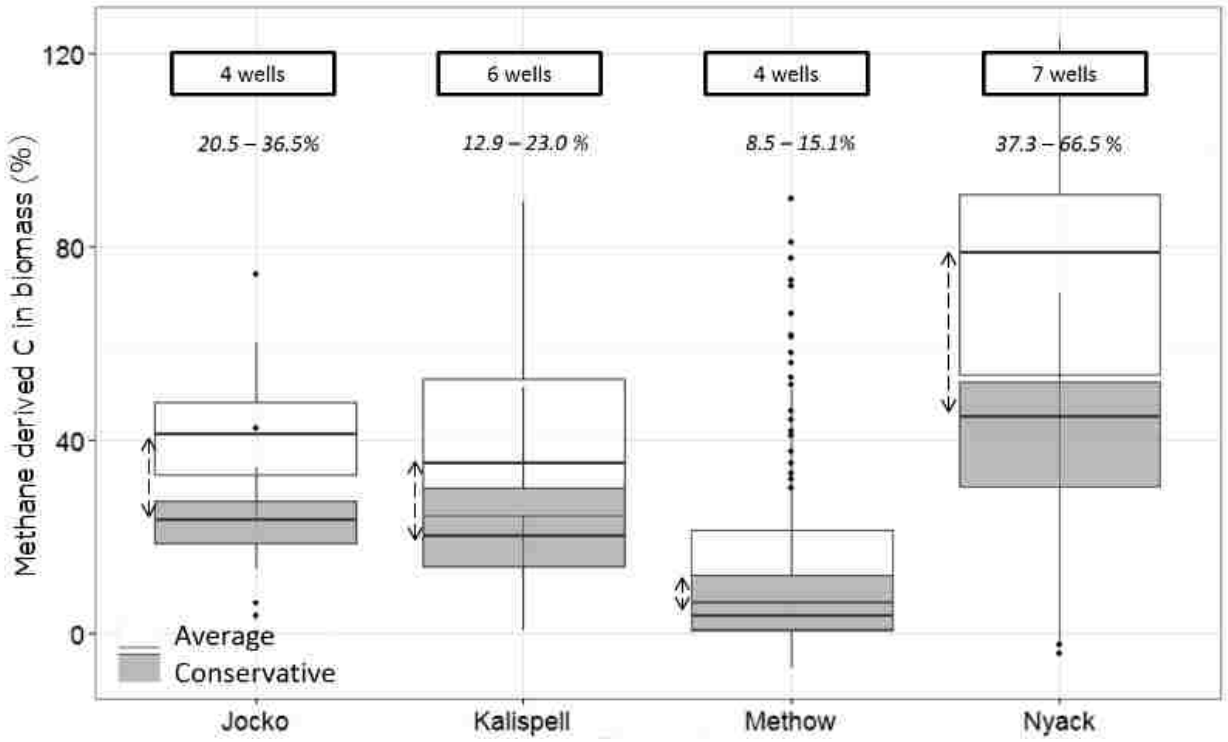

Fig. 5. Stonefly methane dependence across floodplains: boxplots of methane derived carbon contribution to stonefly biomass for each of the floodplains studied using both the average and conservative estimation techniques (see Table S1 for the two estimates). These estimates each assumed an extreme end of a range of potential source $\delta^{13}C$ values for methane (see text). The values displayed above each bar are the average methane dependence values (stratified by well) for each floodplain. Whiskers extend to 1.5 times the inter-quartile range for each set of floodplain estimates.

Extended Data

a

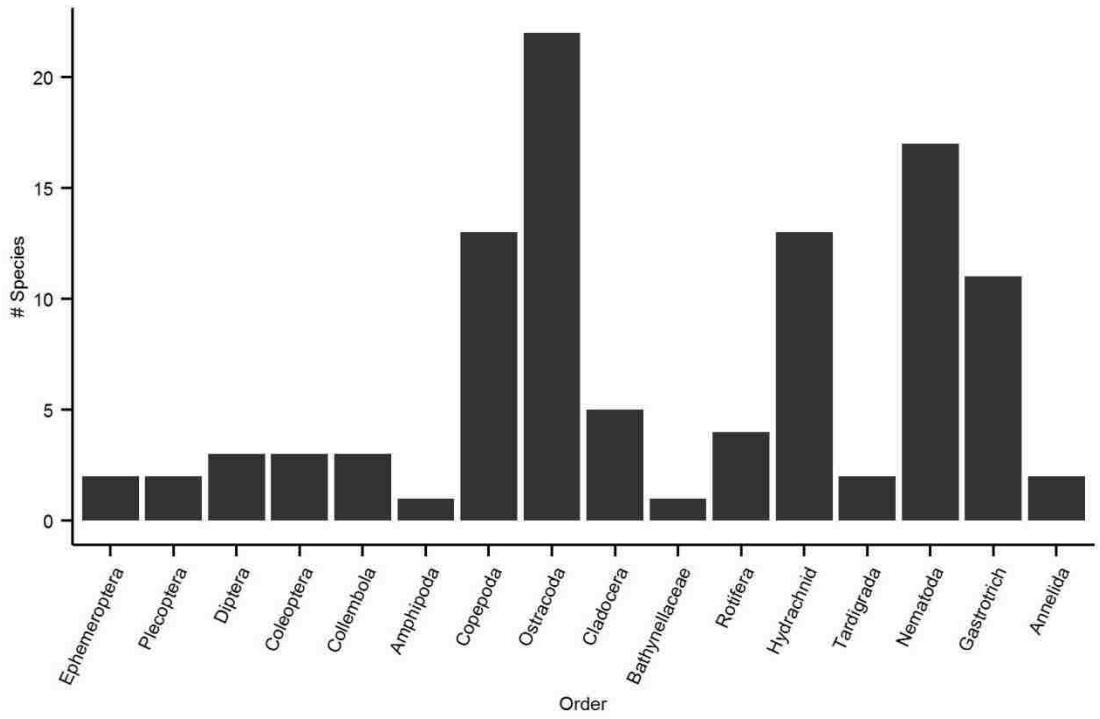

b

Plecoptera Species	Duration larval stage	Wells/locations where common	Diet
Isocapnia crinita	2 years	HA02, HA07, HA10, HA15, HA17	Grazers
Isocapnia grandis	2 years	HA07, HA10, HA15, HA17, Kalispell, Methow	Grazers
Isocapnia integra	2 years	HA02	Grazers
Paraperla frontalis	2-3 years	All Nyack wells, all floodplains	Omnivorous
Kathroperla perdita	2-3 years	All Nyack wells, all floodplains	Omnivorous

Extended Data Figure 1 | Species documented on the Nyack Floodplain A. A total of 104 species have been documented in the hyporheic zone of the Nyack floodplain. Seventeen are Plecoptera, but only 5 Plecoptera species were commonly occurred in well samples (Table 1) and they do not occur in the river channel, spending the entire larval life history in the aquifer. Gibert et al. (*10*), described this novel life history strategy as amphibitic – hatching and growth to larval maturity in the aquifer, adult emergence, mating and egg deposition focused in the river

channel or potentially the adult stage can live in interstices in the floodplain bed sediments above the water table. B. Descriptions and life history characteristics of the five common amphibitic (larval stage underground, adult emergence aboveground) Plecoptera species which were used in our analysis (*8, 10, 14, 41, 42, 48*).

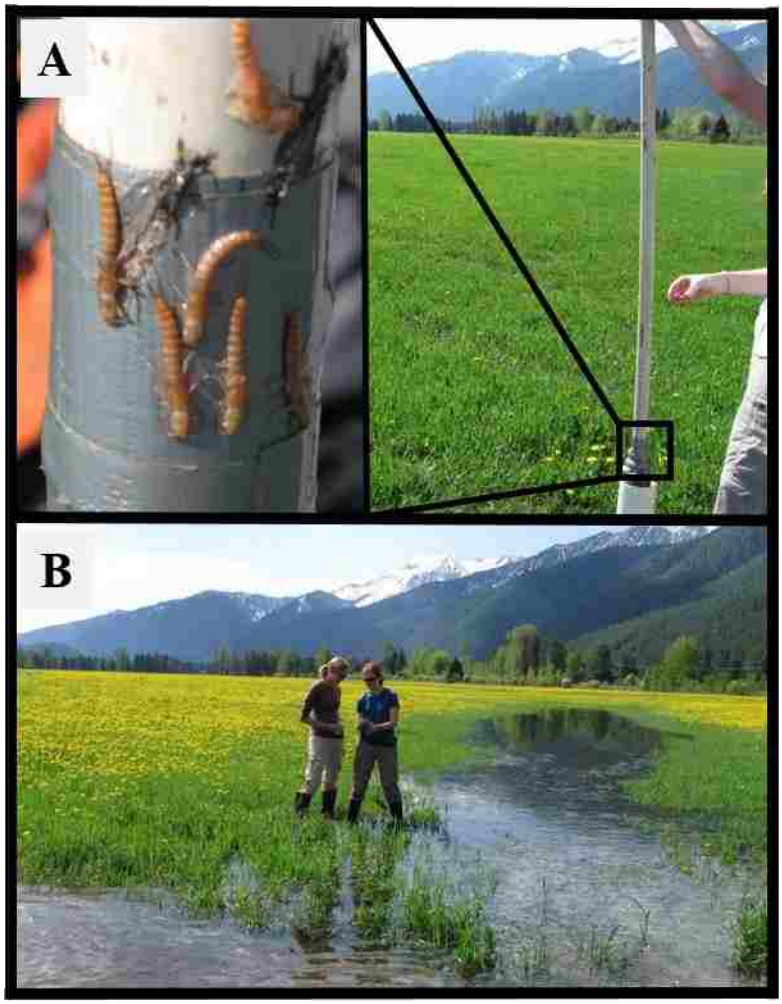

Extended Data Figure 2 | Surface and ground water connectivity A. Large (~2.5 cm) stoneflies (*Paraperla frontalis*) perched on equipment partially removed from well HA05 (Fig 1B) located 1.5 km from the river channel at Nyack. B. Aquifer water emerging at the surface of floodplain in a paleochannel located near the well in A during spring runoff, illustrating the ground and surface water connectivity characteristic of alluvial floodplains like the Nyack. Photos in A are a courtesy of Dr. Ashley Helton.

a

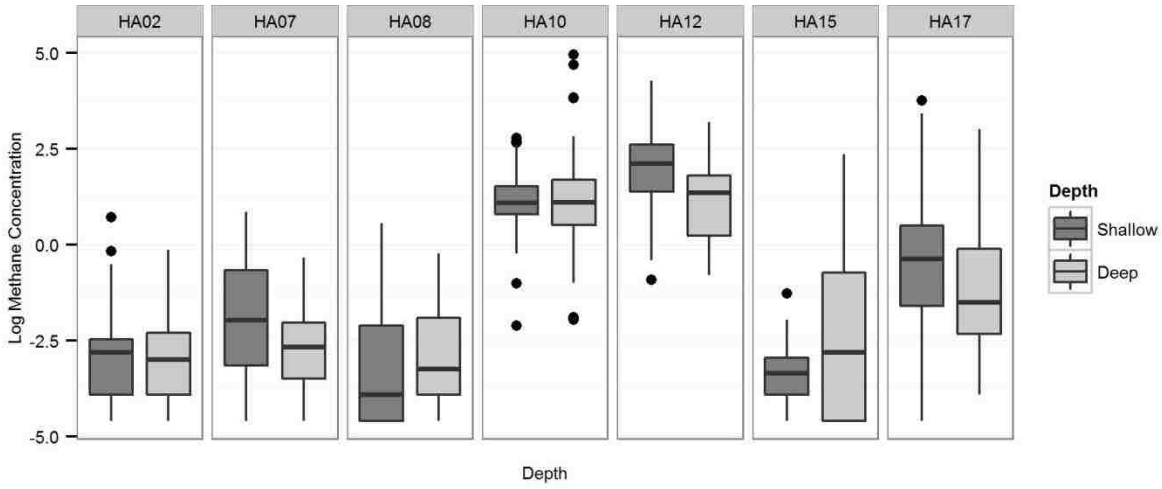

b

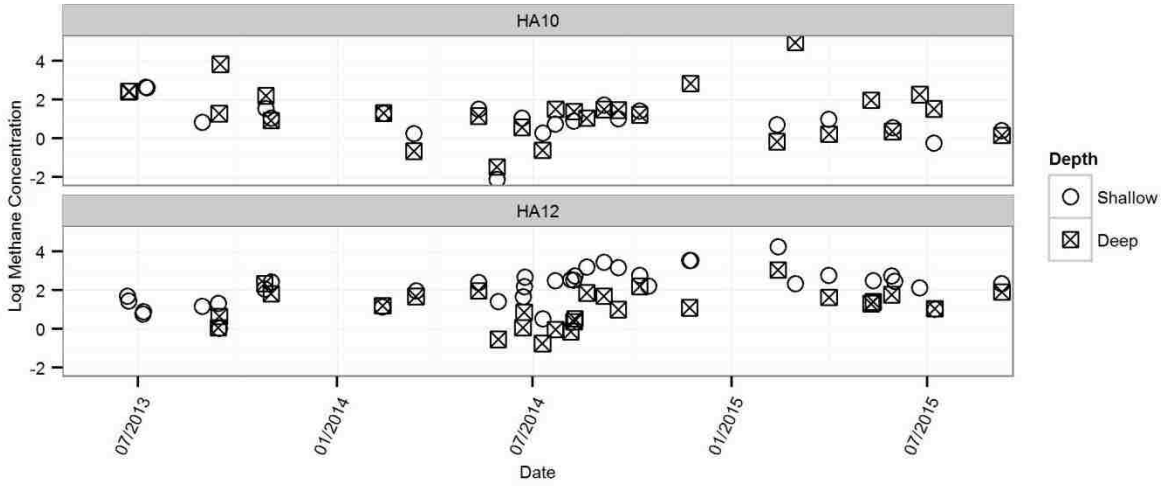

Extended Data Figure 3 | Methane concentrations in the Nyack aquifer A. Boxplots of log-transformed methane concentrations stratified per month show low (<1 µmol/L) methane concentrations in most wells sampled, with significant effects of depth (indicated by the star) occurring at HA10 and HA12. In HA12, shallow methane samples tended to have higher methane concentrations, whereas in HA10 deeper samples tended to have higher methane

concentrations, displaying vertical heterogeneity within the aquifer. B. Methane concentrations are plotted by date sampled from February 2014 to September 2015 (average error <0.17 μmol/L). Deeper HA10 samples show erratic changes in concentration over time.

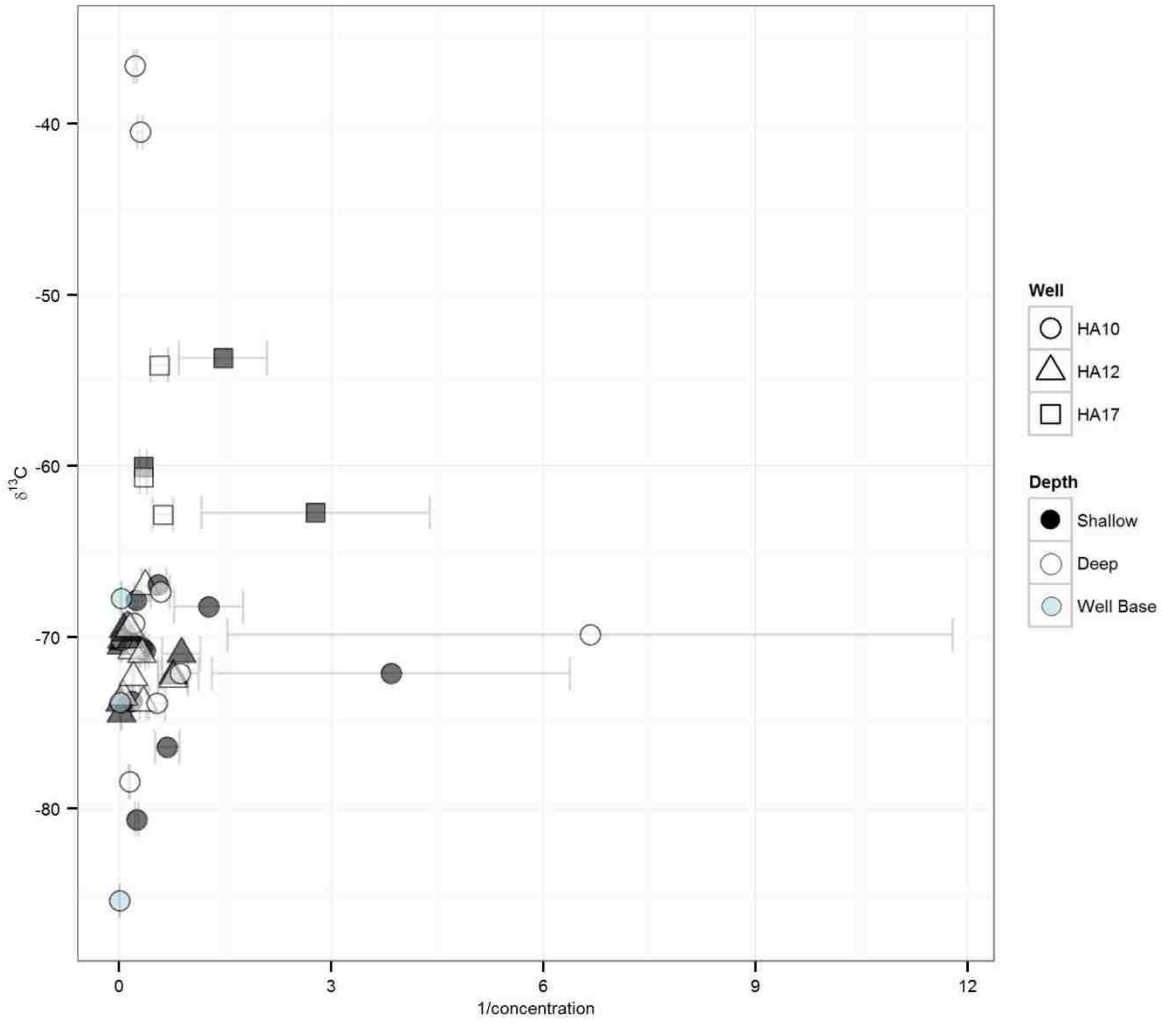

Extended Data Figure 4 | Using a Keeling Plot to determine methane source values A Keeling plot to indicate source $\delta^{13}C$ values of methane that shows a broad range of variation in $\delta^{13}C$ even during periods of high dissolved methane concentrations in the aquifer. We used these relations to parameterize the mixing models using two extreme estimates of source $\delta^{13}C$: the average of $\delta^{13}C$ values in methane samples taken at > 1 µmol/L concentration, and this average fractionated by $\alpha = 30.3$ ‰ (*25*).

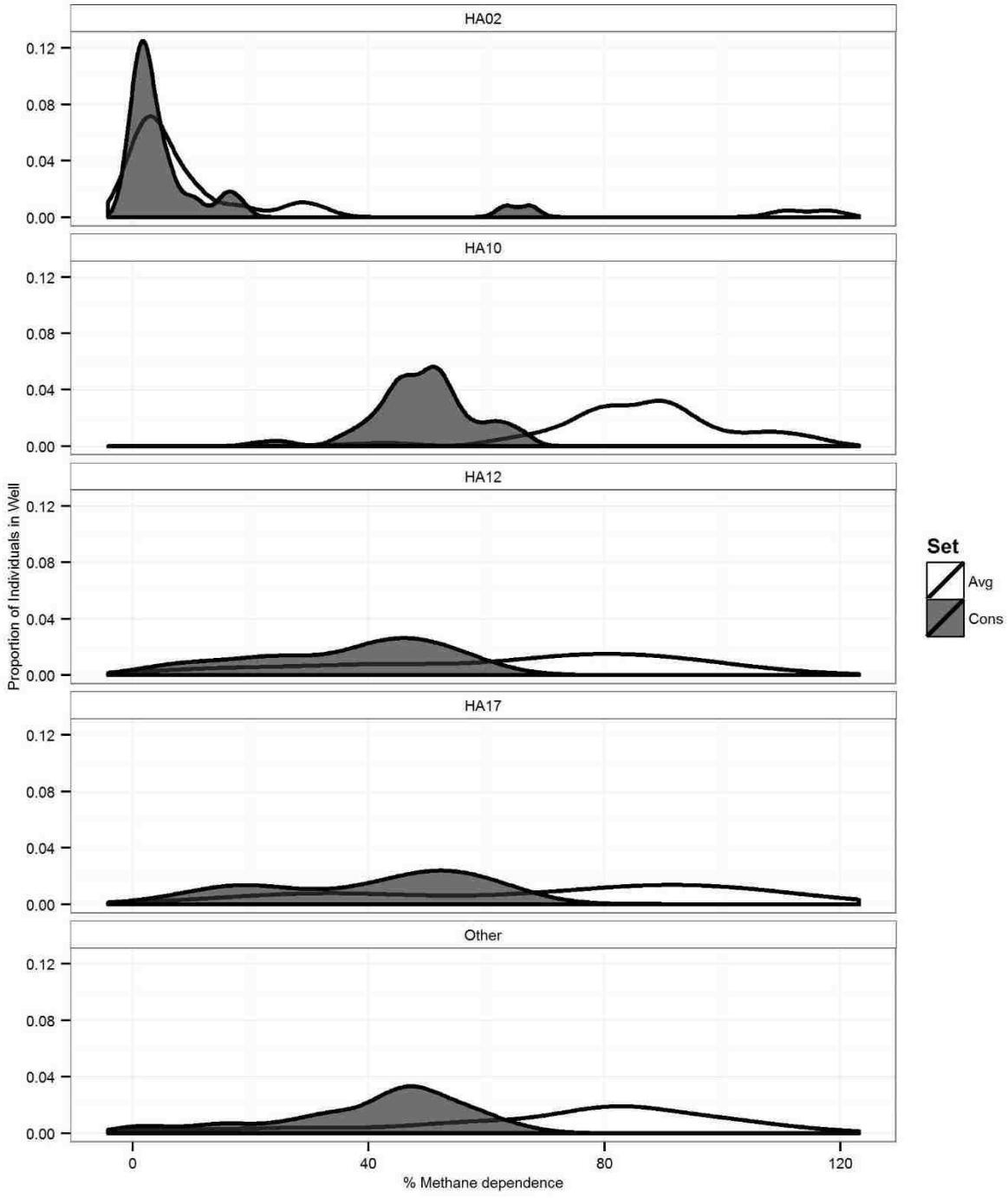

Extended Data Figure 5 | Methane derived carbon contribution across the Nyack aquifer

Average and conservative methane carbon contribution estimates are displayed for focal wells and all other wells ("Other") analyzed in the study. Well HA02, with much lower methane

dependence, was closest to the river and had the shortest residence time (45 days). The rest of the wells were all at similar residence times 117 – 304 days (*17*) (Table S2). Wells HA10 and HA12 both have high levels of measurable methane. Despite these being the only wells with measurable methane, all wells but HA02 showed 40 to 80% methane dependence as measured by stonefly biomass.

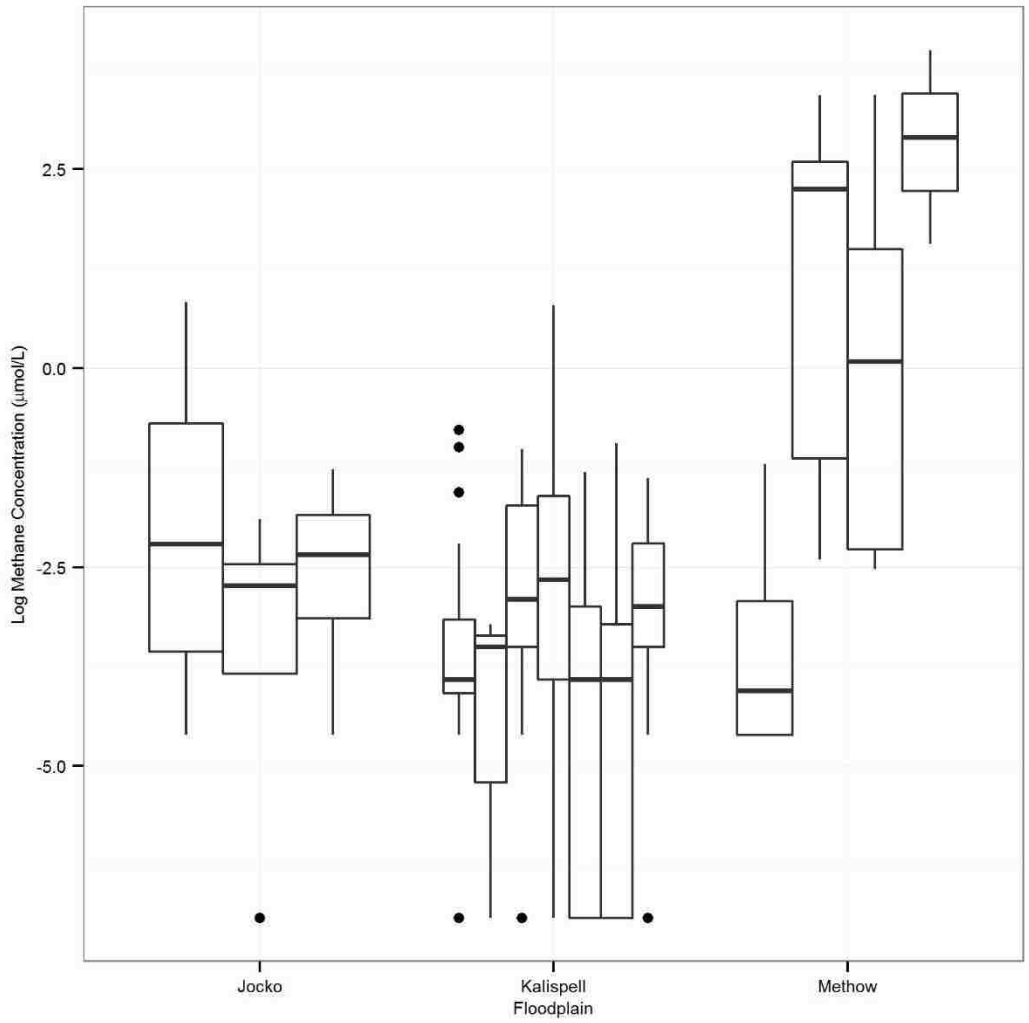

Extended Data Figure 6 | Methane concentrations at other floodplains Log methane concentrations for wells at all other floodplains studied. Most wells had less than 1 µmol/L dissolved methane over the course of study despite producing stoneflies which were clearly dependent on methane-derived carbon.

Extended Data Table 1 | Nyack well characteristics Well residence times and typical dissolved oxygen concentrations are displayed alongside species which we typically observed in each well. Note that we only found methane in wells with at least rare hypoxia.

Well	Easting	Northing	Shallow RT*	Deep RT*	DO character	Observational Notes
HA02	292244	5369912	45	60	Oxic	Near river channel at head of floodplain
HA07	290489	5372413	156	217	Oxic	
HA08	290564	5372617	210	263	Oxic	
HA10	290586	5373203	117	146	Occasional hypoxia	Methane usually present
HA12	292484	5370507	119	179	Occasional hypoxia	Methane usually present
HA15	291560	5371559	133	210	Oxic	
HA17	291846	5371524	167	304	Rare hypoxia	Rare hypoxia in winter, occasionally has methane in low concentrations

*RT = residence time (days). Estimates taken from Helton et al. (2012) (*17*).

Extended Data Table 2 | Radiocarbon-aged methane samples Sample information for all methane samples which were radiocarbon aged. Ancient methane contribution estimates were calculated using the same two-source mixing model equation used for stonefly overall methane contributions, but using radiocarbon signatures and defining ancient methane as radiocarbon-dead. Sample sizes were limited because a) we needed to meet minimum methane concentrations for analysis, and b) sample radiocarbon dating was very cost-prohibitive. Using this data, it is impossible to determine the maximum methane age, especially at HA10, and also to determine the depth at which methane is generated. However, as shown in Figure S2B, methane concentrations tended to be higher at the deeper depth in HA10. Well sample depths are indicated as following: S=shallow, D=deep, and WB=well base.

Date	Well and Depth	Methane $\delta^{13}C$ (‰)	Methane $\Delta^{14}C$ (‰)	Methane age (years BP)	Methane concentration (µmol/L)	CO_2 $\delta^{13}C$ (‰)	CO_2 $\Delta^{14}C$ (‰)	CO_2 age (years BP)	Ancient methane contribution
9/4/2014	HA12 S	-70.49 ± 0.3	-122.6 ± 21.0	990 ± 200	21.99 ± 0.24	-15.7 ± 0.15	-160.4 ± 1.8	1340 ± 20	12.3 %
9/17/2014	HA12 S	-70.16 ± 0.3	-92.8 ± 19.7	720 ± 180	28.39 ± 0.24	-14.8 ± 0.15	-181.0 ± 4 1.	1545 ± 20	9.2 %
11/24/2014	HA12 S	-72.60 ± 0.15	-48.2 ± 1.7	335 ± 15	30.83 ± 0.24	-19.2 ± .15	-158.4 ± 1.7	1325 ± 20	0.5 %
11/24/2014	HA10 S	-70.61 ± 0.3	-580.0 ± 7.2	6910 ± 140	2.80 ± 0.24	-16.8 ± 0.15	-223.4 ± 1.5	1970 ± 20	58.0 %
5/12/2015	HA10 D	-70.76 ± 0.3	-328.5 ± 1.3	3200 ± 20	1.80 ± 0.09	-15.2 ± 0.15	-150.3 ± 1.5	1310 ± 15	32.8 %
8/16/2015	HA10 WB	-84.40 ± 0.15	-253.7 ± 1.3	2350 ± 15	4.92 ± 0.09	-14.9 ± 0.15	-217.2 ± 1.4	1965 ± 15	25.4 %

Extended Data Table 3 | Organic matter pools Mean and standard error values for organic matter pools as measured during July 2013. CPOM (Coarse particulate organic matter) incorporated some stonefly detritus, resulting in its low value. FPOM stands for fine particulate organic matter. The average and standard error were incorporated into the Bayesian mixing model.

OM Type	$\delta^{13}C$	Std. Deviation	n
Biofilm	-28.50	1.81	26
CPOM	-29.71	3.56	28
FPOM	-25.28	1.65	24
Average	**-27.83**	**2.49**	

Extended Data Table 4 | Bayesian modeling scenarios We used four scenarios to represent extremes of two ranges: methane $\delta^{13}C$ and ancient methane $\Delta^{14}C$. These scenarios incorporated the displayed set of values used in parameterizing the Bayesian mixing model. Please mote the differences in OM radiocarbon values; these resulted from varying methane $\Delta^{13}C$ values used to calculate the weighted average of OM $\Delta^{14}C$ (weighted by non-methane based biomass). See methods for more information.

Scenario	**ConsAge**		**AvgAge**		**ConsAnc**		**AvgAnc**	
α	-30.3 ‰		0		-30.3 ‰		0	
Methanogenic methane max age	Measured (6900 yrs BP)		Measured (6900 yrs BP)		Radiocarbon-dead (>50,000 yrs BP)		Radiocarbon-dead (>50,000 yrs BP)	
	$\delta^{13}C$	$\Delta^{14}C$	$\delta^{13}C$	$\Delta^{14}C$	$\delta^{13}C$	$\Delta^{14}C$	$\delta^{13}C$	$\Delta^{14}C$
Modern methane	-100.8 ± 8.5	0 ± 7.2	-68.8 ± 8.5	0 ± 7.2	-100.8 ± 8.5	0 ± 7.2	-68.8 ± 8.5	0 ± 7.2
Aged-Ancient methane	-100.8 ± 8.5	-580 ± 7.2	-68.8 ± 8.5	-580 ± 7.2	-100.8 ± 8.5	-1000 ± 7.2	-68.8 ± 8.5	-1000 ± 7.2
Organic matter	-27.8 ± 2.5	-65.6 ± 75.9	-27.8 ± 2.5	-13.7 ± 32.2	-27.8 ± 2.5	-65.6 ± 75.9	-27.8 ± 2.5	-13.7 ± 32.2

Prepared for *Ecological Monographs*

Final manuscript coauthors: Jack A. Stanford, Bonnie K. Ellis, Jonathan Graham

Chapter 3: Methane dynamics drive the ecology of an expansive alluvial aquifer

Abstract

The alluvial aquifer of the Nyack Floodplain is an extremely oligotrophic system with large bodied hyporheic stoneflies (order: Plecoptera) as consumers. Up to a majority of total stonefly biomass in the Nyack aquifer has been found to contain biogenic methane-derived carbon, clearly demonstrating the importance of methane in the system, but the ecological role of methane in the aquifer is still unexplored. We investigated the role of methane at multiple scales: firstly, we analyzed dissolved organic carbon concentrations in relation to methane dynamics to understand the role of methane in providing an organic carbon source to this system. We then related these particular biogeochemical dynamics to the trophic and community ecology of aquifer biota, with a focus on top consumers: the hyporheic stoneflies. We found that dissolved methane concentration was the best predictor of dissolved organic carbon concentration in the aquifer, while methane concentrations were best predicted by dissolved oxygen concentrations. Stoneflies had distinct isotopic niches (trophic positions) as defined by $\delta^{13}C$ and $\delta^{15}N$ signatures. The distinctions between species could be attributed to varying abilities to access methane-derived carbon resources at oxic-hypoxic interfaces: *Isocapnia grandis* and *Kathroperla perdita* showed tolerance to hypoxia and anoxia in respirometry experiments, and *I. grandis* and *Paraperla frontalis* both showed consumption of methanogenic and methanotrophic microbes found in 16S rRNA gene sequence analysis of gut contents. While

none of the biogeochemical variables we studied were consistently significant in predicting trophic positions, dissolved methane concentrations alone explained 19% of the variation in stonefly species assemblages using NMDS analysis of 73 sampling events, while the combination of all biogeochemical variables considered explained 22%. We concluded that methanogenic methane was clearly important for production in this system, as shown by its correlation with DOC, varying levels of carbon contribution to individual stonefly species, and significance in structuring stonefly species assemblages. Our findings emphasized not only the unique adaptations of aquifer species to a heterogenous and carbon-limited environment, but the need to reconsider basal sources of productivity in a highly oligotrophic and light-limited system.

Introduction

Over the past decades, the conceptualization of productivity in river systems has received multiple upgrades. It has progressed from viewing these as heterotrophic ecosystems as mainly fueled by upstream nutrient export in the river continuum concept (Vannote et al. 1980) to including the importance of terrestrial-derived carbon with the flood pulse concept (Junk et al. 1989) focusing on the dynamic processes that mediate nutrient transfer between various components of the landscape along the river corridor (e.g. Ward and Stanford 1983, Stanford et al. 2005), and partitioning productivity in these systems as driven by both autochthonous and allochthonous carbon (e.g. Thorp and Delong 1994, 2002). The importance of both upstream and local processes is therefore clear in river ecology. Despite the increasingly complex view of productivity in these systems, however, there remains a lack understanding of how a major component of river systems functions: the shallow alluvial aquifers which are distributed along gravel-bedded rivers “like beads on a string” (Stanford and Ward 1993).

These floodplains are hot spots of biodiversity and productivity, yet they are also some of the most threatened ecosystems in the world due to damming, development, diversions, and other anthropogenic alterations (Tockner and Stanford 2002). They are characterized by hydrologic and biogeochemical interchange with the alluvial aquifer (Stanford et al. 2005). The most well-studied floodplain in the world, from which much of this understanding has been derived, is the Nyack Floodplain of Northwestern Montana (Stanford and Ward 1993, Ellis et al. 1998, Craft et al. 2002, Poole et al. 2002, Helton et al. 2014). This alluvial floodplain sits on the 5th order Middle Fork of the Flathead River at the southern boundary of Glacier National Park, encompassing a 3200 km^2 catchment with approximately 9 km of anastomosed river (Figure 1) (Stanford et al. 2005). Approximately 30% of base flow is influent to the aquifer at the upstream end of the floodplain, and upwelling occurs downstream in areas where topographic lows (such as channels and ponds) intersect the water table(Stanford et al. 2005).

The aquifer not only contains a large portion of total river flow, but it helps to maintain productivity and biodiversity (Pepin and Hauer 2002). More than 70 taxa have been documented in the aquifer, 5 of which are large-bodied hyporheic stoneflies (Order: Plecoptera) that are present in the tens of thousands (DelVecchia et al. 2016). These stoneflies spend 1-3 years maturing in the aquifer before emerging from the river channel to mate as short-lived winged adults (Stanford and Gaufin 1974). Because the aquifer is highly oligotrophic and limited by paucity of dissolved organic carbon, the presence of such abundant large macroinvertebrates was a conundrum until it was discovered that 8-70% of consumer biomass was comprised of methane-derived carbon (DelVecchia et al. 2016). The methane was methanogenically derived, and thereby helped to explain another paradox: labile carbon concentrations increase along

flowpaths in the Nyack aquifer, an occurrence that could be due to non-riverine influx or internal production of dissolved organic carbon (DOC) (Helton et al. 2015).

Previous research in the Nyack aquifer has focused extensively on DOC and dissolved oxygen (DO) dynamics, with study of methane concentrations being thus far limited to its known presence in specific aquifer locations and ubiquitous across consumer biomass. DOC and DO concentrations are interrelated and also correlated with other biogeochemical and hydrologic variables: residence time (e.g. Helton et al. 2015), temperature, depth of the sample, and time of year (Figure 2). Along flow paths, dissolved oxygen concentration (DO) and dissolved organic carbon concentration (DOC) both decrease due to respiration of river-supplied nutrients (Lowell et al. 2009, Helton et al. 2015), while temperatures stabilize to the mean annual air temperature at longer flowpaths (Anderson 2005, Poole et al. 2008). DO and DOC can diffuse from the vadose zone, increasing concentrations at locations closer to the water table (Smith et al. 2011). The aquifer also contains matrix subsidies, having organic matter deposits that can subsidize the microbial metabolism in select locations (Reid 2007, Appling 2012, Valett et al. 2014), contributing to increased DOC but diminished DO by stimulating respiration.

Though methane dynamics have not been directly studied in the Nyack aquifer, it is probable given previous Nyack study that locations exist which would be highly suitable for methanogenesis, which can occur in anoxia with or without an organic carbon source as the last and most metabolically inefficient step in microbial decomposition of organic matter (Bowman 2006). Furthermore, if that methane reached an oxic-anoxic interface, it would then stimulate production of methane oxidizing bacteria, or MOB, again contributing to DOC supply but diminishing the available methane and oxygen supplies (Bussmann et al. 2006). All microbial

metabolic processes, including methanogenesis, are affected by changes in temperature (Stanley et al. 2016).

Thus, previous research has elaborated the potential role of multiple biogeochemical and hydrologic processes in determining methane concentrations. Furthermore, work both at Nyack and elsewhere has suggested that methanogenesis and methanotrophy, controlled by these processes, contributes DOC to a carbon limited system (Helton et al. 2015, Craft et al. 2002). Given that up to a majority of site-wide consumer biomass on Nyack is methane-derived carbon (DelVecchia et al.), the importance of methane in this system is clear. However, methane dynamics have been implicated at two vastly different scales: flowpath-mediated biogeochemistry, or the suggestion that methanogenesis contributes to DOC at longer flowpaths, and entire-floodplain consumer biomass. We aimed to relate these scales.

Our overarching goal was to understand how methane dynamics, specifically as related to various other biogeochemical and hydrologic conditions, influenced the ecology of top consumers in the aquifer. Our first objective was to build a more robust understanding of methane dynamics: because DOC limits production in the aquifer, we investigated the relationship between DOC and methane concentrations. We coupled this with study of potential controls on methane production and assimilation: dissolved oxygen, temperature, residence time, timing, and location. Given a better understanding of aquifer biogeochemistry, our second objective was to resolve relationships between these particular biogeochemical dynamics and the trophic and community ecology of aquifer biota, with a focus on top consumers: the hyporheic stoneflies. We took four approaches: 1) we studied a subset of the aquifer food web, including macroinvertebrates, meiofauna, and organic matter types, to delineate stonefly and meiofauna trophic positions in relation to basal resources; 2) we explored potential adaptations of various

stonefly species that could facilitate them to access methane-derived carbon resources; 3) we analyzed relationships between local biogeochemical dynamics and stonefly trophic positions; 4) we analyzed relationships between local biogeochemical characteristics and stonefly species assemblages. Overall, our approaches to these two objectives enabled us to elaborate the niche characteristics of individual stonefly species and how these characteristics, along with species assemblages, were related to methane biogeochemical dynamics within the aquifer (e.g. Figure 2).

Methods

Study Site

The Nyack floodplain is a mosaic of diverse habitat patches arranged along a gradient of succession influenced by flood disturbance: cottonwoods (*Populus* spp.) and willows (*Salix* spp.) dominate early successional patches, mixed conifer forests dominate zones where flooding is less common, and alders (*Alnus* spp.) and birch (*Betula* spp) dominate the dense soils at the fringe of the wetlands (Mouw et al. 2009). Underlying the floodplain is Pleistocene and recent alluvium of extremely high porosity (maximum hydraulic conductivity of 10 $cm \cdot s^{-1}$) confined below by an impermeable clay layer of tertiary age(Stanford and Ward 1993).

The floodplain is equipped with nineteen 3-inch PVC wells with 2 mm slot openings down the length of the pipe (Figure 1). The wells were drilled 8-10 m using a hollow auger drilling. We sampled these wells for insects approximately every 3-6 weeks from June 2013 to October 2015. We measured environmental variables at two depths - 1 and 4 m below the

baseflow water table – every 3-6 weeks from January 2014 to October 2015. At seven of these wells, we sampled at additional times approximately every 3 to 4 weeks; winter sampling (November to March) was also restricted to these wells for feasibility. We chose these wells for additional sampling because they were a) distributed across the entirety of the floodplain, b) were well represented in DelVecchia et al. (2016), and c) were equipped with the RiverNet continuous monitoring system, which we could use to check for consistency in the variables which we measured. The RiverNet system recorded hourly measurements of dissolved oxygen and temperature at approximately 3m below the baseflow water table. While this was not depth-specific, it enabled us to quality control our meter measurements. All analyses presented here were conducted using our meter measurements.

Sample Collection

In order to sample environmental variables dissolved oxygen, dissolved organic carbon, dissolved methane, and temperature, we used a peristaltic pump equipped with PTFE (Teflon) tubing to draw water from depth at each well. We let the pump run for two minutes into a 500-mL Nalgene benthos jar, then proceeded to take measurements. We measured dissolved oxygen concentration (DO) and percent dissolved oxygen saturation (%Sat) using a YSI 85 handheld meter. We measured temperature using a Fisher Scientific high-accuracy (0.01 °C) portable corded thermometer. We collected samples for measuring dissolved organic carbon concentrations (DOC) by using acid-washed 60 mL syringes, then filtering water through ashed Whatman 0.7 μm pore size glass filters (Freshwater Research Laboratory protocol). We analyzed these samples on a Leco carbon analyzer according to standard Flathead Lake Biological Station protocol (Freshwater Research Laboratory protocol). We sampled methane concentrations using a modified active-sampling method as described in DelVecchia (2016).

These samples were analyzed on a greenhouse gas chromatograph (SRI Instruments model 8610C) equipped with a flame ionization detector and SRI PeakSimple Software (DelVecchia et al. 2016). We calculated headspace methane concentrations using a three-point calibration with Scotty gas standards (Air Liquide America). We then used Henry's Law to calculate dissolved methane before headspace equilibration using the solubility constant documented by Yamamoto et al. (1976). Error averaged 0.08 µmol/L initial aqueous concentration and our detection limit was 0.11 µmol/L.

We collected stonefly samples using both trapping and pumping methods. To trap, we had suspended nylon ropes in the wells on which the emergent and resident stoneflies could climb. We pumped the wells using a gas-operated diaphragm pump and collected samples using the methodology in DelVecchia et al. (2016). We froze samples and stored them at -80° C until preparation for stable isotope analysis. We took the same collection approach for collecting organic matter samples for stable isotope analysis, but samples were collected in June to July 2013 and only at the RiverNet wells. We used 64 and 500 µm Nitex mesh to parse out fine and coarse organic matter, respectively. These samples were also frozen until preparation for stable isotope analysis.

We collected biofilm samples at the RiverNet wells by suspending ashed and autoclaved gravel bags at all sampling depths on the Nyack for ten weeks during July and August 2013, then again for six weeks each four times between May 2014 and May 2015 (DelVecchia et al. 2016). We collected and sieved 6-12 mm gravels from Beaver Creek on the Nyack Floodplain. We rinsed and ashed the gravels, then packaged them in synthetic mesh bags. We autoclaved these samplers and suspended them at the shallow and deep depths in each of the seven focal wells. We left them in the wells, undisturbed, for 10 weeks in July-August 2013. Upon removal, we

kept gravel (in the whirl-paks) for stable isotope analysis. To process the biofilm stable isotope samples, we defrosted and gently rinsed samples at the lab, added 150 mL of ultra pure de-ionized water, and sonicated for 40 minutes. We then poured the supernatant into a beaker and dried at 60°C until all water was evaporated. We then scraped the beaker and treated the material as organic matter stable isotope samples.

To prepare stoneflies and organic matter for stable isotope analysis, we followed the methods of DelVecchia et al. (2016). Samples were analyzed on a PDZ Europa ANCA-GSL elemental analyzer interfaced to a PDZ Europa 20-20 isotope ratio mass spectrometer (Sercon Ltd., Cheshire, UK) at the UC Davis Stable Isotope Laboratory. Stable isotope ratios were expressed relative to international standards: V-PDB (Vienna PeeDee Belemnite) for ^{13}C and air for ^{15}N.

Analysis methods, Objective 1: biogeochemical controls on dissolved organic carbon and dissolved methane concentrations

We used the same methods to understand controls on 1) dissolved organic carbon concentrations (DOC), and 2) dissolved methane concentrations (methane).

We performed all data analysis in R (R Core Team 2016). We tested all continuous variables for normality using the Skewness-Kurtosis test, assessing skewness values between -0.5 and 0.5 and kurtosis values less than 3 as symmetric and normal. As both DOC and methane concentrations were highly right skewed, we used a log transformation on both variables. In order to do so for methane, we added 0.001 µmol/L to all values of 0 before the transformation (thus the minimum log-transformed methane concentration was -3). This value was <10% of

measurement error, which was 0.07 µmol/L; thus our addition was an order of magnitude lower than the error range. In order to log-transform the DOC concentrations, we removed two samples of value 0 before the transformation. We then removed all data points which did not have a complete set of temperature, dissolved oxygen (DO), DOC, and methane concentration measurements, bringing our sample size to n = 127.

We also manipulated the day of year variable. Because day was a circular variable, we included it as a fixed effect as follows (Stolwijk et al. 1999):

$$\beta_1 \left| \sin\left(\frac{2\pi(day)}{365}\right) + \cos\left(\frac{2\pi(day)}{365}\right) \right|$$

We termed this our 'day term'.

We tested variables for homoscedasticity using the Fligner-Killeen test. We removed DOC outliers, which we defined as points which were 1.5 times the interquartile range above the third quartile or below the first quartile in each well. We initially assessed potential correlations using ANOVA and Pearson correlation coefficients where assumptions of normality and homoscedasticity were met (all variables but Well and Sampling Depth). We used a one-way test (oneway.test()) to evaluate relationships between variables where assumptions were not met; this was essentially an extension of the Welch t-test.

We constructed linear mixed effects models using the R package nlme (Pinheiro et al. 2016). We assigned the well of collection as a random effect in order to account for unknown differences between the wells. All other variables were assigned as fixed effects. We first accounted for effects of the day term and depth differences in the model, which we inferred

would lead to a joint spatiotemporal correlation in our biogeochemical variables: DO, DOC, and methane. We then assessed if additional predictors would improve the model and compared models using AIC (Akaike information criteria) scores (Akaike 1974).

Analysis Methods, Objective 2, Approach 1: Trophic positions of aquifer macroinvertebrates and meiofauna

We analyzed $\delta^{13}C$ and $\delta^{15}N$ values in order to understand variation in basal carbon resources and variation in trophic position, respectively (e.g. Fry 2006). We included stoneflies, organic matter, and meiofauna in this analysis in order to infer relative trophic positions. We incorporated two previous stable isotope datasets from the Nyack floodplain specifically for this process: the first (n = 239) was collected during July 2012 by Flathead Lake Biological Station research staff, processed according to the same protocol that we used in the 2013-2015 samples, and also sent to the UC Davis Stable Isotope Facility for analysis. The second (n = 61) was collected during 2004 and processed using the same protocol and facility, but also included meiofauna samples and stoneflies from additional wells. Though stonefly stable isotope samples included one individual per sample, this was impossible to follow with meiofauna because of their low masses. Therefore, approximately thirty meiofauna individuals were combined per well per taxa for the stable isotope analysis. These two datasets, along with 2013 collected stoneflies from the focal dataset, were used only in construction of the food web because corresponding environmental data from the dates of collection of these samples was either unavailable or unreliable. All stoneflies examined were later instar larvae because these stages are easiest to identify.

We used all available stable isotope samples across datasets to assemble the food web structure. Our large sample size (n=752) enabled us to resolve a persistent problem in interpretation of food web structure in systems with a methane subsidy: reliance upon methane-derived carbon is known to be correlated with depletion in ^{15}N (Conway et al. 1989, Lee and Childress 1994, Kohzu et al. 2004). This is because MOB fractionate DIN as they preferentially uptaake ammonium and nitrate (Hoch et al. 1992, Lee and Childress 1994). We therefore compared $\delta^{13}C$ values, which indicated a gradient of methane derived carbon in biomass, with $\delta^{15}N$ values. We examined this relationship specifically in consumers (stoneflies and meiofauna), using a varying intercepts model. We chose a varying intercepts model because the relationship between the signatures should remain constant across species, but intercepts should vary as a result of ^{15}N increasing with progressive trophic levels. We found that $\delta^{15}N$ and $\delta^{13}C$ were strongly correlated in all known consumers ($R^2 = 0.627, p < 10^{-4}, n = 719,$ Fig. 4),

We therefore applied this relationship to all consumers and organic matter pools andused y intercepts to represent trophic level differences between species independent of methane derived carbon reliance, making organisms and organic matter pools comparable using stable isotope differences. We calculated the base trophic level for aquifer invertebrates as the average of FPOM and biofilm $\delta^{15}N$ values. We excluded CPOM because CPOM a) was generally too coarse for consumption by the invertebrates, and b) included stonefly detritus such as exuvia. The $\delta^{15}N$ residual value that we used to represent the base food resource, or trophic level 1, was -5.77 ‰.

We used basic linear models compared using ANOVA to determine that well of collection could significantly affect $\delta^{13}C$ and $\delta^{15}N$ signatures, ($Pr(>F) < 10^{-13}$). Therefore we used an unweighted stratification of $\delta^{13}C$ and $\delta^{15}N$ values by well for each species and organic matter classification to account for uneven sampling between wells and unknown differences in abundance between wells. We used these stratified means and standard error values to construct a biplot to understand the food web.

Analysis Methods, Objective 2, Approach 2: Potential adaptations of select stonefly species

We considered two potential adaptations of stoneflies that could facilitate them to access methane derived resources: 1) tolerance to hypoxia and anoxia and 2 consumption of methanotrophic and/or methanogenic microbes.

1. Stonefly respirometry

In August 1994, preliminary respirometry experiments were conducted using individuals collected from the Nyack Floodplain. Using miniature respiration chambers and oxygen microelectrodes, we examined the respiratory response of *I. grandis* and *K. perdita* to hypoxia. Individual stoneflies were placed in respiration chambers containing 0.2 µm Nucleopore filtered hyporheic water from the collection site. Respiration chambers were maintained at ambient temperatures (9.1 - 11.2 + 0.1°C) using a temperature-controlled circulating water bath. Copper-constant thermocouples were used to monitor temperatures for consistency throughout experiments. Dissolved oxygen concentration was measured using Strathkelvin 781 oxygen meter with model 1302 oxygen microelectrodes (FEP membranes). Electrode calibration

followed Strathkelvin procedures with zero baseline utilizing 5% sodium sulphite and 100% DO saturation following bubbling. During incubation, oxygen concentration was measured every 10 seconds using Datacan V data acquisition software by Sable Systems. Organisms were placed in miniature respiration chambers containing pebbles (DI washed and autoclaved) suspended on a plastic mesh with a slowly circulating micro magnetic spinbar below. Chamber volume ranged from 2.4 to 39 ml, depending upon organism size. Initial oxygen saturation was 90 - 100% and the animal was allowed to remove oxygen from the water down to 0% saturation. Respiration rates were standardized by body weight of each stonefly and recorded as µg O_2 /XX/mg organism body weight. After the experimental chamber reached 0% oxygen saturation, organisms were transferred to oxygen saturated water and the time to recovery was recorded, unless the organism died before reaching 0% oxygen saturation.

2. Stonefly gut contents

In order to assess whether or not these organisms consume methanogenic and methanotrophic microbes, we analyzed the 16S rRNA gene in stonefly gut contents and biofilm collected from the well gravel bag samplers. We used 16 individuals collected during July 2013. Because our sample sizes were small, we regarded this as a qualitative analysis to understand what taxa were indeed present in both collection locations (gut and well), and to establish if there was indeed a significant contribution of methanogen/methanotroph taxa to the composition of stonefly gut contents.

In order to collect DNA from stonefly gut contents, we immediately identified and froze stonefly nymphs using liquid nitrogen. To later remove the gut contents, we defrosted and dissected each individual, cutting the abdomen to remove hindgut and foregut contents using

flame-sterilized tools (e.g. Blankenship and Yayanos 2005, Deagle et al. 2005). For both gravel bag samples and gut samples, we extracted DNA using the MO-BIO Powersoil Kit, then stored extracted DNA at -80 C until samples were sent to the laboratory of Dr. Carl Yeoman (Montana State University) for amplification and sequencing on an Illumina MiSeq platform.

We ran all analysis in QIIME (Caporaso et al. 2010). We assembled the paired-end MiSeq reads using pandaseq (Masella et al. 2012). We used the uclust method to choose OTUs (operational taxonomic units) with 97% sequence similarity and a 100 bp prefilter length. We assigned taxonomy using the rdp classifier method with the most recent SILVA database (version 111, "SILVA Terms of Use/License Information").

Analysis Methods, Objective 2, Approach 3: relationships between local biogeochemical dynamics and stonefly trophic positions

In order to understand potential explanations for stonefly trophic positions, we compared the inclusion of methane-derived carbon (MDC) in biomass as well as $\delta^{15}N$ residuals to biogeochemical characteristics at the time of sample collection. Though insect tissue stable isotope values turn over on the scale of hours to days, we hypothesized that MDC values would be correlated with biogeochemical characteristics because either a) stoneflies were within the vicinity the of the well for some time (hours to days) before collection, or b) well characteristics from a given day were representative of conditions in the preceding days. We also assumed that the well conditions would be related to what food resources were available to the insects. Therefore, a correlation might imply suggest which biogeochemical characteristics would be most important in characterizing stonefly diets.

We first corrected the $\delta^{13}C$ values of stonefly, amphipod, and meiofauna biomass using the estimates of trophic level calculated using the $\delta^{15}N$ residuals, as follows:

$$Corrected\ \partial^{13}C = Measured\ \partial^{13}C - 0.5(TL - 1)$$

Where TL represents the trophic level. This adjustment was miniscule relative to overall $\delta^{13}C$ values, as the mean trophic level adjustment was 2.2 ‰.

We used the corrected methane derived carbon (MDC) estimates and $\delta^{15}N$ residual values from stonefly biomass to investigate potential correlations with environmental variables measured at the corresponding times and locations. We repeated the analysis for both depths at which these variables were measured, and focused on the "average" estimates of MDC. We then calculated percent MDC in consumer biomass using a two-source stable isotope mixing model using $\delta^{13}C$ values (Fry 2006) (Eq. 1):

$$\%\ MDC = \frac{Stonefly\ \partial^{13}C - OM\partial^{13}C}{Methane\ \partial^{13}C - OM\partial^{13}C} \bullet 100$$

To represent any possible contribution of organic matter to stonefly diet, we used 'organic matter' as a surrogate for any component of stonefly biomass that was not methane-derived carbon. For this purpose, we used a stratified average of $\delta^{13}C$ values from all organic matter pools that we measured within the aquifer: FPOM, CPOM, and biofilm. We used the methane $\delta^{13}C$ values explained in DelVecchia et al. (2016) to represent a full range of potential methane contributions to stonefly biomass.

In analyzing potential effects of the well and day of collection (transformed to day term, as defined above) on each $\delta^{15}N$ residuals and methane dependence, we were able to use the entire

dataset, which included 751 observations. ANOVA analysis indicated that species and well of collection, but not day term, were significant in predicting MDC in the stoneflies ($p<10^{-16}$). We therefore took multiple approaches to understanding potential correlations with environmental variables: 1) we calculated Pearson correlation coefficients and f-test statistics using ANOVA for each variable individually for each species; 2) we used the same linear regression subsets approach that we used for the biogeochemical variables; 3) we ran linear mixed effects models using well as a random effect and included as fixed effects the species and day of collection, evaluating biogeochemical variable inclusion to the model as additional predictors. We used the multiple analyses to search for consistencies. We repeated each analysis for biogeochemical variables measured at the shallow and deep sampling depths in each well on each sampling day. We compared linear mixed effects models using AIC scores and log-likelihood values (Akaike 1981). All of these analyses were run using the 2014-2015 stable isotope dataset (n=127) because all stable isotope values in this dataset corresponded with measured biogeochemical variables.

Analysis Methods, Objective 2, Approach 4: relationships between local biogeochemical variables and stonefly species assemblages

The purpose of approach 4 was to understand how the biogeochemical variables that we measured affected stonefly species assemblages. In order to compare methane, DO, and DOC values to stonefly assemblages, we needed to subset the data to that which met the following requirements: a) species abundance values needed to correspond with a complete set of measured environmental variables, b) at least one individual of any species needed to be present in a sample, and c) only species which were found at more than 10 (half) of the wells could be considered. These requirements were necessary to run a meaningful ordination analysis through

non-metric multidimensional scaling (NMDS). NMDS is process to geometrically arrange samples such that inter-point distances reflect the experimental differences (Kruskal 1964). After screening for our set requirements for this analysis, we were able to include samples only from 2013-2015, eventually amounting to n=76. We represented these samples in three dimensions.

We identified stoneflies according to multiple keys (Baumann et al. 1977, Stewart et al. 1988, Zenger and Baumann 2004)and focused on rope (trapping) and pump collected insects. In order to assemble the ordination data, we included only species *Isocapnia grandis, Isocapnia crinita, Isocapnia integra, Paraperla frontalis, Kathroperla perdita,* and *Stygobromous spp.* (amphipod) because these species were all abundant during multiple sampling events. Because stonefly collections were not depth-specific, in order to compare stonefly assemblages to environmental variables we needed to average environmental variables for both depths measured on the day of collection at each well. In addition, our stringent requirements for samples to be included caused discrepancies between sample sizes per well and sampling time. We therefore included both variables in the analysis to ensure that any effects of environmental variables were true rather than a result of confounding with the well and day of collection (day term). We then ran the NMDS analysis through the R platform using the vegan package (Oksanen et al. 2016).

Results

Results, Objective 1: Biogeochemical controls on dissolved organic carbon and dissolved methane concentrations

Our initial analysis of the variables using Pearson correlation coefficients, ANOVA, and one-way analysis of variation showed that well of collection and the day term all significantly affected each DO, DOC, and methane concentrations (Table 2). This was expected given that each of these concentrations were known to vary spatiotemporally and this variation was evident in our data (Figure 3). Methane was the only concentration that did not vary with the sampling depth, temperature, or residence time, suggesting that methane concentrations might not be as prone to flow path effects or potential diffusion from the vadose zone as the other two variables – DO and DOC -- could be. However, the three concentrations were all significantly related. We had expected this because we had expected that all concentrations would be spatiotemporally correlated and therefore correlated with each other.

We then progressed to using the linear mixed effects models to assess correlations between the variables. We therefore evaluated linear mixed effects models including as fixed effects the day term and sampling depth and as a random intercept the well of collection, thereby accounting for variation occurring from spatiotemporal correlation. We compared base models including these terms to models including temperature, residence time, DO, and either DOC or methane (Table 3). We found that even after accounting for spatiotemporal correlation in the base models, methane and temperature were significant predictors of DOC, with methane being the most improvement to the base model (Table 4). This suggested that methane and DOC were indeed correlated more extensively than both being affected by location and time of year. Similarly, dissolved oxygen, DOC, and residence time were significant predictors of methane, with DO making the biggest improvement to the base model. This suggested that DO and methane were also correlated more extensively than joint spatiotemporal correlation.

Results, Objective 2, Approach 1: Trophic positions of aquifer macroinvertebrates and meiofauna

The plot of $\delta^{15}N$ residuals vs $\delta^{13}C$ showed clear differences between species which corresponded with trophic levels that have previously been determined using ecological observation (DelVecchia et al. 2016) (Fig. 5, Table 5). The average invertebrate trophic enrichment factor is 2.2 ‰ (Fry 2006), so consumers should be 2.2 ‰ heavier than their food source. Therefore, species with intercepts differing by at least 2.2 ‰ were considered one trophic level apart. Both *K. perdita* and *P. frontalis* were significantly more enriched in ^{15}N than *I. grandis* or *I. integra*, and all *Isocapnia* species appeared to feed at approximately the same trophic level. This suggested that *K. perdita* and *P. frontalis* were more carnivorous than Isocapnia species. We also have observed *P. frontalis* and *K. perdita* consuming early instar larvae.

The differences in $\delta^{15}N$ values between stoneflies and organic matter pools were sufficiently different to show more than one trophic level of separation. The same was true of the other consumers and organic matter classes. However, $\delta^{13}C$ was significantly more depleted in stoneflies than in all OM, meiofauna, and amphipod species examined. This suggested that we did not measure a highly methane-derived organic carbon source that could be directly assimilated by the stoneflies. This could indicate either a) that we did not measure MOB-dominated biofilms, b) that stoneflies were preferentially feeding on MOB, or c) that additional intermediate trophic level MDC consumers were not measured (e.g. early-instar larvae).

We also found that $\delta^{13}C$ signatures varied between species, suggesting in this case varying levels of MDC in biomass (Figure 5). It also suggested a complexity to the food web,

because stoneflies could differ in their access to MDC resources. For example, as methane in the Nyack aquifer was generally produced methanogenically, methane was likely produced in anoxic environments and oxidized at oxic-anoxic interfaces (Bussmann et al. 2006). Differences in $\delta^{13}C$ could then have arisen from species' variable abilities to access the interface where MOB flourished.

Analysis Methods, Objective 2, Approach 2: Potential adaptations of select stonefly species

Stonefly respirometry

I. grandis and *K. perdita* individuals both survived down to near-anoxia (<0.1 mg O_2/L) or anoxia (Figure 6). *I. grandis* 1 stayed below 5% DO saturation for 4.7 hrs, below 1% DO saturation for 47 minutes, and below 0.1% DO saturation for 29 minutes. It then recovered in DO saturated water after 33 minutes recovery in 2 minutes. *I. grandis* 2 was removed at 0% DO saturation and recovered in DO saturated water after 2 minutes. Lines shown are Loess curves with span=0.7. No data existed for the *K. perdita* individual other than that it drew down DO to 0.1 mg/L before dying. While *I. grandis* individuals rapidly dropped their respiration rates as DO %saturation dropped below approximately 25%, *K. perdita* maintained a steady respiration rate throughout the experiment. We concluded that *I. grandis* individuals, given their ability to withstand and recover from anoxia, exemplified a potential ability of the species to withstand anoxic conditions. *K. perdita* was unclear.

Gut content analysis using 16S rRNA sequences

When we analyzed 16S rRNA sequences in stonefly gut contents, we found an average read length of 444 bp, and an average of 41,871 reads per sample. Gut content microbial communities showed the presence of both methanogenic and methanotrophic taxa (Table 6 and Figure 7). The presence of methanogenic taxa in gut contents could suggest that the stoneflies were able to consume resources from anoxic zones, whereas the presence of MOB in gut contents suggested ability to access an oxic-anoxic interface. While we acknowledge the possibility of incorporating gut microbiota into the sample, we consider it more likely that results indicate gut contents given that we used established dissection methods (Blankenship and Yayanos 2005, Deagle et al. 2005).

Methanogenic and methanotrophic taxa were most abundant in samples collected from well HA10. If indeed gut contents qualitatively reflect the microbial communities present in stonefly diets, then the abundance of these taxa in HA10 samples associates well with the fact that HA10 is one of two wells on the floodplain that commonly experiences hypoxia and has measurable methane concentrations. However, samples collected in well HA12, another well with hypoxia and measurable methane concentrations, did not have higher proportions of methanogenic and methanotrophic taxa than the other samples.

Results, Objective 2, Approach 3: relationships between local biogeochemical dynamics and stonefly trophic positions

We found that both MDC and $\delta^{15}N$ residuals were correlated with species and well of collection, but not the day term (ANOVA, $p<10^{-16}$, n=751). When we used the subset data to compare each of these values to environmental variables, our linear regression analysis showed

that none of our biogeochemical variables greatly improved predictions of $\delta^{15}N$ residuals or MDC. However, the combination of day of collection, residence time, and methane predictors resulted in our highest adjusted R^2 value of 0.24 (Table 7). Our linear mixed effects model analysis accounted for the day of collection, species, and well before considering biogeochemical predictors, but showed that inclusion of biogeochemical variables made little improvement to the models (Table 8).

The significance of the day and location of collection in all analyses indicated that the stoneflies' diets varied significantly even within species. The variation in MDC values indicated that the stoneflies did not rely upon consistent basal carbon resources, either because their direct consumption varied across species, or because a consistent direct food source had high variation in MDC. However, the high levels of $\delta^{13}C$ depletion relative to measured biofilm $\delta^{13}C$ and all OM $\delta^{13}C$ combined with observations of amorphous biofilm and organic matter in gut contents clearly suggested that the stoneflies selectively assimilated carbon from methanogenic/methanotrophic microbial components, whether this was a direct choice or one which had moved up the food web. The lack of significance of biogeochemical variables, which could turn over on more rapid time scales, implied that the stoneflies were accessing resources either not directly measurable within well (e.g. fine-scale redox interfaces or hot spots of microbial production), not associated with the biogeochemical variables we measured, or associated with the long-term character of the well rather than immediate conditions (e.g. underlying geology).

Results, Objective 2, Approach 4: relationships between local biogeochemical dynamics and stonefly species assemblages

After clipping the dataset to sampling events which met all of our assumptions (methods), we compared stonefly nymph and amphipod species relative abundance values to the biogeochemical characteristics of each sampling event using the non-metric multidimensional scaling (NMDS) analysis in the vegan package in R (Oksanen et al. 2016). As we could only consider species with raw abundance values >0 for the majority of sampling events, we considered *I. crinita, I. grandis, I. integra, K. perdita, P. frontalis,* and *Stygobromous spp.* After running the NMDS modeling process with a max of 100 iterations, we achieved a stress value of 0.09 and proceeded to compare results to biogeochemical predictors. We found that after accounting for the well of collection, methane and DO concentrations were both significant predictors of community assemblages (Figure 8 and Table 8). Together these variables explained 22% of the variation in community assemblages. Methane concentrations alone explained 19% of the variation.

K. perdita and *I. integra* were consistently found at lower methane concentrations and higher dissolved oxygen concentrations, while *I. crinita* was commonly found at higher methane concentrations. *Stygobromous spp*. tended to cluster at higher DOC concentrations. P. frontalis *and I. grandis* clustered at the lower end of the DO gradient at intermediate methane concentrations.

Discussion

Our first objective was to understand how DOC and methane dynamics were related to each other and to other biogeochemical and hydrologic variables. Our results matched with what we would have expected under these two conditions: methane production and assimilation is

controlled by dissolved oxygen conditions (i.e. methanogenesis occurs anaerobically) (Stanley et al. 2016); and methane cycling stimulates production as evident by dissolved organic carbon concentrations (e.g. as suggested by Helton et al. 2015). Indeed, all modeling approaches agreed that methane concentrations were best predicted by considering the sampling event and dissolved oxygen concentrations, while dissolved organic carbon concentrations were best predicted by dissolved methane concentrations.

The correlation between DOC concentrations and methane concentrations on the Nyack floodplain suggested that either a) that carbon fixation occurred via methanogenesis, or b) that an external methane source (if present) could have stimulated production of DOC at specific sites. In fact, DelVecchia et al. (2016) showed that methane measured in the Nyack aquifer was mostly methanogenic, but could have included a thermogenic contribution at HA10. These findings, combined with those of Helton et al. (2015) showing that labile DOC increased along flow paths, our evidence that DOC concentrations were extremely low at all sites sampled (<2mg/L), and the carbon limitation present in the aquifer (Craft et al. 2002b) strongly suggest that methanogenic carbon fixation is a significant contribution to the aquifer DOC supply. This conclusion was supported by our analysis of 16S rRNA sequences, which revealed the presence of hydrogenotrophic methanogens.

The correlation between methane concentrations and dissolved oxygen concentrations was most informative when considering that stoneflies across the floodplain had methane derived carbon in their biomass, that hypoxia was only present in the wells that did have methane concentrations, and that all methanogens documented in the 16S analysis were strict anaerobes. As insect tissue $\delta^{13}C$ values have been found to turn over at rates of 6 hours to 22 days (Ostrom 1996), we do expect that stonefly biomass $\delta^{13}C$ values do, to an extent, reflect food resources

found in the vicinity of a well, even if they are mobile. Together these show that the aquifer must contain fine-scale biogeochemical cycling, because methane must have been produced in zones of anoxia and consumed where oxygen was present, yet even where methane was not documented it showed presence in the food web. We therefore suspect that the aquifer contains fine-scale biogeochemical heterogeneity such that anoxic pockets are present for the production of methane via anaerobic methanogenesis, as has been shown for oxygen (Malard and Hervant 1999). Because this methane is oxidized rapidly in oxic conditions (Bussmann et al. 2006), perhaps methane is only measurable where anoxic pockets are prevalent enough to show a DO decrease in the well itself.

However, given the carbon limitation present in the aquifer, it was surprising that methane was measurable even in oxic conditions at wells HA10 and HA12. Given that we used a low-flow peristaltic pump to sample water from the wells, we do not expect to have greatly disturbed anoxic and oxic pockets during the pumping process. Furthermore, pumping experiments showed that methane concentrations in the wells were high in wells HA10 and HA12 both before and after disturbing the surrounding water column using the gas diaphragm pump (DelVecchia et al. unpublished data). Therefore, the only likely explanation for methane concentrations being measurable in oxic conditions is that the rate of methane production and diffusion into oxic zones surpassed the rate of methane oxidation in the oxic zones. This could result from a biogeochemical limit to methane oxidation (e.g. by mineral nitrogen, Bodelier and Laanbroek 2004), or top-down control from stoneflies grazing on methanotrophs (e.g. Devlin et al. 2015). We believe that the controls on methane oxidation in the Nyack aquifer merit further experimentation and observation.

Our second objective was to resolve relationships between methane biogeochemical dynamics and the trophic and community ecology of hyporheic stoneflies. We used four approaches: 1) we studied a subset of the aquifer food web; 2) we explored potential adaptations of various stonefly species that could facilitate them to access methane-derived carbon resources; 3) we analyzed relationships between local biogeochemical dynamics and stonefly trophic positions; 4) we analyzed relationships between local biogeochemical characteristics and stonefly species assemblages. Overall, our findings from these four approaches showed that aquifer macroinvertebrates were consistently distinguished in their ecological niche space by both the proportions of methane derived carbon in their biomass and their relative abundance in relation to methane and dissolved oxygen concentrations. The differences between species could be attributed to their diet preferences or their ability to withstand the oxic-hypoxic interface.

When we used the full dataset (n=751) to construct the stable isotope biplot in approach (1), we found that both the species and well of collection were significant in determining stonefly biomass MDC and $\delta^{15}N$ residuals. This suggested intra-species and inter-species variation. Each stonefly species not only varied in basal carbon resources but also in the trophic levels at which they fed, as shown by the variation in $\delta^{15}N$ residuals. While trophic position (the combination of isotopic signatures) was significantly different between species, individual signatures were also significantly affected by the day of collection, DO, and dissolved methane concentrations as shown by the linear regressions and linear mixed effects models in approach (3). This showed niche partitioning between species both in basal carbon resources and in trophic level, helping to explain how such diversity might exist in the aquifer. A more complete survey of aquifer meiofauna communities could expand our understanding of the food web. However, approach

(2) helped us to understand what adaptations of stoneflies could facilitate the niche partitioning we observed.

Approach (2) led us to two major conclusions: some stonefly species have the potential for anoxia tolerance, and some stonefly species have also shown consumption of methanogenic and methanotrophic microbes which must be present in the aquifer. The respirometry experiments showed that *I. grandis* has the ability to tolerate anoxia, and *K. perdita* has the ability to tolerate hypoxia at least for a limited time. Despite this approach being limited to these two species, it provided evidence that some amphibitic species with partially hypogean life histories – the larval phase which we analyzed – have the ability to tolerate low oxygen conditions, which could facilitate access to oxic-anoxic interfaces. These findings were similar to those on hypogean crustaceans which can tolerate hypoxia and anoxia for limited times (Malard and Hervant 1999). These crustaceans are able to withstand and move through patches of anoxia, hypoxia, and oxygenated conditions because they maintain low metabolic rates and rapidly synthesize and store fermentable fuels such as glycogen (Malard and Hervant 1999). Additional experimental approaches to determine the adaptability of individual aquifer macroinvertebrates to low DO could quantitatively elaborate the roles of the various aquifer species.

While tolerance to hypoxia and anoxia allowed us to infer whether stoneflies might have the ability to access methane-based food resources, the 16S rRNA sequence analysis showed that *I. grandis* and *P. frontalis* do indeed consume methanogenic and methanotrophic taxa. These findings make the stoneflies similar to lake profundal chironomid larvae, which graze on methane-cycling bacteria and also display highly depleted ^{13}C signatures (Kiyashko et al. 2004, Jones et al. 2008). Furthermore, these findings definitively showed the presence of these

methane-cycling taxa in the aquifer, especially in individuals collected from HA10, where methane was usually present at relatively high concentrations.

When we dissected variation in stable isotope values and biomass methane derived carbon contributions using approach (3), we could not directly and consistently relate stable isotope values to biogeochemical conditions in the well of collection on each sampling event. This could suggest that the well conditions did not reflect the areas in which the stoneflies had been feeding for the stable isotope turnover time preceding collection. In other insects, whole-insect stable isotope turnover time can be 21 days (Ostrom et al. 1996). If the stoneflies have a similar turnover time for whole-insect biomass, these results suggest that the stoneflies are highly mobile or not accessing the resources we measure in-well. Overall, the well of collection was clearly important for predicting stonefly stable isotope values but biogeochemical conditions were not, still showing heterogeneity across the floodplain.

Despite the coherence between biogeochemical measurements and stonefly stable isotope signatures in approach (3), approach (4) showed the importance of these variables in structuring species assemblages. The findings from approach (4) were roughly consistent with conclusions from approaches (1) and (2). In particular, *K. perdita* and *I. integra* were both found most often during low dissolved methane and high DO sampling events as shown by the NMDS analysis; both species were also the least comprised of MDC as shown by the stable isotope analysis in approach (1). *I. crinita* was found at the highest methane concentrations, and was also the species with the highest levels of MDC. In addition, *I. grandis* and *P. frontalis* were present at intermediate levels of both variables and *I. grandis* demonstrated the potential to tolerate hypoxia and anoxia, which we would expect in interfaces between methane production and assimilation zones. Despite the highly oligotrophic nature of the aquifer, multiple stonefly species had

distinct isotopic niches and assemblages which were structured by the availability of dissolved methane, dissolved oxygen, and dissolved organic carbon. Surprisingly, DO and methane were more significant than dissolved organic carbon in structuring species assemblages, updating previous work on the ecological role of aquifer biogeochemistry. Specifically, Datry et al. demonstrated that organic carbon concentrations supplied by surface water recharge were significant in structuring biodiversity (2005).

We concluded from the intersection of the four approaches that the ability of aquifer macroinvertebrates to assimilate MDC was likely related to their ability to tolerate low DO, such as might be found at the interface between methane production and assimilation zones. This was shown by the ability of some species to tolerate hypoxia and anoxia and the role of DO in structuring species assemblages. The value of accessing oxic-anoxic interfaces was shown not only by the high proportions of MDC in biomass, but by the presence of methanogenic and methanotrophic microbes in gut contents as was demonstrated in approach (3). The combination of these findings indicated that the macroinvertebrate species present in the aquifer are each uniquely adapted to survive in the highly oligotrophic environment. These findings also underscored the ecological importance of methanogenic methane production.

Conclusions

In conclusion, we found that methanogenic methane produced within the Nyack aquifer is valuable for stimulating production, as shown by both its correlation with DOC and its significant carbon contribution to consumer biomass. DO affects methane concentrations, and thereby indirectly affects production within the aquifer. Well measurements do not seem to

encompass the range of biogeochemical heterogeneity present on the floodplain, but stonefly tissue indicates that this heterogeneity must be present because methane is a contributor to biomass even in well-oxygenated wells. Our evidence that these biogeochemical variables structure stonefly species assemblages not only shows the ecological importance of methane dynamics, but also emphasizes the unique adaptations present in each species that allow them to coexist in this system. Overall, this study is evidence for the need to reconsider major sources of productivity in highly oligotrophic shallow aquifers.

Literature Cited

Akaike, H. 1974. A new look at the statistical model identification. Automatic Control, IEEE Transactions on 19:716–723.

Akaike, H. 1981. Likelihood of a model and information criteria. Journal of econometrics 16:3–14.

Anderson, M. P. 2005. Heat as a ground water tracer. Ground water 43:951–968.

Appling, A. 2012. Connectivity drives function: carbon and nitrogen dynamics in a floodplain-aquifer ecosystem. Duke University.

Balch, W. E., G. E. Fox, L. J. Magrum, C. R. Woese, and R. S. Wolfe. 1979. Methanogens: reevaluation of a unique biological group. Microbiological Reviews 43:260–296.

Baumann, R. W., A. R. Gaufin, and R. F. Surdick. 1977. The stoneflies (Plecoptera) of the Rocky Mountains. American Entomological Society.

Blankenship, L. E., and A. A. Yayanos. 2005. Universal primers and PCR of gut contents to study marine invertebrate diets. Molecular Ecology 14:891–899.

Bonin, A. 2008. Population genomics: a new generation of genome scans to bridge the gap with functional genomics. Molecular ecology 17:3583–3584.

Bowman, J. 2006. The Methanotrophs — The Families Methylococcaceae and Methylocystaceae. Pages 266–289 *in* M. D. P. Dr, S. Falkow, E. Rosenberg, K.-H. Schleifer, and E. Stackebrandt, editors. The Prokaryotes. Springer New York.

Bussmann, I., M. Rahalkar, and B. Schink. 2006. Cultivation of methanotrophic bacteria in opposing gradients of methane and oxygen. FEMS microbiology ecology 56:331–344.

Caporaso, J. G., J. Kuczynski, J. Stombaugh, K. Bittinger, F. D. Bushman, E. K. Costello, N. Fierer, A. G. Peña, J. K. Goodrich, J. I. Gordon, G. A. Huttley, S. T. Kelley, D. Knights, J. E. Koenig, R. E. Ley, C. A. Lozupone, D. McDonald, B. D. Muegge, M. Pirrung, J. Reeder, J. R. Sevinsky, P. J. Turnbaugh, W. A. Walters, J. Widmann, T. Yatsunenko, J. Zaneveld, and R. Knight. 2010. QIIME allows analysis of high-throughput community sequencing data. Nature Methods 7:335–336.

Conway, N., J. M. Capuzzo, and B. Fry. 1989. The role of endosymbiotic bacteria in the nutrition of Solemya velum: evidence from a stable isotope analysis of endosymbionts and host. Limnology and Oceanography 34:249–255.

Craft, J. A., J. A. Stanford, and M. Pusch. 2002. Microbial respiration within a floodplain aquifer of a large gravel-bed river. Freshwater Biology 47:251–261.

Deagle, B. E., S. N. Jarman, D. Pemberton, and N. J. Gales. 2005. Genetic screening for prey in the gut contents from a giant squid (Architeuthis sp.). Journal of Heredity 96:417–423.

DelVecchia, A. G., J. A. Stanford, and X. Xu. 2016. Ancient methane subsizes contemporary food web.

Doronina, N., E. Kaparullina, and Y. Trotsenko. 2014. The Family Methylophilaceae. Pages 869–880 *in* E. Rosenberg, E. F. DeLong, S. Lory, E. Stackebrandt, and F. Thompson, editors. The Prokaryotes. Springer Berlin Heidelberg.

Ellis, B. K., J. A. Stanford, and J. V. Ward. 1998. Microbial assemblages and production in alluvial aquifers of the Flathead River, Montana, USA. Journal of the North American Benthological Society 17:382–402.

Fry, B. 2006. Stable Isotope Ecology. Springer New York, New York, NY.

Garcia, J.-L., B. Ollivier, and W. B. Whitman. 2006. The Order Methanomicrobiales. Pages 208–230 *in* M. D. P. Dr, S. Falkow, E. Rosenberg, K.-H. Schleifer, and E. Stackebrandt, editors. The Prokaryotes. Springer New York.

Helton, A. M., G. C. Poole, R. A. Payn, C. Izurieta, and J. A. Stanford. 2014. Relative influences of the river channel, floodplain surface, and alluvial aquifer on simulated hydrologic residence time in a montane river floodplain. Geomorphology 205:17–26.

Helton, A. M., M. S. Wright, E. S. Bernhardt, G. C. Poole, R. M. Cory, and J. A. Stanford. 2015. Dissolved organic carbon lability increases with water residence time in the alluvial aquifer of a river floodplain ecosystem. Journal of Geophysical Research: Biogeosciences 120:693–706.

Hoch, M. P., M. L. Fogel, and D. L. Kirchman. 1992. Isotope fractionation associated with ammonium uptake by a marine bacterium. Limnology and Oceanography 37:1447–1459.

Junk, W. J., P. B. Bayley, and R. E. Sparks. 1989. The flood pulse concept in river-floodplain systems. Canadian special publication of fisheries and aquatic sciences 106:110–127.

Kohzu, A., C. Kato, T. Iwata, D. Kishi, M. Murakami, S. Nakano, and E. Wada. 2004. Stream food web fueled by methane-derived carbon. Aquatic Microbial Ecology 36:189–194.

Kruskal, J. B. 1964. Nonmetric multidimensional scaling: a numerical method. Psychometrika 29:115–129.

Lee, R. W., and J. J. Childress. 1994. Assimilation of inorganic nitrogen by marine invertebrates and their chemoautotrophic and methanotrophic symbionts. Applied and Environmental Microbiology 60:1852–1858.

Lowell, J. L., N. Gordon, D. Engstrom, J. A. Stanford, W. E. Holben, and J. E. Gannon. 2009. Habitat heterogeneity and associated microbial community structure in a small-scale floodplain hyporheic flow path. Microbial ecology 58:611–620.

Lumley, T., and A. Miller. 2009. Leaps: regression subset selection.

Masella, A. P., A. K. Bartram, J. M. Truszkowski, D. G. Brown, and J. D. Neufeld. 2012. PANDAseq: paired-end assembler for illumina sequences. BMC Bioinformatics 13:31.

Mouw, J. E. B., J. A. Stanford, and P. B. Alaback. 2009. Influences of flooding and hyporheic exchange on floodplain plant richness and productivity. River Research and Applications 25:929–945.

Oksanen, J., F. G. Blanchet, R. Kindt, P. Legendre, P. R. Minchin, R. O'Hara, G. L. Simpson, P. Solymos, M. H. H. Stevens, and H. Wagner. 2016. vegan: Community ecology package.

Pepin, D. M., and F. R. Hauer. 2002. Benthic responses to groundwater–surface water exchange in 2 alluvial rivers in northwestern Montana. Journal of the North American Benthological Society 21:370–383.

Pinheiro, J., D. Bates, S. Debroy, D. Sarkar, EISPACK authors, S. Heisterkamp, B. V. Willigen, and R-core. 2016. nlme: Linear and Nonlinear Mixed Effects Models.

Poole, G. C., S. J. O'Daniel, K. L. Jones, W. W. Woessner, E. S. Bernhardt, A. M. Helton, J. A. Stanford, B. R. Boer, and T. J. Beechie. 2008. Hydrologic spiralling: the role of multiple interactive flow paths in stream ecosystems. River Research and Applications 24:1018–1031.

Poole, G. C., J. A. Stanford, C. A. Frissell, and S. W. Running. 2002. Three-dimensional mapping of geomorphic controls on flood-plain hydrology and connectivity from aerial photos. Geomorphology 48:329–347.

R Core Team. 2016. R: A Language and Environment for Statistical Computing. R Foundation for Statistical Computing, Vienna, Austria.

Reid, B. L. 2007. Energy flow in a floodplain aquifer ecosystem. The University of Montana.

SILVA Terms of Use/License Information. 2015, February. . http://www.arb-silva.de/fileadmin/silva_databases/qiime/LICENSE.txt.

Smith, M. G., S. R. Parker, C. H. Gammons, S. R. Poulson, and F. R. Hauer. 2011. Tracing dissolved O 2 and dissolved inorganic carbon stable isotope dynamics in the Nyack aquifer: Middle Fork Flathead River, Montana, USA. Geochimica et Cosmochimica Acta 75:5971–5986.

Stanford, J. A., M. S. Lorang, and F. R. Hauer. 2005. The shifting habitat mosaic of river ecosystems. Verh. Internat. Verein. Limnol. 29:123–136.

Stanford, J. A., and J. V. Ward. 1993. An ecosystem perspective of alluvial rivers: connectivity and the hyporheic corridor. Journal of the North American Benthological Society 12:48–60.

Stanley, E. H., N. J. Casson, S. T. Christel, J. T. Crawford, L. C. Loken, and S. K. Oliver. 2016. The ecology of methane in streams and rivers: patterns, controls, and global significance. Ecological Monographs:n/a–n/a.

Stewart, K. W., B. P. Stark, and others. 1988. Nymphs of North American stonefly genera (Plecoptera). Entomological Society of America.

Stolwijk, A. M., H. Straatman, and G. A. Zielhuis. 1999. Studying seasonality by using sine and cosine functions in regression analysis. Journal of epidemiology and community health 53:235–238.

Thorp, J. H., and M. D. Delong. 1994. The riverine productivity model: an heuristic view of carbon sources and organic processing in large river ecosystems. Oikos:305–308.

Thorp, J. H., and M. D. Delong. 2002. Dominance of autochthonous autotrophic carbon in food webs of heterotrophic rivers. Oikos 96:543–550.

Tockner, K., and J. A. Stanford. 2002. Riverine flood plains: present state and future trends. Environmental conservation 29:308–330.

Valett, H. M., F. R. Hauer, and J. A. Stanford. 2014. Landscape influences on ecosystem function: local and routing control of oxygen dynamics in a floodplain aquifer. Ecosystems 17:195–211.

Vannote, R. L., G. W. Minshall, K. W. Cummins, J. R. Sedell, and C. E. Cushing. 1980. The River Continuum Concept. Canadian Journal of Fisheries and Aquatic Sciences 37:130–137.

Ward, J. V., and J. A. Stanford. 1983. The serial discontinuity concept of lotic ecosystems. Dynamics of lotic ecosystems 10:29–42.

Yamamoto, S., J. B. Alcauskas, and T. E. Crozier. 1976. Solubility of methane in distilled water and seawater. Journal of Chemical and Engineering Data 21:78–80.

Zenger, J. T., and R. W. Baumann. 2004. The Holarctic winter stonefly genus Isocapnia, with an emphasis on the North American fauna (Plecoptera: Capniidae). Monographs of the Western North American Naturalist 2:65–95.

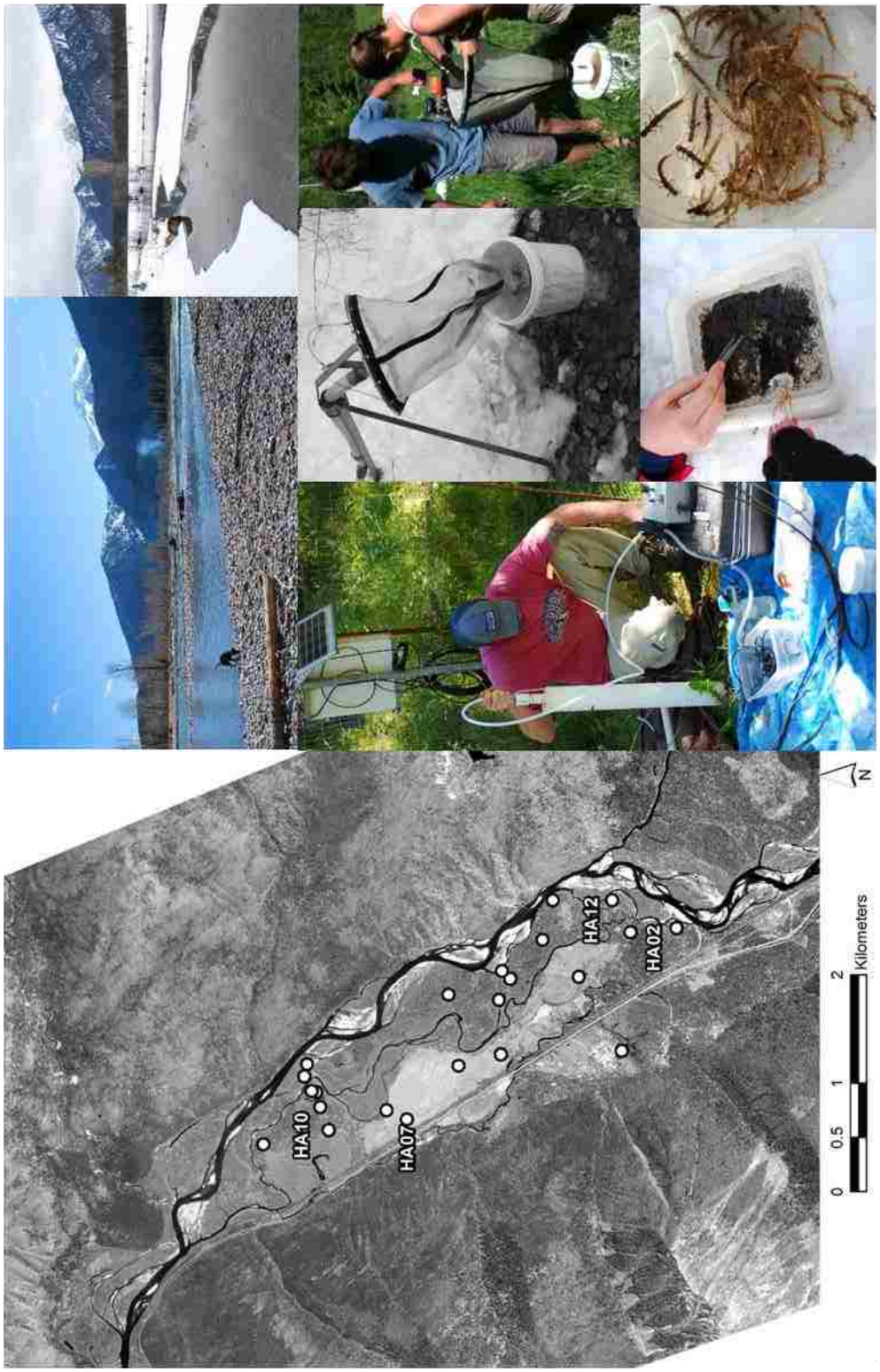
HA10
HA07
HA12
HA02
N
0
0.5
1
2
Kilometers

Figure 1. A. A view of the Middle Fork of the Flathead, close to the head of the floodplain. The cottonwood and spruce galleries, large woody debris, and active scour bars demonstrate the dynamic nature of the floodplain. B. Beaver Creek is completely groundwater fed in the winter and is an example of a crucial off channel habitat on the floodplain. C. A volunteer assists by holding pumping gear for collection of water samples for dissolved oxygen, dissolved organic carbon, and dissolved methane. RiverNet sensor setup is in the background. D. Insect samples were collected by using a diaphragm pump to filter water through mesh 330 micron netting. E. Volunteers rinse netting to collect groundwater macroinvertebrates. F. Even in winter months, the groundwater is kept at near mean annual air temperature, making it a suitable habitat for the macroinvertebrates. G. An example collection from one pumping event on the floodplain – each insect in this example is approximately 2.5 to 3 cm long.

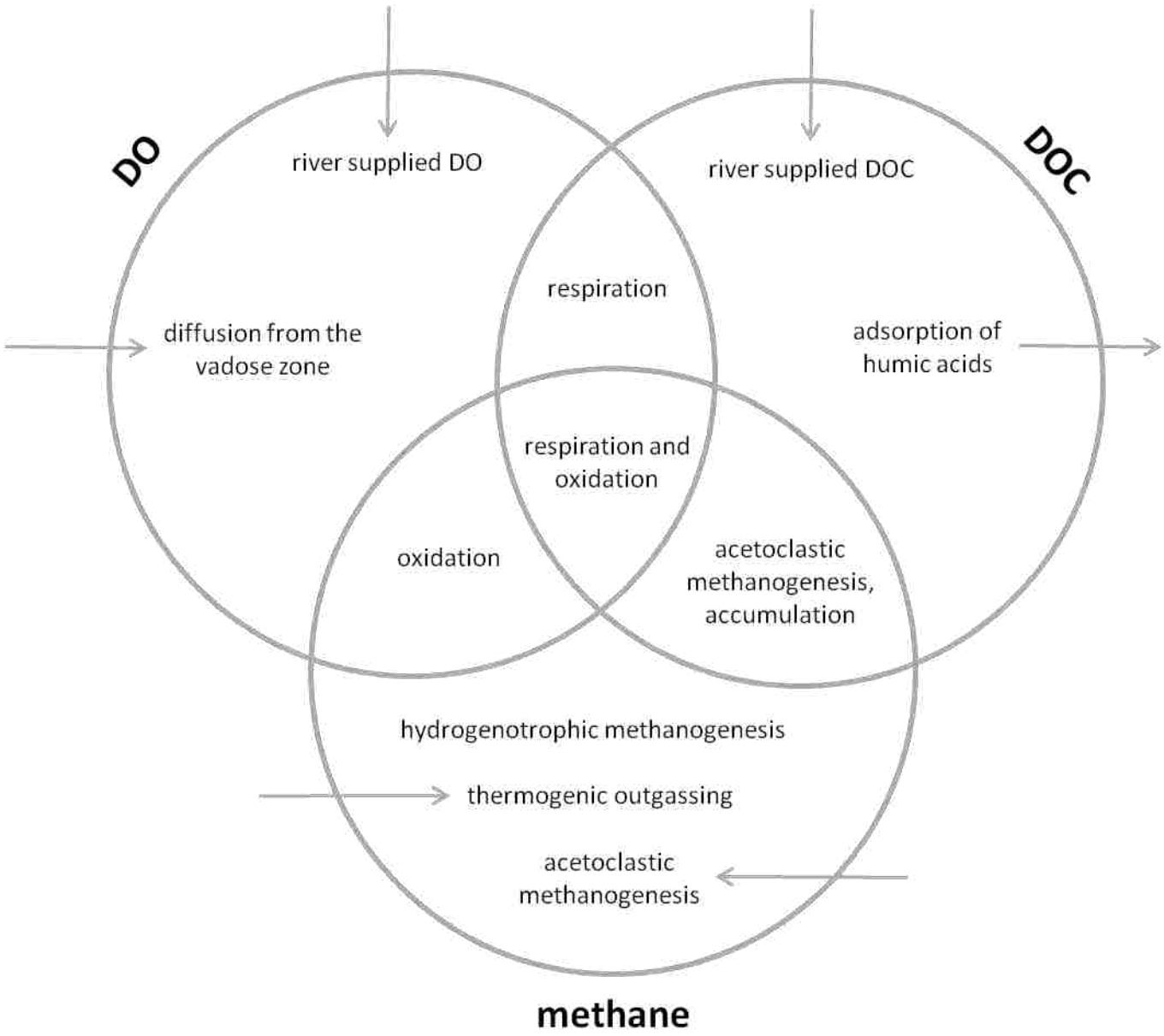

Figure 2. A simplified representation of processes that affect concentrations of the three focal biogeochemical constituents along flowpaths. Overlaps indicate interactive processes, or those which occur when both constituents are present. Arrows in and out indicate external subsidies or exports. All constituents can change from flowpath mediated processes (e.g. respiration of river supplied nutrients along flowpaths) or from spatial subsidies (e.g. fossil methane subsidy, stored OM, or a vadose zone interaction).

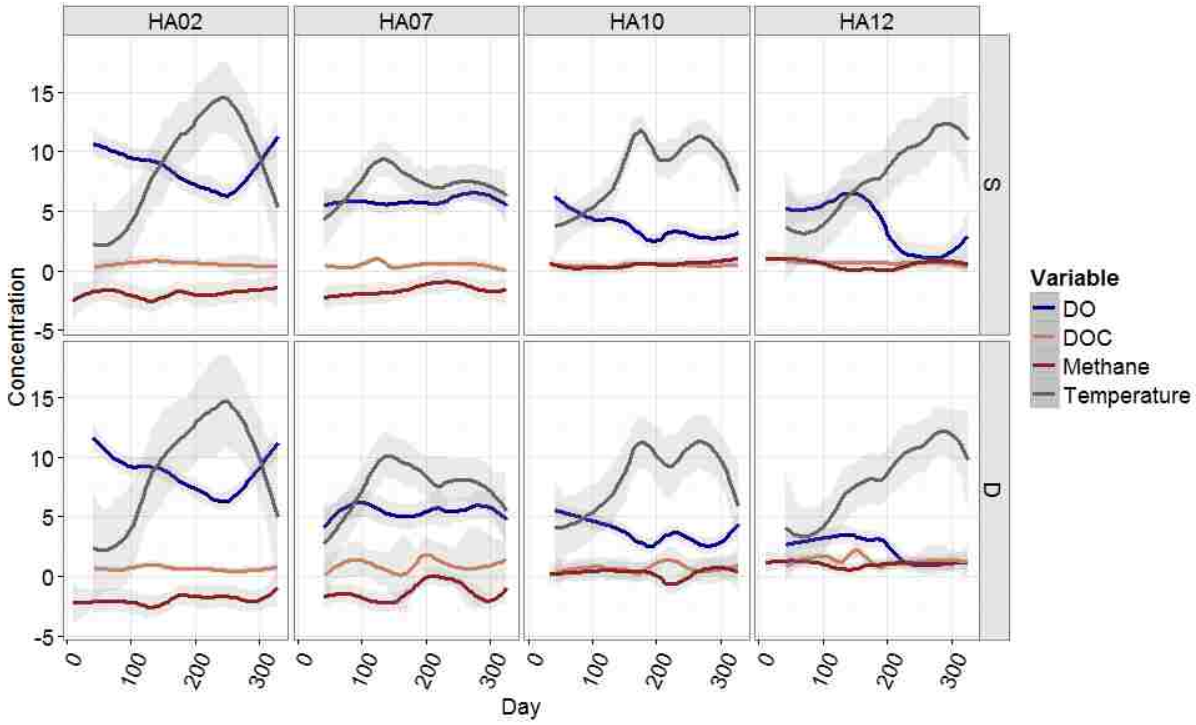

Figure 3: Loess curves (span=0.5) of temporal patterns of biogeochemical constituent concentrations in four of the wells (HA02, HA07, HA10, HA12) which represent a broad range of characteristics. HA02 is in the parafluvial zone with a RT of 45 days, so it receives more river-supplied DO and DOC, with negligible methane concentrations. HA07 and HA12 are both at longer flowpaths in the orthofluvial zone, but HA12 is often hypoxic in the summer months and has measurable methane concentrations. Methane is expressed in terms of log(umol/L), while DO and DOC are expressed in terms of mg/L.

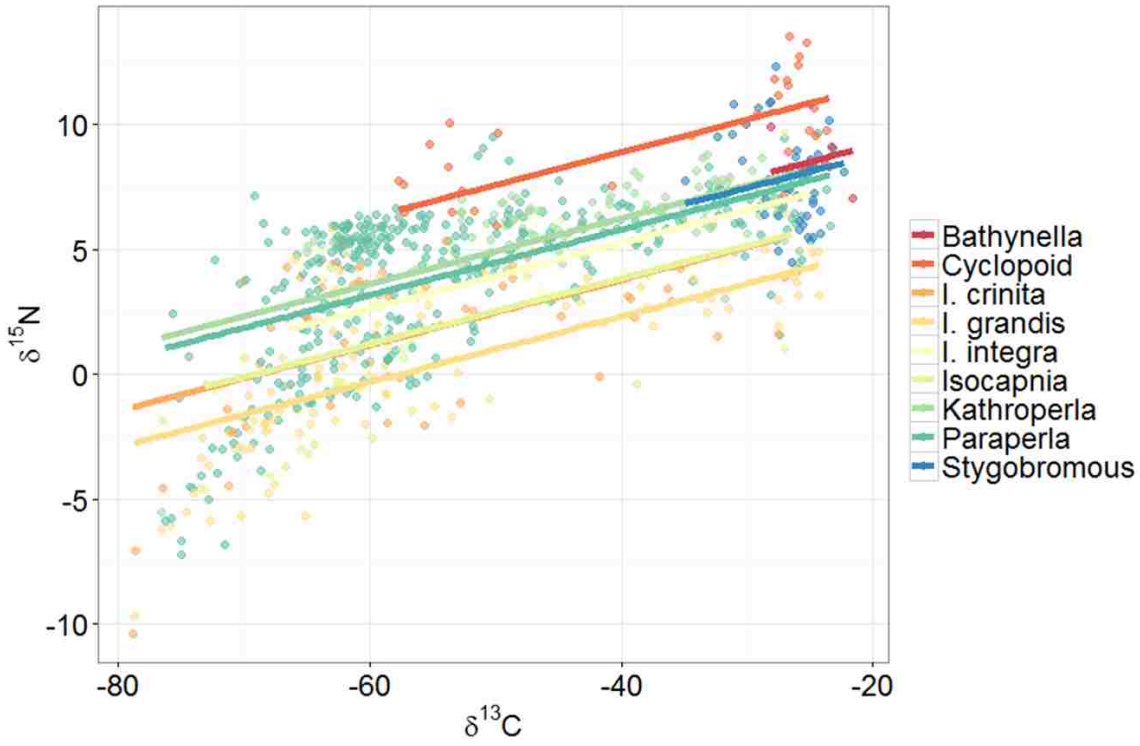

Figure 4. $\delta^{15}N$ values are known to be depleted in methanotrophs and higher trophic levels which use methane derived carbon, thereby causing $\delta^{15}N$ and $\delta^{13}C$ to be correlated in methane-dependent food webs. We therefore used the linear regression of these stable isotope signatures to account for changes in $\delta^{15}N$ as a result of methane assimilation, then regarded the intercepts as more indicative of changes in $\delta^{15}N$ caused by trophic level differences alone. Linear regression is shown with 95% confidence interval.

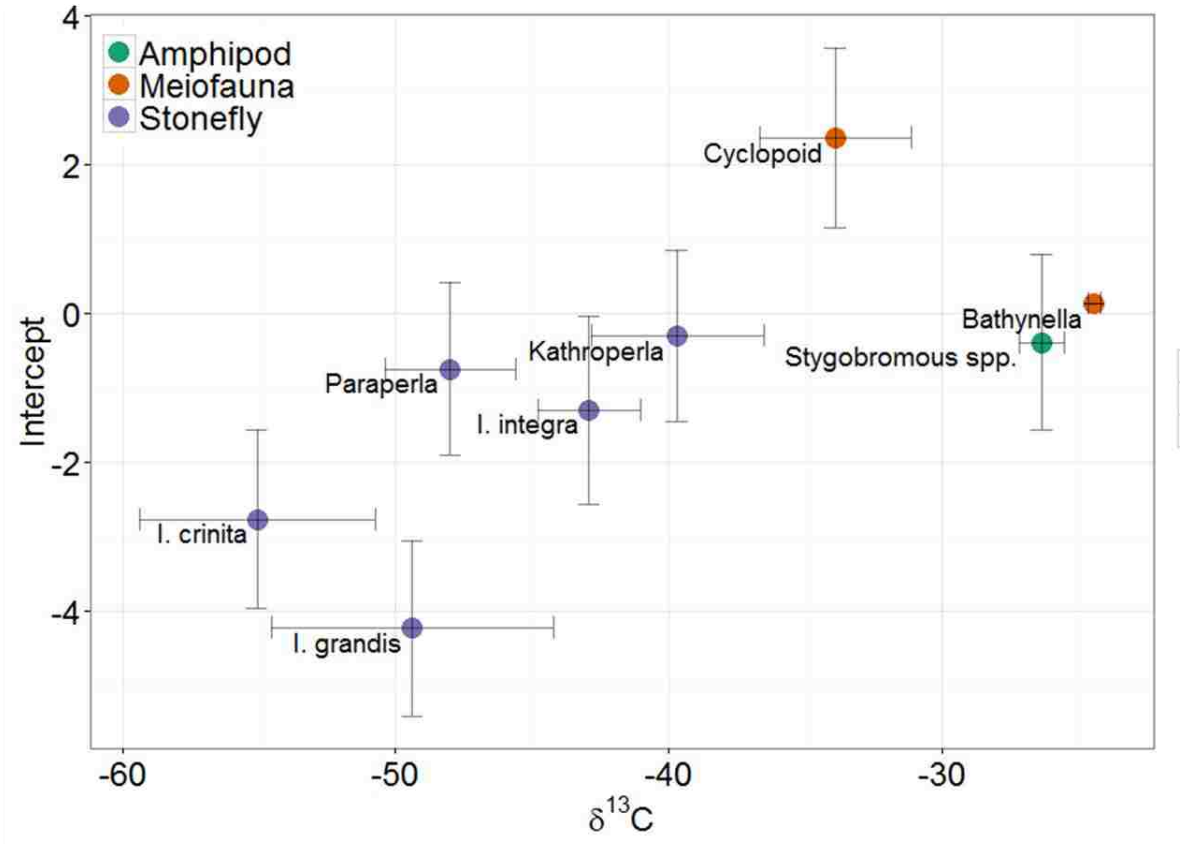

Figure 5. A biplot of stable isotope values (intercepts from the relationship shown in Figure 4 vs δ^{13} C values) for each organism in the aquifer for which we had data. Bars represent standard error. Information on collection and sample sizes is displayed in Table 6. Periphyton estimates adapted from Michelle Anderson.

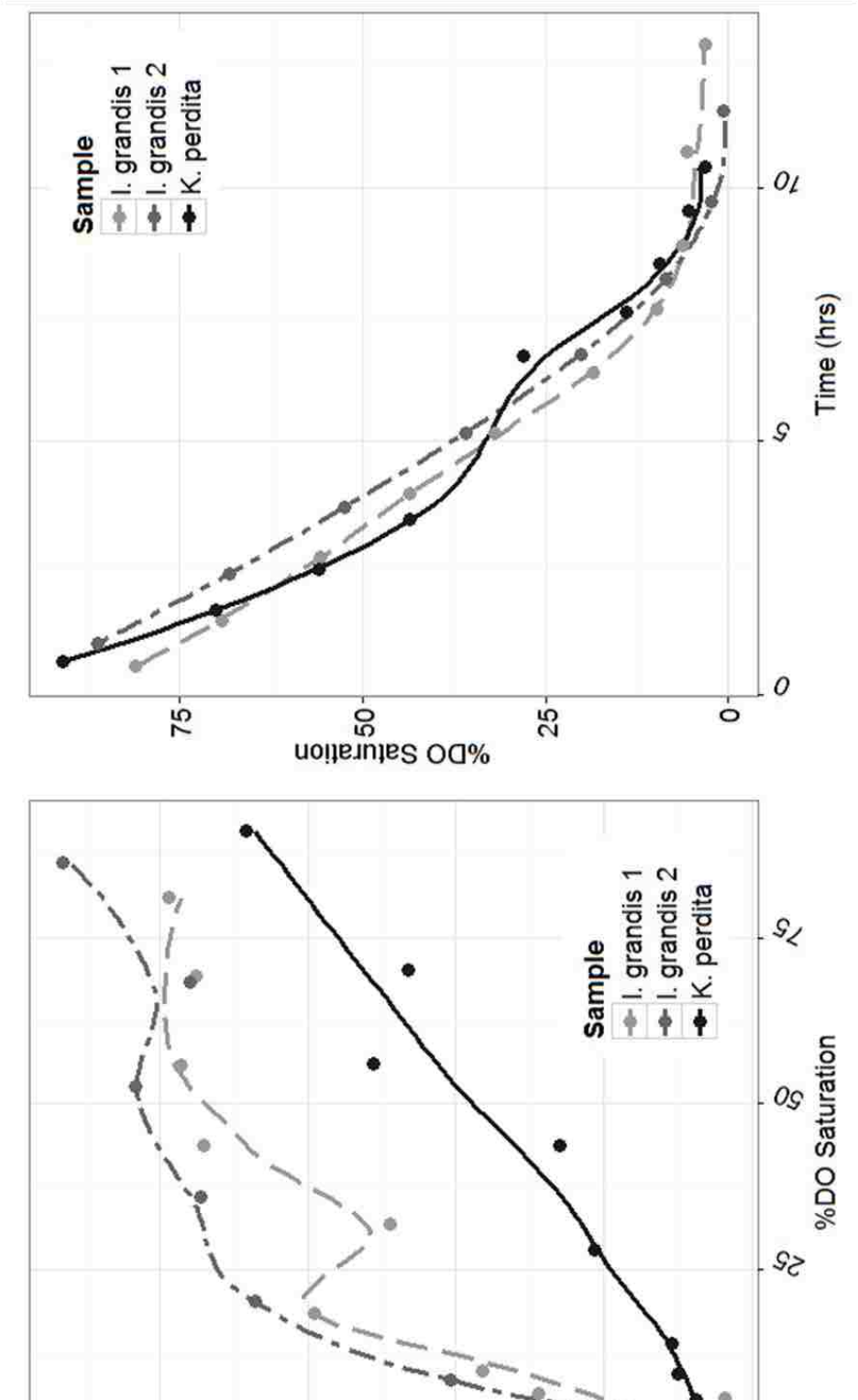
Sample
I. grandis 1
I. grandis 2
K. perdita
%DO Saturation
0
25
50
75
0
5
10
Time (hrs)
Sample
I. grandis 1
I. grandis 2
K. perdita
%DO Saturation
25
50
75

Figure 6. Three individual stoneflies were included in respirometry experiments in August 1994, showing the potential for these organisms to survive in low dissolved oxygen conditions for extended periods of time. I. grandis 1 stayed below 5% DO saturation for 4.7 hrs, below 1% DO saturation for 47 minutes, and below 0.1% DO saturation for 29 minutes. It then recovered in DO saturated water after 33 minutes recovery in 2 minutes. I. grandis 2 was removed at 0% DO saturation and recovered in DO saturated water after 2 minutes. Lines shown are Loess curves with span=0.7.

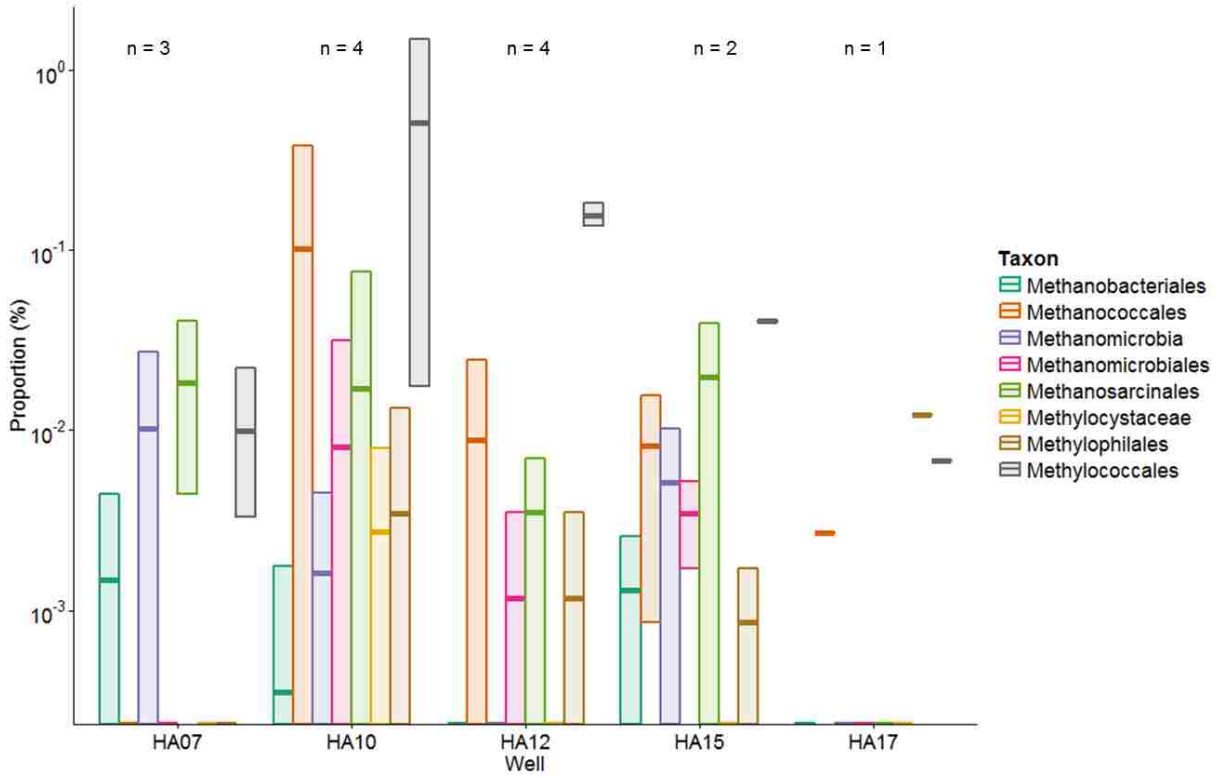

Figure 7. Mean, minimum, and maximum values for the percentage contribution of each methanogen and methanotroph taxon to total number of 16S rRNA sequences identified in stonefly gut contents from each well. The numbers above each set of bars indicate the total number of individuals examined for each well. All individuals except those collected from HA07 were *P. frontalis*, while HA07 individuals were solely *I. grandis*. Functional ecology for each taxon is displayed in Table 7.

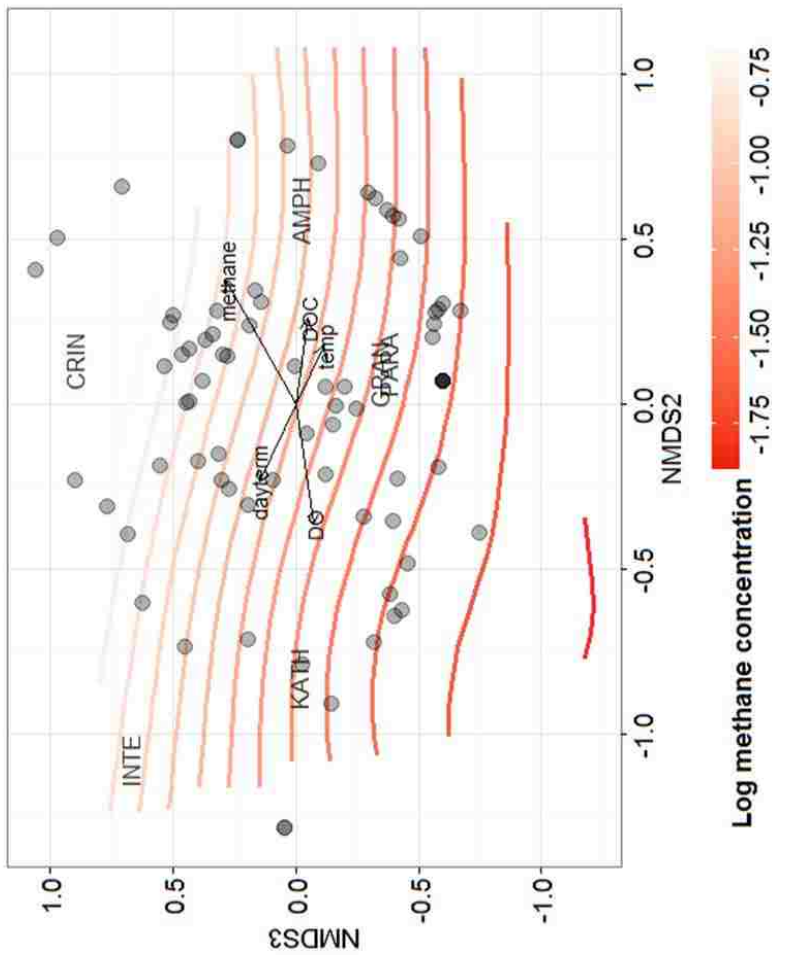
NMDS3
NMDS2
1.0
0.5
0.0
-0.5
-1.0
CRIN
INTE
KATH
AMPH
GRAN
PARA
methane
DOC
temp
daytem
DO
Log methane concentration
-0.75
-1.00
-1.25
-1.50
-1.75

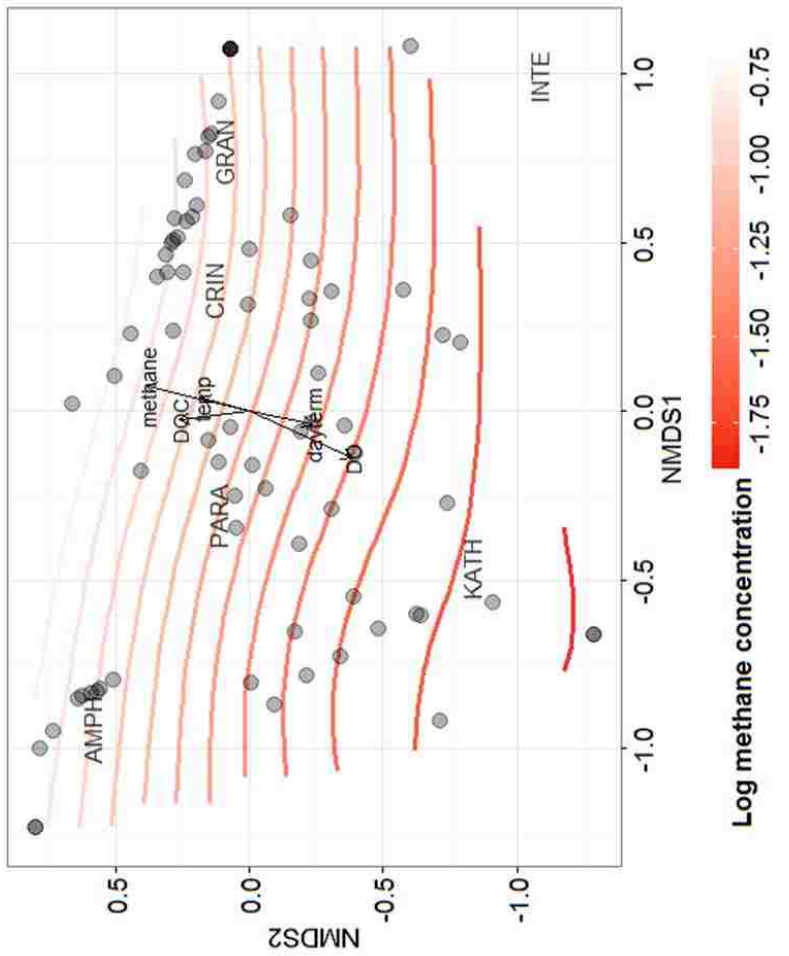
NMDS2
NMDS1
1.0
0.5
0.0
-0.5
-1.0
AMPH
GRAN
CRIN
INTE
PARA
KATH
methane
DOC
temp
daytem
DO
Log methane concentration
-0.75
-1.00
-1.25
-1.50
-1.75

Figure 8. NMDS plots for stonefly species assemblages in relation to concentrations of DO, DOC, temperature, methane, the well of collection, and the day of collection. Arrows represent the strength and direction of correlations with each of the biogeochemical constituents. Distances are Bray-Curtis. Correlation coefficients and significance values are displayed in Table 10.

Table 1. Well residence times and coordinates

Well	Easting (UTM)	Northing (UTM)	Shallow Residence Time (Days)	Deep Residence Time(Days)
HA01	291112	5370422	164.1	219.9
HA02	292244	5369912	45.4	60.5
HA04	291796	5370827	54.2	139.0
HA05	291080	5371541	180.1	270.2
HA06	290976	5371934	156.4	217.8
HA07	290489	5372413	156.4	217.8
HA08	290564	5372617	210.6	263.0
HA09	290386	5373176	178.0	284.5
HA10	290586	5373203	117.4	146.8
HA12	292484	5370507	119.7	179.7
HA13	292498	5371054	46.9	159.6
HA15	291560	5371559	133.3	210.3
HA16	291770	5371453	167.1	304.5
HA17	291846	5371524	167.1	304.5
HA18	291626	5372018	110.1	221.9
HA19	290984	5373323	147.8	291.7
HA20	290870	5373349	147.8	291.7
SarN	290740	5373291	130.7	277.3
SarS	290731	5373249	117.4	146.8

Table 2. Pearson correlation coefficients and ANOVA significance values were calculated for each of the interacting variables independently. Bold values are <0.05 p values. Many variables are known to change along flowpaths and thus many were deemed significant in this preliminary test. However, we suspect that the residence time was rarely significant in this procedure because the residence time estimates were similar for many of the wells (Table 1).

Sampling Depth		Day term			Residence Time		
ANOVA	n	Pearson	ANOVA	n	Pearson	ANOVA	n
<0.0001	367	0.259, **<0.0001**	**<0.0001**	479	-0.110, **0.016**	**0.003**	479
<0.0001	367	-0.095,0.084	**0.004**	329	-0.063, 0.251	**0.001**	329
0.6319	367	-0.101, **0.015**	**0.003**	566	0.025, 0.54	0.445	566

		DO			DOC			Methane		
	n	Pearson	ANOVA	n	Pearson	ANOVA	n	Pearson	ANOVA	n
	227				-0.19, <**0.0001**	**0.007**	271	-0.526, **<.0001**	**<0.0001**	479
	232	-0.19, **0.001**	**0.017**	271				0.323, **<.0001**	**<0.0001**	329
	232	-0.526, <**0.001**	**<0.0001**	479	0.323, **<0.0001**	**<0.0001**	329			

Table 3. Linear mixed effects model summary statistics are displayed for all combinations of predictors assessed for each DOC and methane concentrations. AIC scores represent the Akaike Information Criterion. Bold models are those which we considered best. All models included the well of collection as a random effect and the day term and sampling depth as fixed effects. We performed the analysis as such in order to assess which predictors could improve the model once variation caused by the nuances of sampling were accounted for.

Fixed effects (Dependent: log(DOC))	AIC	Log Likelihood
Dayterm	-146.9	77.4
Dayterm + SD	-176.7	93.3
Dayterm + SD + log(methane)	**-182.1**	**97.1**
Dayterm + SD + Temp	-178.4	95.2
Dayterm + SD + RT	-174.7	93.3
Dayterm + SD + DO	-177.3	94.6
Dayterm + SD + log(methane) + Temp	**-184.7**	**99.4**
Dayterm + SD + log(methane) + Temp + DO	-182.8	99.4

Fixed effects (Dependent: log(methane))	AIC	Log Likelihood
Dayterm	516.1	-254.0
Dayterm + SD	517.3	-253.6
Dayterm + SD + log(DOC)	513.3	-250.6
Dayterm + SD + Temp	518.3	-253.2
Dayterm + SD + RT	517.1	-252.5
Dayterm + SD + DO	**501.7**	**-244.9**
Dayterm + SD + DO + log(DOC)	499.2	-242.6
Dayterm + SD + DO + log(DOC) + ResTime	**499.1**	**-241.5**

Table 4. Coefficients from the best linear mixed effects models indicated in Table 4. Bold values indicate significance ($p<0.05$).

Predictor	Log(DOC)		Log(methane)	
	3 term	4 term	3 term	5 term
Intercept	**-0.255**	**-0.329**	**-0.582**	**-0.983**
Dayterm	**-0.035**	-0.008	**-0.139**	**-0.114**
Depth (Shallow)	**0.114**	**0.105**	-0.036	0.113
Log(methane)	**0.038**	**0.041**		
Log(DOC)				**0.603**
DO			**-0.124**	**-0.117**
Residence Time				0.002
Temperature		**0.012**		

Table 5. Total number of individuals, wells from which they were collected, and datasets of origin are displayed with means and standard errors for each $\delta^{13}C$, $\delta\ ^{5}N$, and $\delta\ ^{5}N$ residuals.

Table 6. Functional ecology for each taxon in Figure 6. *Bonin and Boone 2006, ^Balch et al 1979, ‘ Garcia et al, **Bowman 2006, & Doronina 2014

Taxon	Functional Ecology
Methanobacteriales*	Hydrogenotrophic or use formate or alcohols as electron donors, freshwater and marine environments, strictly anaerobic
Methanococcales*^’	Hydrogenotrophic or use formate as electron donor, strictly anaerobic, require NaCl for optimum growth, marine environments, mesophilic to hyperthemophilic, require selenium for growth
Methanomicrobia; other	
Methanomicrobiales’	Hydrogenotrophic or use formate or alcohols as electron donors, freshwater and marine environments, require acetate for growth, mesophilic, strictly anaerobic
Methanosarcinales’	Hydrogenotrophic or acetoclastic, strictly anaerobic, freshwater and marine environments
Rhizobiales; Methylocystaceae**	Type II methanotroph, freshwater environments with steady methane and oxygen supply
Methylophilales&	Non-methanotrophic methylotrophs found in freshwater environments, often in association with methanotrophs
Methylococcales**	Type I methanotroph, freshwater environments with steady methane and oxygen supply

Table 7. Linear mixed effects model summary statistics are displayed for all combinations of predictors assessed for each methane dependence and $\delta^{15}N$ residuals. AIC scores represent the Akaike Information Criterion. Bold models are those which we considered best. All models included the well of collection as a random effect and the day term and sampling depth as fixed effects. We performed the analysis as such in order to assess which predictors could improve the model once variation caused by the nuances of sampling were accounted for.

Fixed effects (Methane dependence – S)	AIC	Log Likelihood
Species	608.39	-297.14
Dayterm	607.73	-296.87
Log(methane)	610.17	-301.1
DO	611.84	-301.92
Log(DOC)	610.90	-301.45
Dayterm + Species	596.89	-290.44
Dayterm + Species + DO	**596.11**	**-289.06**
Dayterm + Species + log(methane)	598.59	-290.30
Dayterm + Species + log(DOC)	598.80	-290.40

Fixed effects (Methane dependence – D)	AIC	Log Likelihood
Species	884.94	-435.47
Dayterm	882.78	-437.39
Log(methane)	887.56	-439.78
DO	887.49	-439.74
Log(DOC)	884.92	-438.46
Dayterm + Species	**881.56**	**-432.78**
Dayterm + Species + DO	883.16	-432.58
Dayterm + Species + log(methane)	883.07	-432.53
Dayterm + Species + log(DOC)	882.22	-432.11

Fixed effects (Resids – S)	AIC	Log Likelihood
Species	278.00	-132.00
Dayterm	318.39	-155.19
Log(methane)	318.66	-155.33
DO	311.82	-151.91
Log(DOC)	315.43	-153.71
Dayterm + Species	**278.20**	**-131.10**
Dayterm + Species + DO	280.19	-131.10
Dayterm + Species + log(methane)	279.20	-130.60
Dayterm + Species + log(DOC)	280.17	-131.09

Fixed effects (Resids – D)	AIC	Log Likelihood
Species	406.84	-196.42
Dayterm	443.66	-217.82
Log(methane)	444.61	-218.30
DO	438.78	-215.39
Log(DOC)	444.23	-218.11
Dayterm + Species	405.54	-194.77
Dayterm + Species + DO	406.78	-194.39
Dayterm + Species + log(methane)	**404.51**	**-193.26**
Dayterm + Species + log(DOC)	407.08	-194.54

Table 8. Correlations and significance values obtained using NMDS of stonefly species assemblages in relation to listed variables. Significance values less than 0.05 are in bold.

	NMDS1	NMDS2	R^2	Pr(>r)
Log(methane)	0.19	0.98	0.160	**0.002**
DO	-0.34	-0.94	0.169	**0.002**
DOC	-0.09	1.00	0.067	0.074
Temperature	0.22	0.97	0.033	0.304
Dayterm	-0.15	-0.99	0.055	0.134
Well			0.310	0.060

	NMDS2	NMDS3	R^2	Pr(>r)
Log(methane)	0.82	0.58	0.221	**0.001**
DO	-0.99	-0.16	0.139	**0.005**
DOC	0.97	-0.23	0.070	0.060
Temperature	0.81	-0.58	0.044	0.180
Dayterm	-0.82	0.57	0.077	0.063
Well			0.192	0.762

Prepared for submission to *The American Naturalist*

Chapter 4: Desynchronized growth and emergence in hyporheic stoneflies (Plecoptera) of the Nyack aquifer, Montana

Final manuscript coauthor: Jack A. Stanford

Abstract

Stoneflies (order: Plecoptera) are some of the most dominant macroinvertebrates in stream ecosystems, yet few of the species identified in North America have known life histories. The stoneflies with known life histories show remarkable synchronicity in emergence in relation to annual temperature patterns. However, little is known about the hyporheic stoneflies – amphibionts that spend their entire larval stages in the interstitial spaces of shallow aquifers before emerging as winged adults. We studied the growth and emergence patterns of five hyporheic species that are notably abundant in the expansive alluvial aquifer (essentially a massive hyporheic zone) of the Nyack Floodplain on the Middle Fork of the Flathead River in Northwestern Montana. We found desynchronized emergence in *Isocapnia crinita, Isocapnia grandis,* and *Isocapnia integra*, with extended emergence periods in *Paraperla frontalis* and *Kathroperla perdita*. None of the species had significant differences in emergence timing. *P. frontalis* additionally had desynchronized growth across the aquifer, with significant effects of well, river, and air temperature patterns. Mean daily air temperature was the only significant predictor of *P. frontalis* emergence, the most abundantly occurring species. We concluded that the constancy of temperature patterns in habitats within this expansive aquifer contributed to

desynchronization of both growth and emergence in hyporheic species, highlighting a behavioral adaptation to the aquifer environment.

Introduction

Plecoptera is one of the most dominant macroinvertebrate orders in cold stream ecosystems (Stewart et al. 1988) in temperate latitudes. It is also one of the most important orders because these species are used as ecological indicators for stream water quality (Armitage et al. 1983). In 1974, the discovery of stonefly nymphs living in subterranean interstitial spaces introduced a new facet to Plecoptera ecology, recognizing some of these species as amphibionts living in the hyporheic zone (Stanford and Gaufin 1974; Gibert et al. 2009). Since then, surprisingly little has been documented regarding the ecology of these hyporheic taxa, which are distributed across the Rockies and Pacific Northwest north to Alaska (Stewart et al. 1988).

Hyporheic stoneflies are amphibionts which spend 1-3 years underground as larvae in the shallow but expansive alluvial aquifers of gravel bedded floodplains (Gibert et al. 1994*b*). These are essentially massive hyporheic zones since predominate recharge is from the river (Boulton et al. 1998). Amphibitic stoneflies display morphological and behavioral adaptations to life in the dark waters of alluvial aquifer systems: larvae have reduced eye size, loss of pigment at early instars, long bodies, reduced wing size, tolerance to hypoxia, and dependence on chemosynthetic carbon resources (Gibert et al. 1994*b*; DelVecchia et al. 2016). These stoneflies presumably travel through the aquifer gradually maturing and then moving to the river channel to emerge as flying or crawling adults. They deposit eggs in the river channel and the newly hatched larvae apparently emigrate into the aquifer in strong contrast to most stonefly species that stay in the

river channel and do not burrow beyond a few centimeters into the saturated bed sediments(Gibert et al. 1994*b*).

Previous study has suggested that Plecoptera require both the accumulation of degree days and a threshold temperature in order to emerge as adults (Ward and Stanford 1982). Emergence has been found to be earlier at lower elevations and in warmer years, and varying emergence patterns can temporally segregate coexistent species (Ward and Stanford 1982). Aboveground habitats contain more temporal temperature variation than the hyporheic and shallow aquifer environments, where temperatures stabilize at longer residence times to closely follow the mean annual air temperature of 6-7°C (; Poole et al. 2008 Stanford et al., 2016). Reduced temperature amplitude is expected to cause emergence patterns to desynchronize.

Indeed, growth of a cavernicolous stonefly: *Protonemura gev*i, a Palearctic cave stonefly of the Iberian peninsula, Spain, was desynchronized in the constantly dark and stable temperatures of the cave environment, with a wide range of sizes are present at a given sampling time (López-Rodríguez and de Figueroa 2012). Still, the cave environment, at 50m from opening to stream pool, is orders of magnitude smaller than the vast shallow aquifer environment in which hyporheic stoneflies persist. Thus, more desynchrony might be expected in the aquifer where degree day accumulations and temperature thresholds have more potential to vary over longer residence times.

We studied the growth and emergence of the five common species of amphibitic stoneflies in the expansive alluvial aquifer of the Nyack Floodplain on the Middle Fork of the Flathead River, Montana: *Isocapnia grandis, Isocapnia crinita, Isocapnia integra* (formerly *I. missourii*), *Paraperla frontalis*, and *Kathroperla perdita*. On this floodplain, we used a network

of twenty wells, six of which were equipped with continuous monitoring systems ('RiverNet') that logged temperature and dissolved oxygen (DO) data. The wells a range of temperature and DO variation, with varying levels of cohesiveness with air and river conditions. We therefore also analyzed how the growth and emergence patterns of the most abundant species, *P. frontalis*, related to temperature and dissolved oxygen concentrations across the aquifer.

Materials and Methods

Study Site

The Nyack floodplain is on the 5th order Middle Fork of the Flathead River at the southern boundary of Glacier National Park, encompassing a 3200 km^2 catchment with approximately 9 km of anastomosed river (Figure 1) (Stanford et al. 2005). The floodplain is constrained by upstream and downstream knick points, with a 9x2 km floodplain area. Underlying the floodplain is 20-100m deep Pleistocene and recent alluvium of extremely high porosity (maximum hydraulic conductivity of 10 cm s^{-1}) confined below by an impermeable clay layer of tertiary age (Stanford and Ward 1993). Approximately 30% of base flow is influent to the aquifer at the upstream end of the floodplain, and upwelling occurs downstream in areas where topographic lows (such as channels and ponds) intersect the water table (Stanford et al. 2005).

The floodplain was equipped with twenty instrumented 3-inch PVC wells with 2 mm slot openings down the length of the pipe (Figure 1). The wells were drilled to 8-10 m using a hollow auger drilling rig. Six of the wells were instrumented in 2012 with the RiverNet

continuous monitoring system, which recorded hourly measurements of depth, dissolved oxygen concentration and saturation (RDO dissolved oxygen probe), and temperature, all at approximately 3 m below the base flow water table. The RiverNet system also recorded hourly measurements of air temperature at well HA07 (Figure 1) and river temperature. DO sensors were calibrated monthly.

Sample collection

We sampled the RiverNet wells for stoneflies approximately every 2-6 weeks from June 2013 to August 2015. We sampled all other wells approximately every 6 weeks from April-October each year. We used two methods: trapping and pumping. To trap, we suspended nylon ropes to the bottom of each well. The ropes went to the top of the well, where they ended in a PVC trap for adults (inverted funnel, mesh). These ropes enabled teneral adults to crawl up the rope emerge through the well where they would be caught in the PVC trap above. Stonefly larvae were also able to perch on the rope. We collected adults (trap collected) and larvae (rope collected) separately into 95% ethanol. We only collected live adults, such that the number collected reflected individuals that had emerged in approximately the last day. We pumped by using a gas-operated diaphragm pump that output water through 2.5" Tigerflex tubing into a 330 micron Nitex mesh net. We kept pumping time and speed constant between all wells and sampling events. After pumping was completed, we elutriated the samples retained in the net, collecting stoneflies caught in the net and transferring them to distilled water (DI). At the lab, we rinsed the stoneflies and transferred them to 95% Ethanol.

We identified the stoneflies to the species level as much as possible using 6-50X magnification on a stereo-dissecting microscope fitted with 20X eyepieces. We measured

growth as head capsule width (HCW): the widest distance across the eyes. We measured this with a calibrated ocular micrometer attached to the microscope for pump-collected individuals specifically collected in 2014-2015 only. We only measured pump individuals to avoid incorporating any bias from the rope samples (e.g. more likely for teneral individuals to be present on the rope). We referred to multiple keys and reference collections from the Middle Fork of the Flathead to identify species (Baumann et al. 1977; Stewart et al. 1988; Gibert et al. 1994*a*; Zenger and Baumann 2004). Identification was not possible in early instar *Isocapnia* larvae.

Statistical Methods

We used sampling data from all 20 wells in our analysis of desynchronization in growth and emergence across the floodplain (first objective). Because six of these wells were instrumented, we constrained analysis of the factors affecting *P. frontalis* growth and emergence to those six wells (second objective).

We performed all data analysis in R (R Core Team 2016). We tested continuous variables for normality using the Skewness-Kurtosis test, assessing skewness values between -0.5 and 0.5 and kurtosis values less than 3 as symmetric and normal. Numbers of emerged stoneflies were right-skewed, so we used log transformations before data analysis. We controlled for quality in the RiverNet data by removing any observations that changed 0.5°C relative to the observations the hour before and the hour after; this removed any sampling points that were the result of removing the sensors for calibration and sampling. We averaged temperature readings from three different temperature probes per well (same depth), the

calculated the mean and maximum temperature readings per day. We also calculated mean DO concentration per day.

In addition to the RiverNet variables, we measured the shortest linear distance to the river as the shortest linear distance from the well to the base flow water level on Google Earth Imagery from July 2014 (Google Earth Imagery 2014). This was an important variable to consider because if hyporheic stoneflies emerge from the river as thought in previous study (Stanford and Gaufin 1974; Gibert et al. 1994*b*), they could be emerging from wells differentially as they make their way to the river. We tested for significance of well locations, date, daily mean temperature (well, river, and air), daily maximum air temperature, daily mean DO concentration, and shortest linear distance to river. . We used Pearson correlation coefficients to determine collinearity between variables (Table 1), using only those which were not significantly correlated in the linear mixed effects models, then used a linear mixed effect model with log-transformed *Paraperla* emergence as a response variable and well as a random effect with all other variables as fixed effects. We used only the well temperature, distance to river, mean air temperature, day/month of year, and DO concentration as independent variables for predicting Paraperla growth and emergence (log-transformed) because all other variables were correlated with the mean air temperature.

Results

Temperature and DO conditions in the aquifer compared to the river channel

RiverNet data showed that measured well variables had varying levels of correspondence in temperature patterns in wells with the river and with air temperature (Figure 2, 3A). Well temperatures at longer residence times stabilized to the mean annual air temperature of 6-7°C.

DO patterns were similarly less synchronous with the river for wells at longer residence times. The river was consistently close to 10 mg/L DO concentration, which is approximately saturation (Figure 2B). Well HA02, closer to the river channel, more closely mimicked the DO patterns of the river but all other wells displayed consistently lower DO concentrations that are normally considered stressful for stream stonefly species (Nagell 1973). In fact, wells HA10 and HA12 went hypoxic during the summer months.

Synchronization in growth and emergence among the five widely distributed and abundant stonefly species

Larvae of all species were distributed across the wells sampled (Figure 4). As shown in previous study of the Nyack aquifer (DelVecchia et al. 2016), abundance of each species varied between wells but the stoneflies were present throughout the well grid that spans the entire aquifer. DelVecchia et al. (2016) found that dissolved oxygen and methane concentrations contributed to structuring stonefly species assemblages because individual species had varying reliance on methane derived resources and tolerance to hypoxic environments. Therefore, we inferred that differences in abundance between species were a result of these factors.

The four *Isocapnia* species each had a wide range of HCW values, but too few individuals were found at each given time to determine larval life history duration. Similarly, almost all individuals of *K. perdita* we collected were at later instars, with few individuals found with small head capsule sizes. *P. frontalis* was the most abundant and ubiquitous, with a wide

range of head capsule widths represented in the samples. *P. frontalis* was the only species for which we considered the sample size and range sufficient to examine distributions of head capsule widths over time. We found that a wide range of *P. frontalis* sizes were present across the six wells at most sampling times and emergence and the emergence spanned 8-12 weeks (Figure 5). By the large range of head capsule widths present even immediately preceding emergence, we determined that *P. frontalis* had at least a 2-year larval stage. The lower quantities of *Isocapnia* species and *K. perdita* in our samples made it unclear as to how many cohorts were actually present, or if there was simply a continuous size range. We did not have data on *I. integra* larvae head capsule widths because *I. integra* and *I. crinita* are particularly difficult to distinguish as larvae, though *I. crinita* develops some distinctive characteristics such as hoariness which can lead us to definitively identify that species.

When we examined emergence patterns, we pooled the number collected by day across all wells sampled enabling us to qualitatively compare emergence of each species over time without incorporating effects of the well itself. We found that *I. integra* showed extreme desynchronization, emerging yearlong from wells across the floodplain (Figure 6). Many of the winter emergers which we examined were dwarf micropterous. *I. crinita* and *I. grandis* had less desynchronization, but still emerged over five month periods from February to July. *P. frontalis* and *K. perdita* had the most synchronized emergence of the species, but emerged over a two to three month period. When we used ANOVA to test for correlations between the number of individuals emerged and the month of year and species, we found that the month was significant to $p = 0.10$ ($p = 0.085$) but the species was not ($p = 0.249$).

Synchronization in growth and emergence of P. frontalis compared to RiverNet variables

We further analyzed *P. frontalis* growth and emergence in particular because *P. frontalis* had the most widespread and abundant specimens collected. We found that the only significant variable in predicting *P. frontalis* emergence was the daily mean air temperature (Table 2). We found that variation between wells was <10-9 of variation within wells, suggesting that the well explained a very low proportion of the variation in emergence values. When we repeated the same analysis using P. frontalis head capsule widths, we found that all variables but DO were significant ($p < 0.05$, Table 3).

The daily mean air temperature had a negative coefficient for the number of emerged insects occurred because the dataset did not include values of 0 for days when no emergent insects were found (Table 4). Peak *Paraperla* emergence is in July, but peak air temperatures are in August. Therefore, with this limited dataset, the model reflected that over the time period which *Paraperla* are emerging, numbers emerged decreased at higher air temperatures.

The positive coefficients of air temperature and linear distance to river in relation to head capsule width could reflect that the most *Paraperla* are pre-emergence (and thus at their largest) in the summer, so perhaps this is why the sizes are correlated with air temperature . The sizes could be correlated with distance to river because perhaps the Paraperla are moving to the river as they prepare to emerge, but this conclusion can only be a vague speculation because these individuals were collected from only 7 wells that could not possibly encompass a continuous range of distance to the river.

Discussion

RiverNet data demonstrated a constancy of temperature at the annual mean air temperature at longer residence times, but wells closer to the river had more coherence with air and river temperatures. Dissolved oxygen was generally in lower concentrations in wells than in the rivers, with two wells exhibiting occasional hypoxia. Nonetheless, the four stoneflies for which we included larval HCW data were distributed within the aquifer. Abundance of each species varied between wells because species were dependant on the dissolved oxygen, dissolved methane, and dissolved organic carbon concentrations within wells, which have been found to explain 22% of the variation in stonefly species assemblages and thus were important for determining species abundance (DelVecchia et al. 2016).

When examining growth and emergence patterns among the five species across the aquifer, we found that synchronicity in growth and emergence patterns varied between species but were most desynchronized in the *Isocapnia* species. The *Isocapnia* species were almost completely asynchronous, remarkably similar to the cave dwelling nemourid reported by López-Rodríguez and de Figueroa (2012). *I. integra* emerged over the course of the year, though many of the winter-emerging individuals were dwarf micropterous, suggesting either a disadvantage to flying in the winter months, or a tradeoff to emergence during the winter (Hynes 1976; Costello 1988). *P. frontalis* and *K. perdita* were somewhat more synchronous but in any case emergence timing was not significantly different between species. All species had more extended durations of emergence timing than those previously described in aboveground ecosystems (eg. Stanford 1976, Dewalt 1995).

We analyzed *P. frontalis* to understand what might drive differences in growth and emergence. For many aquatic insects in the temperate zone, temperature is the most important factor regulating these behaviors (Ward and Stanford 1982). Individuals must acquire both sufficient degree days and a threshold temperature in order to emerge (Stanford 1975, p. 197; Ward and Stanford 1982). While temperature patterns alone are complex in the aquifer's network of residence times ranging from hours to years-long residence times (Helton et al. 2014), there are many other complexities that could have affected desynchronized growth and emergence in this environment. For example, DelVecchia et al. (2016) showed that *I. grandis* and *K. perdita* reacted to hypoxic conditions differently, with *I. grandis* being able to withstand almost an hour of complete anoxia before recovering in oxygenated water. We therefore would expect that many of the hyporheic stoneflies, including *P. frontalis*, would have variation in tolerance to hypoxia, which was present in two of the six wells we used in this study. When we examined temperature and DO patterns in relation to *P. frontalis* growth, our results showed that temperature was significant in predicting *P. frontalis* growth but dissolved oxygen was not. We therefore inferred that species are constrained to habitats based on their dietary needs and DO preferences, but are subject to the temperature regimes of the aquifer environments that suit them. If stoneflies are mobile and moving throughout the aquifer, accumulation of degree days can vary drastically by individual depending on its location, which we have no way of knowing for the period preceding collection.

Though in-well measured variables helped explain growth in *P. frontalis*, they were insignificant in predicting emergence timing. Only the mean daily air temperature was significant in predicting quantities of emerged adults. While the emergence of stream aquatic insects is closely tied to air temperatures (Ward and Stanford 1982), the same cue seems unlikely

in aquifer insects which are sometimes found 10m below the water table. We inferred that either *P. frontalis* individuals are moving to the water table before emergence to actually respond to air temperature, or that air temperature was significantly correlated with another factor that we did not measure, such as the degree day accumulation by each individual.

Conclusion

We concluded that amphibitic stonefly growth and emergence was radically desynchronized by temperature patterns that trend toward the mean annual air temperature of 6-7° C at longer residence times. The widespread distribution and abundance of these five species of hyporheic stoneflies across Nyack, despite such lack of synchronicity in growth and emergence, underscores unique behavioral adaptation of these hyporheic species to live in the expansive aquifer environment. As these species are distributed in alluvial aquifers across the Pacific Northwest and into Alaska (Stewart et al. 1988; DelVecchia et al. 2016), understanding their mechanisms for survival in such a unique environment is important for maintaining biodiversity. Additionally, knowledge of the biology and functional roles of these organisms contributes to our ability to understand and conserve freshwater ecosystems.

Literature Cited

Anderson, M. P. 2005. Heat as a ground water tracer. Ground water 43:951–968.

Armitage, P., D. Moss, J. Wright, and M. Furse. 1983. The Performance of a New Biological Water-Quality Score System Based on Macroinvertebrates Over a Wide-Range of Unpolluted Running-Water Sites. Water Research 17:333–347.

Baumann, R. W., A. R. Gaufin, and R. F. Surdick. 1977. The stoneflies (Plecoptera) of the Rocky Mountains. American Entomological Society.

Boulton, A. J., S. Findlay, P. Marmonier, E. H. Stanley, and H. M. Valett. 1998. The functional significance of the hyporheic zone in streams and rivers. Annual Review of Ecology and Systematics 29:59–81.

Costello, M. J. 1988. Preliminary Observations on Wing-Length Polymorphism in Stoneflies (Plecoptera: Insecta). The Irish Naturalists' Journal 474–478.

DelVecchia, A. G., J. A. Stanford, and X. Xu. 2016. Ancient methane subsizes contemporary food web. Nature.

DeWalt, R. E., and K. W. Stewart. 1995. Life histories of stoneflies (Plecoptera) in the Rio Conejos of southern Colorado. The Great Basin Naturalist 1–18.

Gibert, J., D. C. Culver, M.-J. DOLE-OLIVIER, F. Malard, M. C. Christman, and L. Deharveng. 2009. Assessing and conserving groundwater biodiversity: synthesis and perspectives. Freshwater Biology 54:930–941.

Gibert, J., D. Danielopol, and J. A. Stanford. 1994. Groundwater ecology (Vol. 1). Academic Press.

Google Earth Imagery. 2014.

Helton, A. M., G. C. Poole, R. A. Payn, C. Izurieta, and J. A. Stanford. 2014. Relative influences of the river channel, floodplain surface, and alluvial aquifer on simulated hydrologic residence time in a montane river floodplain. Geomorphology, Discontinuities in Fluvial Systems 205:17–26.

Hynes, H. B. N. 1976. Biology of Plecoptera. Annual Review of Entomology 21:135–153.

López-Rodríguez, M. J., and J. M. T. de Figueroa. 2012. Life in the Dark: On the Biology of the Cavernicolous Stonefly Protonemura gevi (Insecta, Plecoptera). The American Naturalist 180:684–691.

Nagell, B. 1973. Oxygen-Consumption of Mayfly (ephemeroptera) and Stonefly (plecoptera) Larvae at Different Oxygen Concentration. Hydrobiologia 42:461–489.

Poole, G. C., S. J. O'Daniel, K. L. Jones, W. W. Woessner, E. S. Bernhardt, A. M. Helton, J. A. Stanford, et al. 2008. Hydrologic spiralling: the role of multiple interactive flow paths in stream ecosystems. River Research and Applications 24:1018–1031.

R Core Team. 2016. R: A Language and Environment for Statistical Computing. R Foundation for Statistical Computing, Vienna, Austria.

Stanford, J. A. 1975. *Ecological studies of Plecoptera in the Upper Flathead and Tobacco Rivers, Montana*. University of Utah.

Stanford, J. A., and A. R. Gaufin. 1974. Hyporheic Communities of Two Montana Rivers. Science 185:700–702.

Stanford, J. A., M. S. Lorang, and F. R. Hauer. 2005. The shifting habitat mosaic of river ecosystems. Internationale Vereinigung fur Theoretische und Angewandte Limnologie Verhandlungen 29:123–136.

Stanford, J. A., and J. V. Ward. 1993. An ecosystem perspective of alluvial rivers: connectivity and the hyporheic corridor. Journal of the North American Benthological Society 48–60.

Stewart, K. W., B. P. Stark, and others. 1988. Nymphs of North American stonefly genera (Plecoptera). Entomological Society of America.

Ward, J. V., and J. A. Stanford. 1982. Thermal responses in the evolutionary ecology of aquatic insects. Annual review of entomology 27:97–117.

Zenger, J. T., and R. W. Baumann. 2004. The Holarctic winter stonefly genus Isocapnia, with an emphasis on the North American fauna (Plecoptera: Capniidae). Monographs of the Western North American Naturalist 2:65–95.

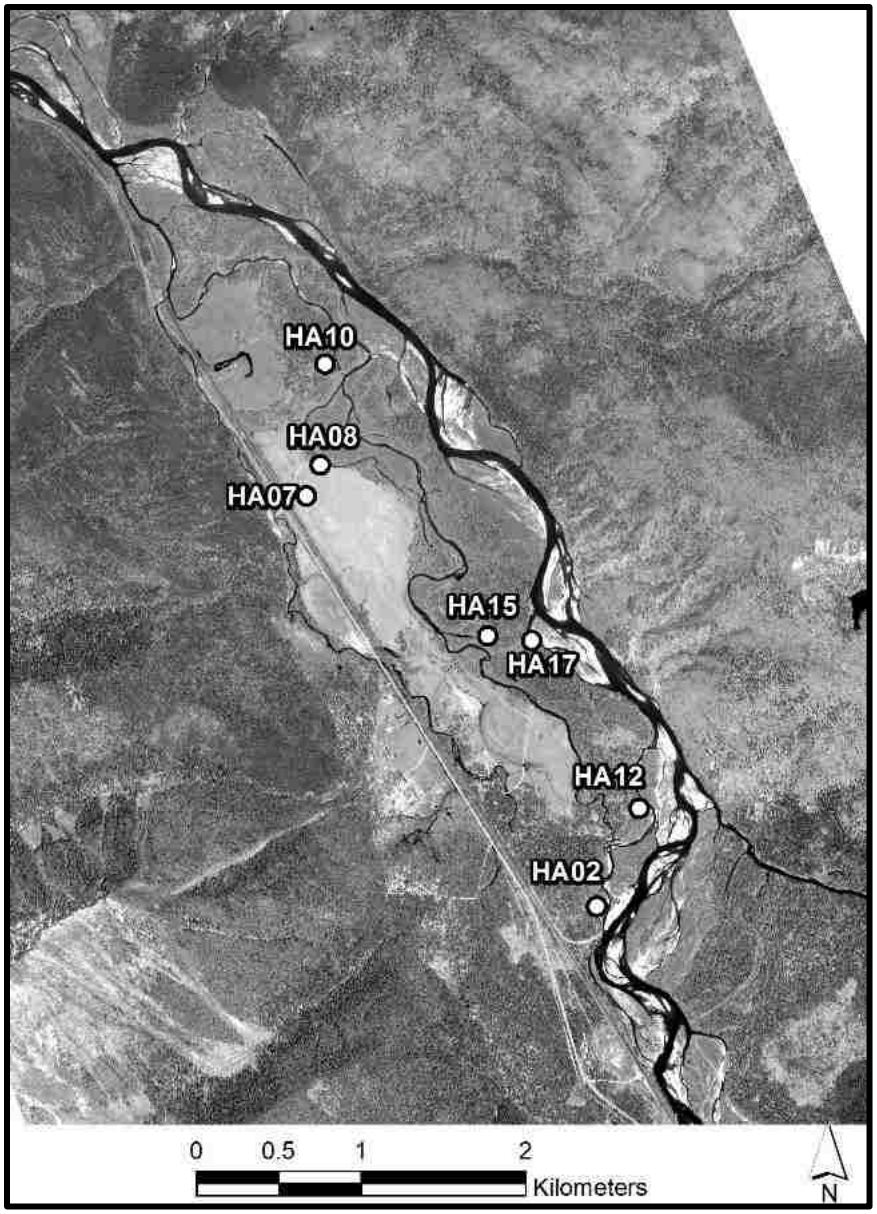

Figure 1. Locations of the twenty aquifer monitoring wells installed in the Nyack floodplain where amphibitic stoneflies were sampled. Those labeled HA were equipped with the RiverNet continuous monitoring system (see text) that measured dissolved oxygen concentration and temperature within the aquifer.

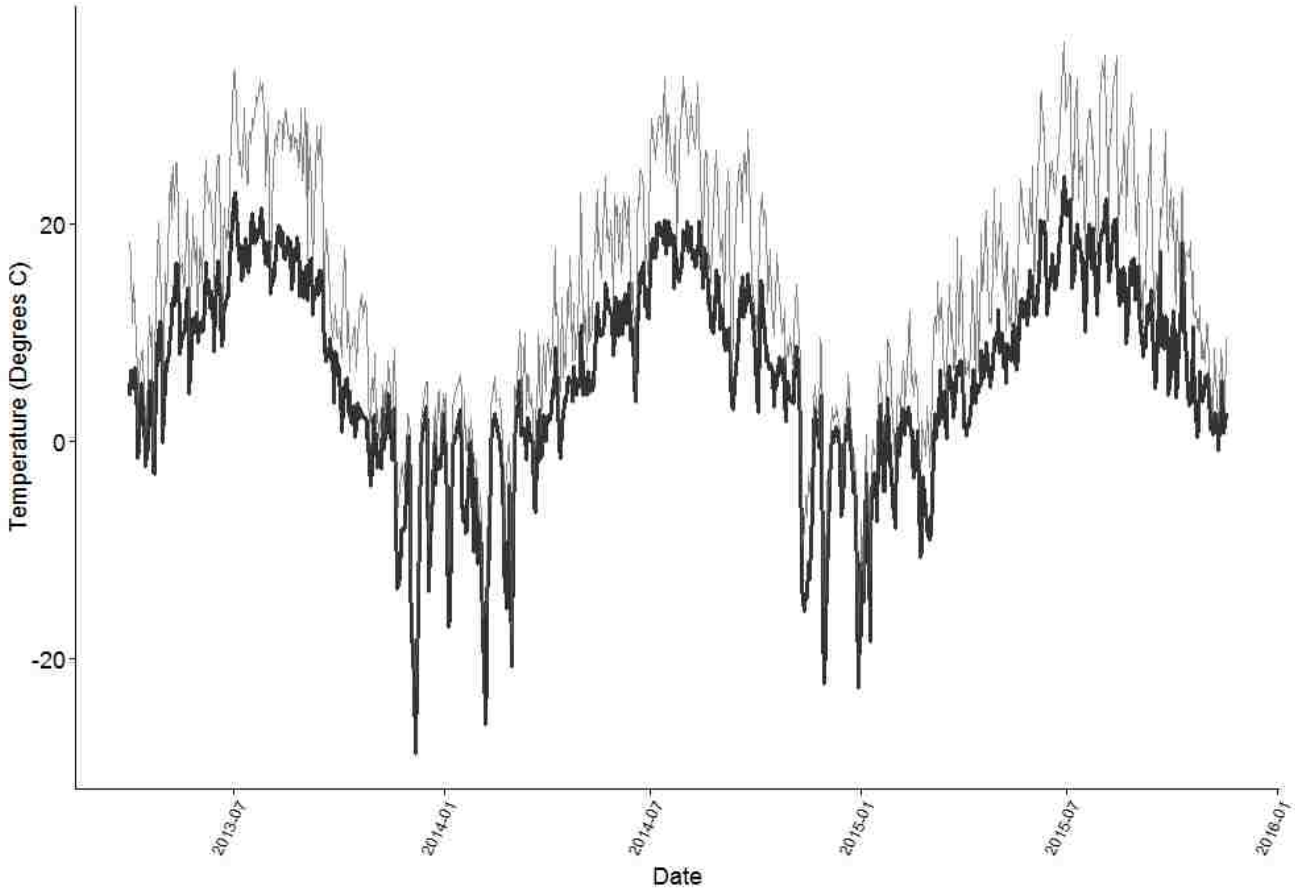

Figure 2. Mean (black) and maximum (grey) daily air temperatures on the Nyack Floodplain from 2013-2016. Temperatures were measured by a meteorological station located at well HA07 (Figure 1).

A.

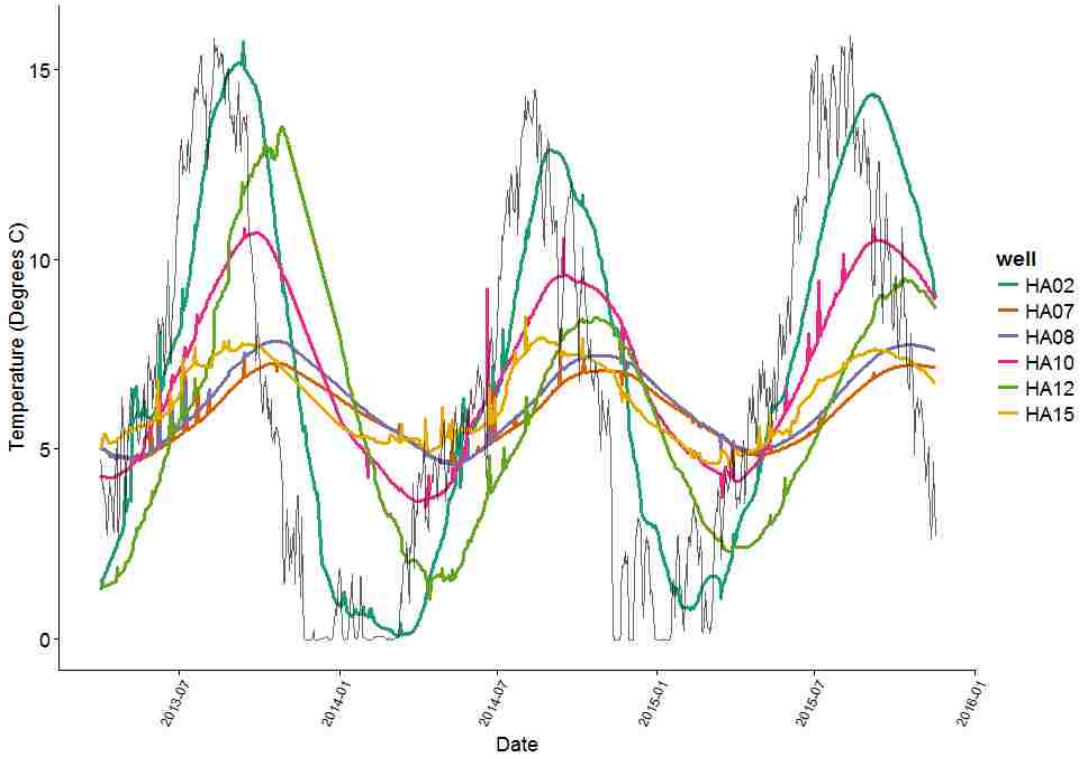
Temperature (Degrees C)
15
10
5
0
2013-07
2014-01
2014-07
2015-01
2015-07
2016-01
Date
well
HA02
HA07
HA08
HA10
HA12
HA15

B.

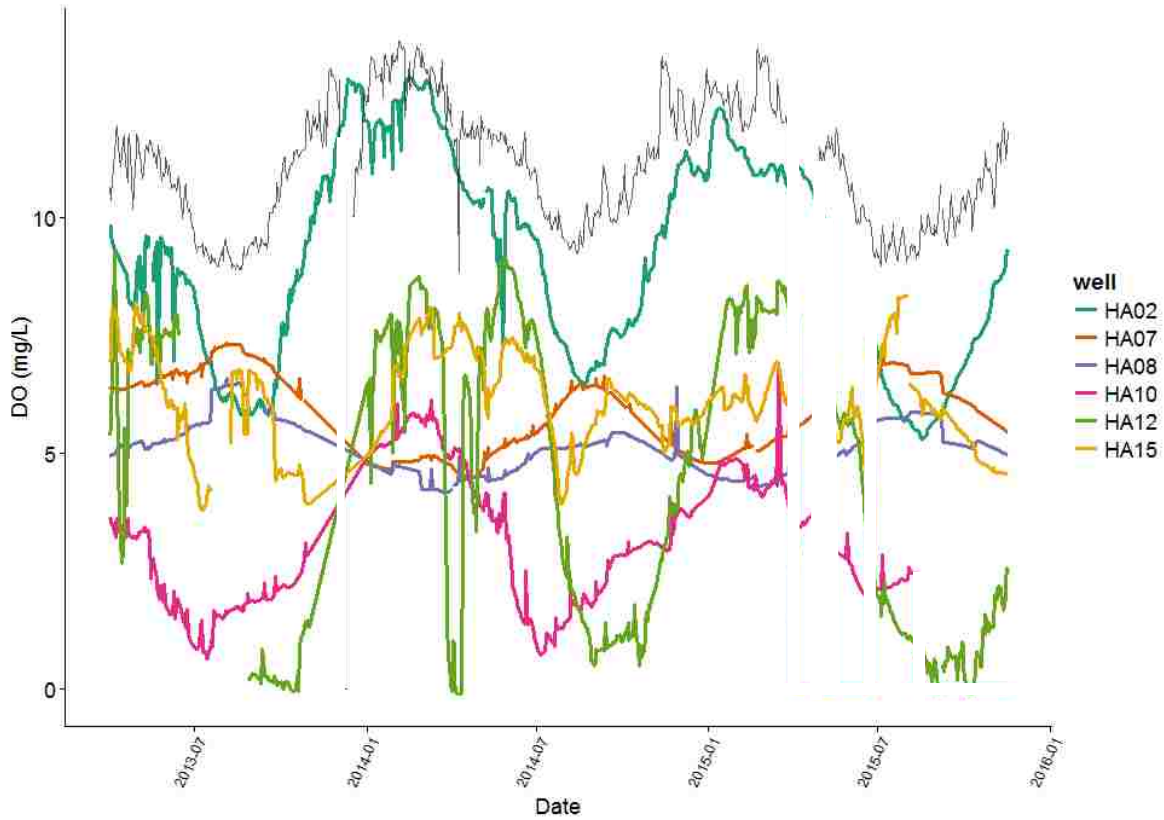
DO (mg/L)
10
5
0
2013-07
2014-01
2014-07
2015-01
2015-07
2016-01
Date
well
HA02
HA07
HA08
HA10
HA12
HA15

Figure 3. Aquifer water temperatures and dissolved oxygen concentrations measured by the RiverNet monitoring system at each of the six wells (colored) compared to measurements in the river channel (grey). Wells such as HA15 and HA08 at longer flowpaths tend to have dampened temperature and DO variation compared to the river. Variation across the wells shows the diversity of habitat types for stoneflies within the aquifer.

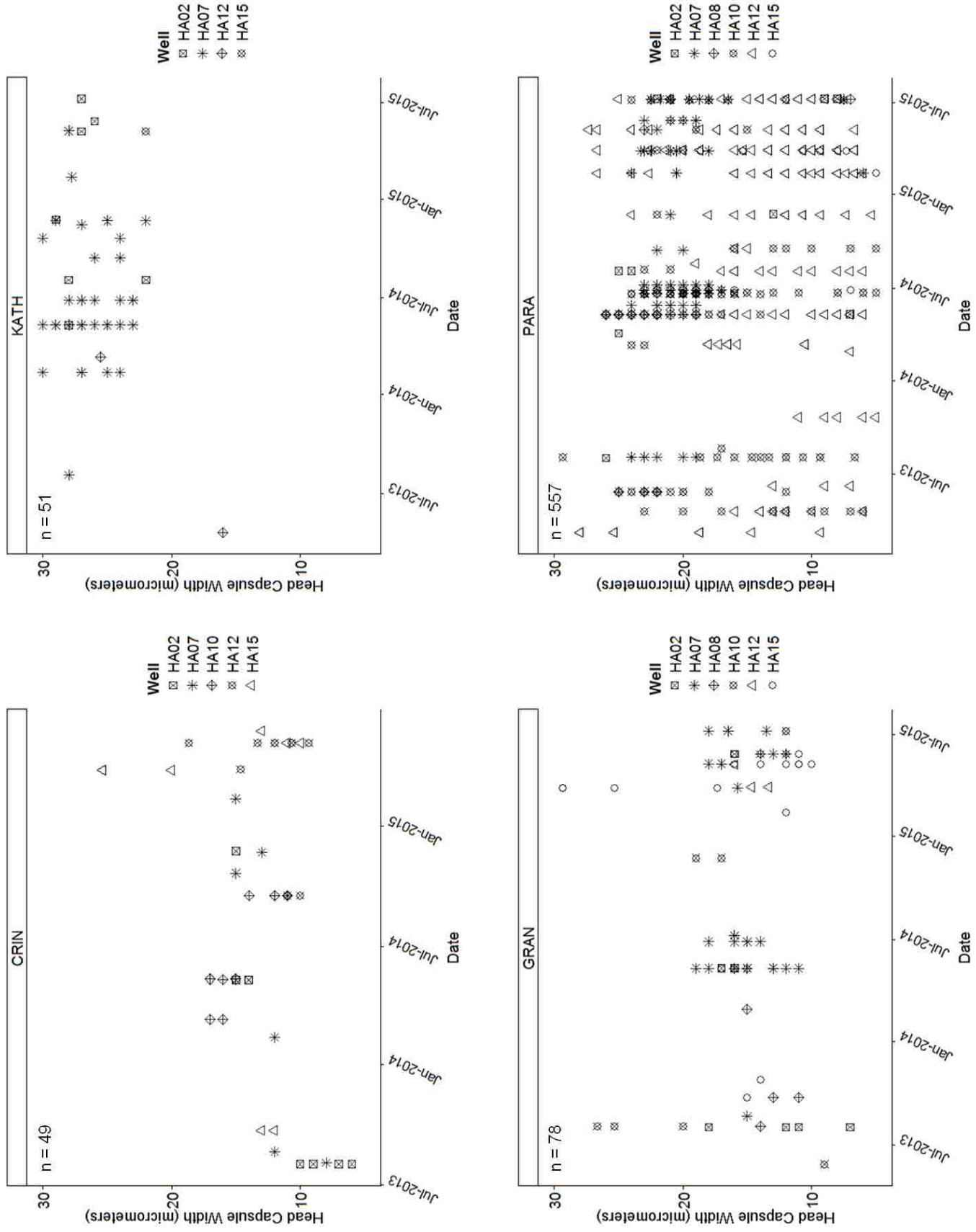
KATH
n = 51
PARA
n = 557
CRIN
n = 49
GRAN
n = 78
Well
HA02
HA07
HA08
HA10
HA12
HA15
Head Capsule Width (micrometers)
30
20
10
Jul-2013
Jan-2014
Jul-2014
Jan-2015
Jul-2015
Date

Figure 4. Head capsule widths of amphibitic stoneflies in the Nyack aquifer sorted by species and measured over time in 5 wells that encompassed the range of temperature and dissolved oxygen in the aquifer. All species but I. integra were present across the floodplain (CRIN = I. crinita, GRAN = I. grandis, KATH = K. perdita, PARA = P. frontalis) . I. integra is not displayed because none of the larvae in our samples could be unequivocally identified as I. integra.

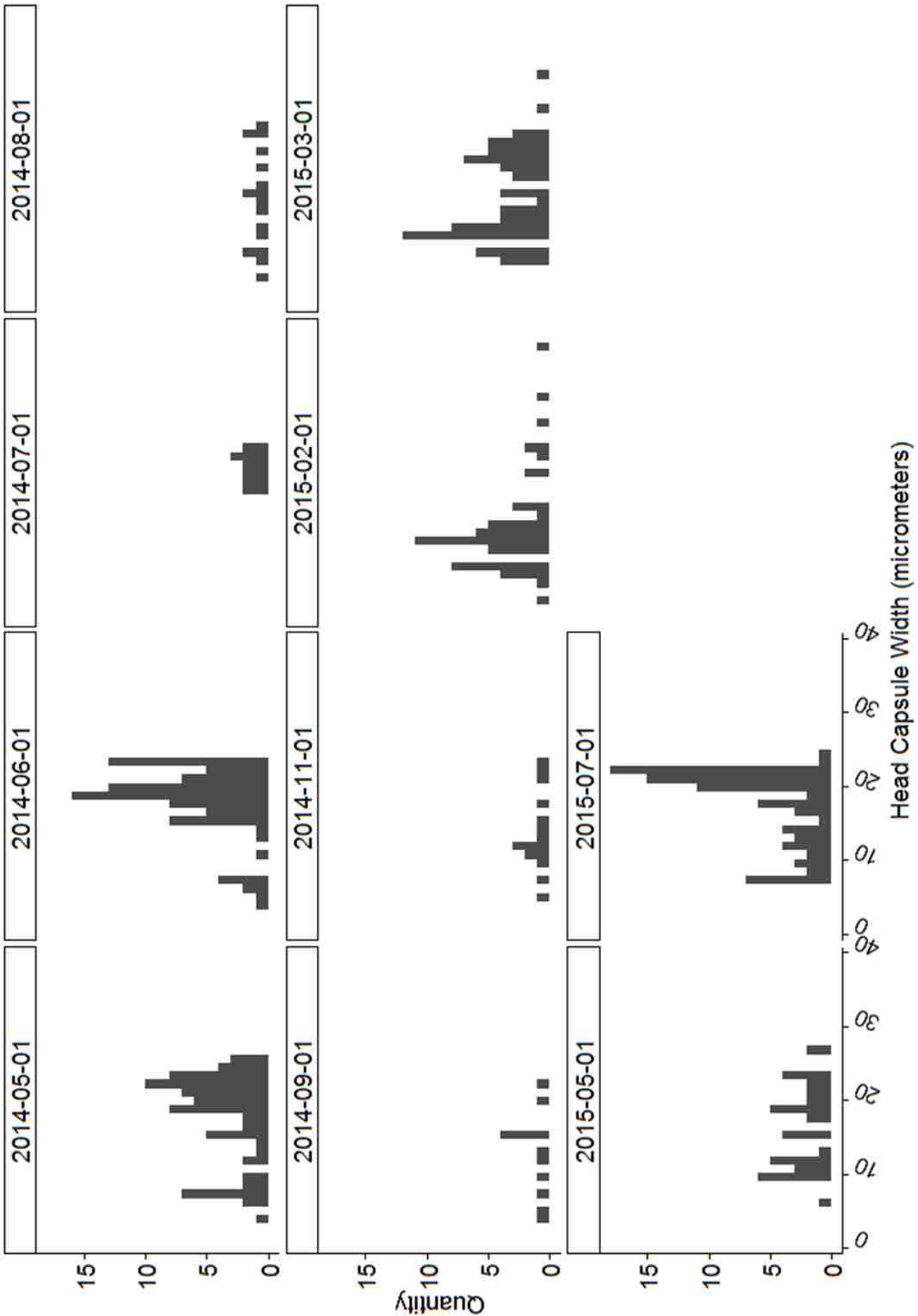
2014-05-01
2014-06-01
2014-07-01
2014-08-01
2014-09-01
2014-11-01
2015-02-01
2015-03-01
2015-05-01
2015-07-01
Quantity
Head Capsule Width (micrometers)
0
5
10
15
20
30
40

Figure 5. *P. frontalis* head capsule widths per month, all well samples combined. Arrows indicate that emergence occurred during that month. Please note that sampling months are not spaced evenly. The presence of early instar larvae in the aquifer even during emergence time and the wide distribution of sizes indicate a multi-year larval stage for *P. frontalis.*

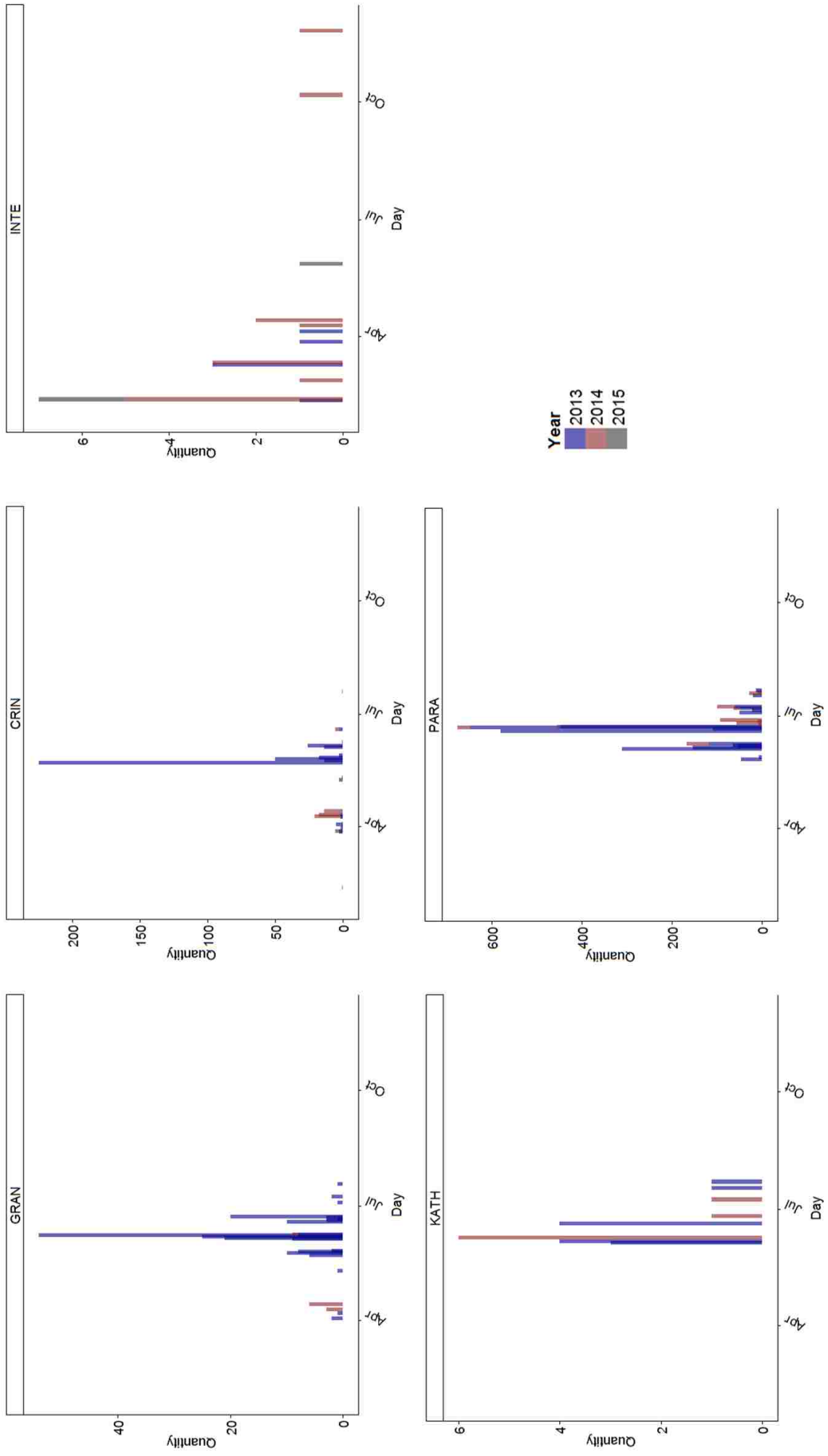
INTE
CRIN
PARA
GRAN
KATH
Quantity
Day
Apr
Jul
Oct
Year
2013
2014
2015

Figure 6. Quantities of teneral (newly emergent) adults of each species found on each sampling day by year, all well samples combined. Please note that y axes are not even and species labeling as in Figure 4 Note in particular that teneral *I. integra* (INTE) were present year around, although peaking in early spring, strongly suggesting a completely desynchronized life cycle. *P. frontalis* (PARA) and *K. perdita* (KATH) also had extended emergence periods of 2-3 months per year, but were more synchronized than the other species.

Table 1. Pearson correlation coefficients for each variable considered for inclusion in the linear mixed effects models. Only mean air temperature, mean well temperature, mean DO concentration, and linear distance to river were included in the linear mixed effects models to avoid collinearity problems.

Variable	Daily mean well temperature	Daily mean river temperature	Daily mean air temperature	Daily maximum air temperature	Daily mean DO concentration	Linear distance to river
Daily mean well temperature		0.464	0.269	0.288	-0.365	-0.092
Daily mean river temperature	0.464		0.886	0.897	-0.253	0.015
Daily mean air temperature	0.269	0.886		0.957	-0.200	0.014
Daily maximum air temperature	0.288	0.897	0.957		-0.205	0.014
Daily mean DO concentration	-0.365	-0.253	-0.200	-0.205		-0.138
Linear distance to river	-0.092	0.015	0.014	0.014	-0.138	

Table 2. ANOVA significance values for each variable tested as a predictor of growth and emergence of *P. frontalis*. Bold values indicate significance ($p < 0.05$). Emergence quantities were incorporated as log-transformed emergence per day.

Variable	Growth	Emergence
Month and day of year	**0.003**	0.174
Daily mean well temperature	**<0.0001**	0.906
Daily mean river temperature	**0.013**	0.236
Daily mean air temperature	**0.002**	**0.051**
Daily maximum air temperature	**<0.0001**	0.348
Daily mean DO concentration	0.876	0.795
Linear distance to river	**<0.0001**	0.824
Well of collection	**<0.0001**	0.215

Table 3. AIC and R^2 values for linear mixed effects models using various combinations of fixed effect variables.

Predictors	Growth		Emergence	
	AIC	Adj. R^2	AIC	Adj. R^2
Month and day of year	3521.29	0.008	74.66	0.054
Daily mean well temperature	3513.93	0.220	77.79	-0.015
Daily mean air temperature	3504.51	0.039	**68.62**	**0.175**
Daily mean DO concentration	3516.51	0.001	74.07	-0.017
Linear distance to river	3407.41	0.196	78.08	-0.022
Daily mean air temperature + Month and day of year	3506.49	0.037	70.58	0.156
Daily mean air temperature + Linear distance to river	**3403.59**	**0.210**	70.49	0.158

Table 4. Coefficients, standard errors, and p values for each of the fixed effect variables used in the best fit model.

Predictors	Growth			Emergence		
	Coefficient	Std. Err	p	Coefficient	Std. Err	p
Intercept	9.411	0.655	<0.0001	2.269	0.419	<0.0001
Daily mean air temperature	0.107	0.0444	<0.0001	-0.092	0.028	0.003
Linear distance to river	0.012	0.001	<0.0001			

Supplemental Table 1. Well coordinates, residence time estimates, and linear distance to river values. Bolded well names are wells equipped with RiverNet, which were the wells we used in analysis of *P. frontalis* growth and emergence patterns.

Well	Easting (UTM)	Northing (UTM)	Residence Time (Days)	Linear Distance to River (m)
HA01	291112	5370422	164.1	
HA02	292244	5369912	45.4	130
HA04	291796	5370827	54.2	
HA05	291080	5371541	180.1	
HA06	290976	5371934	156.4	
HA07	290489	5372413	156.4	824
HA08	290564	5372617	210.6	694
HA09	290386	5373176	178.0	
HA10	290586	5373203	117.4	419
HA12	292484	5370507	119.7	323
HA13	292498	5371054	46.9	
HA15	291560	5371559	133.3	280
HA16	291770	5371453	167.1	
HA17	291846	5371524	167.1	
HA18	291626	5372018	110.1	
HA19	290984	5373323	147.8	
HA20	290870	5373349	147.8	
SarN	290740	5373291	130.7	
SarS	290731	5373249	117.4	

Chapter 5: Synthesis

My dissertation work furthered the legacy of Nyack research and the fields of groundwater ecology and river ecology in three ways: it explained a long-standing conundrum on how diverse and abundant macroinvertebrate species survive in a dark and extremely carbon-limited system, it developed a new conceptualization of basal productivity in river floodplain aquifers, and it underscored the unique adaptations of hyporheic stoneflies.

The second chapter demonstrated the importance of a chemoautotrophic carbon source in supporting consumer biomass. It provided the first report of freshwater consumers supported by ancient methane-derived carbon and the most diverse and geographically widespread example thus far of a river ecosystem supported by methane-derived carbon. Not only was a majority of site-wide stonefly biomass on Nyack comprised of methane derived carbon, but four other floodplain aquifers contained high proportions of methane derived carbon in biomass. This chapter thereby emphasized the importance of unconventional carbon sources in river systems.

The third chapter focused on connecting the different scales at which methane has been implicated in the Nyack aquifer ecosystem. Prior to my dissertation, methanogenesis was suggested as a potential explanation for the imbalance in the Nyack carbon budget and the increase in labile dissolved organic carbon along flowpaths. My first chapter then showed the role of methane in supporting consumers. My second chapter connected these scales by elaborating the ecological connections between methane and dissolved organic carbon biogeochemical dynamics and stonefly biology and ecology. This work showed that methane concentrations were a predictor of dissolved organic carbon concentrations within the aquifer, that some stonefly species had tolerance to hypoxia and consumed methanogenic and

methanotrophic microbes, and that stonefly species assemblages were largely explained by methane and dissolved oxygen concentrations within the aquifer. In summary, this chapter demonstrated the role of dissolved methane in trophic and community ecology within the aquifer. It highlighted the functional roles of various stonefly species in a methane subsidized ecosystem.

Finally, the fourth chapter demonstrated that hyporheic stoneflies in the Nyack Floodplain were behaviorally adapted to the aquifer environment. Temperature is known to be the most important cue for stonefly emergence, but in the aquifer temperature patterns had increasingly less coherence with the river at longer residence times, stabilizing to maintain the mean annual air temperature of 6-7°C year-round. The constancy of temperature regime in the aquifer led to desynchronized growth and emergence in all five common hyporheic stoneflies that we studied because neither degree day accumulation nor threshold temperature cues had the same temporal variability in the aquifer as they did in the river channel. Despite their desynchronized emergence, however, the stoneflies were still abundant across the aquifer, showing that they must be adapted to persist despite their emergence patterns. These findings furthered those of the first two chapters because not only are the distributions of these stoneflies related to the biogeochemical heterogeneity of the aquifer, but their life history patterns reflect their adaptation to aquifer hydrology.

Overall, my dissertation work has contributed a comprehensive understanding of the ecology of the expansive alluvial aquifer, with a specific focus on dominant macroinvertebrates. It has explained how diverse and abundant consumers can survive in an extremely oligotrophic component of river ecosystems and thereby highlighted the role of landscape complexity in maintaining biodiversity and ecosystem function. In addition, it has shown that an unperturbed

floodplain ecosystem is valuable for converting and assimilating a powerful greenhouse gas, elaborating a broader impact of my dissertation in showing that a natural floodplain ecosystem is valuable for maintaining ecosystem services. Finally, my dissertation showed that the aquifer maintains functional diversity in addition to overall species diversity in terms of the unique adaptations of hyporheic stoneflies.

Broader Impacts

As stated, floodplains are valuable but threatened ecosystems. My dissertation further elaborated why these ecosystems in their natural state are so valuable for maintaining productivity, biodiversity, and ecosystem services. The shallow aquifer system produces, converts, and assimilates a powerful greenhouse gas, thereby maintaining productivity while also providing an ecosystem service. In addition, it contains diverse species which are uniquely adapted to the carbon-poor and expansive aquifer environment, showing that the aquifer is valuable for maintaining functional diversity in addition to overall species diversity.

My second and third chapters demonstrated the role of the aquifer in converting and assimilating methane, a powerful greenhouse gas and potential water contaminant. The aquifer ecosystem, as it functions on the near-pristine Nyack floodplain, had such fine-scale heterogeneity that methane could be produced microbially in anoxic zones that we very rarely measured, then assimilated in zones where oxygen was replenished via flow from the river channel or exchange with the vadose zone. Methane derived carbon provided a carbon source for production of large macroinvertebrates, which then subsidized the above-ground ecosystem when they emerged as adult stoneflies. This methane cycle helped to explain why an aquifer

carbon budget that did not consider chemoautotrophy within the aquifer was unbalanced (Appling 2012). Therefore, my dissertation showed that a complex biogeochemical mosaic within the aquifer was necessary for regulating an important aspect of the carbon cycle both in terms of greenhouse gas assimilation and maintaining productivity. Furthermore, this work implied that if this cycle were to be disturbed, we could expect to lose productivity and perhaps have buildup of this greenhouse gas.

My third and fourth chapters demonstrated the unique adaptations of hyporheic stoneflies, further developing the importance of the floodplain as a hotspot of biodiversity. My second chapter showed that the five common species of stonefly had different niche characteristics related to their reliance on methane derived carbon. These species had distinct trophic positions defined both by their trophic levels and the percentage of their biomass provided by methane-derived carbon. The ability for these stoneflies to access methane derived carbon was provided by varying tolerance to hypoxia and consumption of methanogenic and methanotrophic microbes. The role of methane derived carbon in community ecology was additionally shown by the fact that methane concentrations explained 19% of the variation in species assemblages across the aquifer.

Not only did the stonefly species have specific niche characteristics that facilitated their coexistence in this methane-subsidized system, but they also demonstrated adaptation to the temperature regime of the aquifer. My third chapter highlighted the uniqueness of these hyporheic species for their abundance despite desynchronization in growth and emergence. Most stream stoneflies emerge once they have acquired enough degree days and reach a threshold temperature; thus, emergence of a species generally occurs within a 20 day period (Dewalt and Stewart 1995). The five hyporheic stoneflies that we studied emerged over periods

ranging from 2 to 10 months, likely because temperatures were constant over the course of the year. Despite the desynchronization in their emergence, these stoneflies were still present in the aquifer in the tens of thousands, showing that they were able to persist despite potential difficulty of finding mates. Together, the many extremely unique adaptations of these insects elaborated in chapters 2 and 3 showed that floodplains are hotspots of both species diversity and functional diversity.

Application to Systems Ecology

The Systems Ecology program is focused on "developing fundamental, interdisciplinary understanding of interactions of physical, chemical and biological factors affecting ecological systems across spatial and temporal scales and the factors affecting coupled natural and human systems". River floodplains are ideal systems in which to study systems ecology by linking patterns and processes across spatial and temporal scales. They are especially conducive to understanding the processes that create and maintain environmental heterogeneity, and the effects of environmental heterogeneity on ecosystem functioning and biodiversity (Tockner et al. 2010). Heterogeneity, biodiversity, and productivity are maintained in floodplains by the flux of water, materials, and organisms between habitat patches that are spatially variable over time, as described by the shifting habitat mosaic (Stanford et al. 2005, Whited et al. 2007). In particular, floodplains are characterized by extensive exchange between the aquifer and surface environments (Stanford et al. 2005).

My dissertation demonstrated 1) that biogeochemical heterogeneity was crucial for maintaining biodiversity and productivity within the aquifer, and 2) that this heterogeneity was

spatially and temporally structured by nutrient and temperature dynamics maintained by flow path influence and surface-groundwater interactions. Biogeochemical heterogeneity was necessary for microbial processes to produce and assimilate methane in varying dissolved oxygen conditions, and then for various stonefly species to differentially use this carbon source. Heterogeneity was maintained, among other factors, by varying levels of heat and dissolved oxygen supplied by river influence, thereby varying with the seasons and residence time length at each well location.

Floodplains exemplify coupled human and natural systems because they naturally provide us disturbance regulation, water supply, and waste treatment, they are hubs of biodiversity and productivity, and yet they are also some of the most threatened ecosystems from uses such as damming, diversion, and development (Tockner et al. 2010). Study of relatively pristine floodplains such as the Nyack are necessary for understanding a baseline status of these ecosystems, including the services that they can provide us in their natural state.

Literature Cited

Stanford, J. A., M. S. Lorang, and F. R. Hauer. 2005. The shifting habitat mosaic of river ecosystems. Verh. Internat. Verein. Limnol. 29:123–136.

Tockner, K., M. S. Lorang, and J. A. Stanford. 2010. River flood plains are model ecosystems to test general hydrogeomorphic and ecological concepts. River Research and Applications 26:76–86.

Whited, D. C., M. S. Lorang, M. J. Harner, F. R. Hauer, J. S. Kimball, and J. A. Stanford. 2007. Climate, hydrologic disturbance, and succession: drivers of floodplain pattern. Ecology 88:940–953.